IN-25-12

university of california • santa barbara

MECHANICAL PROPERTIES OF AEROGELS

Kelly E. Parmenter and Frederick Milstein

Department of Mechanical Engineering
University of California
Santa Barbara, CA 93106

National Aeronautics and Space Administration
Research Grant Number: NAG 2-930

FINAL FEB 27 1996

CASI

MECHANICAL PROPERTIES OF AEROGELS

Kelly E. Parmenter and Frederick Milstein

Department of Mechanical Engineering
University of California
Santa Barbara, CA 93106

National Aeronautics and Space Administration
Research Grant Number: NAG 2-930

ABSTRACT

Aerogels are extremely low density solids that are characterized by a high porosity and pore sizes on the order of nanometers. Their low thermal conductivity and sometimes transparent appearance make them desirable for applications such as insulation in cryogenic vessels and between double paned glass in solar architecture. An understanding of the mechanical properties of aerogels is necessary before aerogels can be used in load bearing applications. In the present study, the mechanical behavior of various types of fiber-reinforced silica aerogels was investigated with hardness, compression, tension and shear tests. Particular attention was paid to the effects of processing parameters, testing conditions, storage environment, and age on the aerogels' mechanical response. The results indicate that the addition of fibers to the aerogel matrix generally resulted in softer, weaker materials with smaller elastic moduli. Furthermore, the testing environment significantly affected compression results. Tests in ethanol show an appreciable amount of scatter, and are not consistent with results for tests in air. In fact, the compression specimens appeared to crack and begin to dissolve upon exposure to the ethanol solution. This is consistent with the inherent hydrophobic nature of these aerogels. In addition, the aging process affected the aerogels' mechanical behavior by increasing their compressive strength and elastic moduli, while decreasing their strain at fracture. However, desiccation of the specimens did not appreciably affect the mechanical properties, even though it reduced the aerogel density by removing trapped moisture. Finally, tension and shear test results indicate that the shear strength of the aerogels exceeds the tensile strength. This is consistent with the response of brittle materials. Future work should concentrate on mechanical testing at cryogenic temperatures, and should involve more extensive tensile tests. Moreover, before the mechanical response of reinforced aerogels can be fully understood, more tests of unreinforced aerogels are necessary. Unreinforced aerogels are of particular use because their birefringent nature allows for visual determination of stress fields during mechanical testing. The success of any future tests depends on the availability of a large supply of quality specimens with well-documented preparation and storage histories.

TABLE OF CONTENTS

NOMENCLATURE

A	indent surface area (mm^2)
a,b	dimensions (mm)
D	indenter diameter (mm)
E	elastic modulus (MPa)
F	load (N)
H	hardness (MPa)
L	maximum load (N)
S	compressive strength (MPa)
V	shear force (N)

Greek Symbols

δ	indent depth (mm)
ε_f	strain at fracture (mm/mm)
σ	standard deviation of data

1. INTRODUCTION

Silica aerogels are high porosity, extremely low density solids composed of interconnected particles that form an "open" microstructure. As a result of the low solid thermal conductivity of silica, and pore sizes on the order of nanometers, the thermal conductivity of silica aerogel is very low. The low thermal conductivity along with a sometimes transparent appearance make silica aerogels desirable for a wide variety of insulating applications, including cover layers for windows and solar collectors, and as replacements for hazardous CFC insulating foams in cryo-vessels [Fricke, 1992]. However, the same properties of aerogels that make them such good insulators (high porosity and low solid thermal conductivity) also make them inherently fragile and brittle. Thus, their use in load-bearing applications is challenging. Currently, attention is being placed on improving the mechanical properties of aerogels without sacrificing their other unique properties.

Relatively few experiments to determine the mechanical properties of aerogels have been carried out to date. The experiments that are most applicable to the present work include the following tests done with unreinforced silica aerogels. No results for fiber-reinforced silica aerogels have been found in the literature. In earlier work, Gronauer et al. [1986] measured the Young's modulus of unreinforced silica aerogels using sound velocity measurement techniques. Subsequently, Woignier and Phalippou measured the Young's modulus and fracture strength with a three point flexural technique, and the toughness with a single edge notched beam in three point bending technique. More recently, ultrasonic and static compression experiments have been undertaken to determine the elastic modulus [Cross et al., 1989; Gross and Fricke, 1992; Gross et al., 1992].

The present work investigates the mechanical behavior of fiber-reinforced and unreinforced silica aerogels. Silica aerogel is manufactured by first dissolving an alcoholate (silicon methylate (l)) in an organic solvent (methanol (l), 5-30% by volume). The mixture is then hydrolyzed at room temperature by adding between 2 and 20 moles of water, and silica is produced. After the pH is adjusted as desired, the mixture is put into an autoclave and heated to above the solvent's critical temperature to dry the solvent while eliminating its saturated vapor phase. (If not supercritically dried, the porous structure is destroyed by surface tension forces between the vapor-liquid interface.) The vapor is then evacuated, and the product is cooled with dry nitrogen gas [Teichner et al., 1976].

Two processing parameters--the mass percentage of fiber reinforcements and the target density--were altered to obtain aerogels with differing physical characteristics. The target density is a rough prediction of the final aerogel density based on the mass of the original ingredients and the volume of the aerogel mold. It is useful for comparing the properties of aerogels manufactured with the same target density, but it does **not** reflect the final aerogel density. The final aerogel densities are significantly larger than the target densities. The mass percentage of reinforcements was varied from 0% to 25%, and the target density was varied from 40 kg/m^3 to 80 kg/m^3. The reinforced aerogels contained a mixture of 68% silica, 20% alumina, and 12% aluminaborosilicate fibers, with diameters of 3 μm, 2-4 μm, and 8 μm, respectively. All fibers had lengths of 1.27 cm. Table 1.1 is a summary of the materials received and tested.

The mechanical behavior of the aerogels was studied by traditional techniques of mechanical testing (including hardness, compression, and tension tests), and modifications thereof. Particular attention was paid to the effects of processing parameters, testing conditions, storage environment, and age on the aerogels' mechanical behavior. The following paragraphs summarize the procedures and findings of this study.

Table 1.1
Summary of Materials

NASA Batch Number	Specimen Name	Number of Specimens	Fiber Percentage (%)	Target Density (kg/m^3)	Final Density (kg/m^3)	Types of Tests
1,2	-	~6	unreinforced	-	-	Vickers, Knoop, Photoelasticity, Hardness
1,2	-	~6	reinforced	-	-	Vickers, Knoop, Hardness
3	1*	1	reinforced	-	250	Hardness (time at max displacement)
3	2*	1	reinforced	-	300	Hardness (load dependence)
3	4*	1	reinforced	-	210	Hardness (rate dependence)
3	5*	1	reinforced	-	240	Hardness
3	A*	1	25	50	200	Hardness
3	B*	1	10	50	220	Hardness
4	1*	11	25	80	240	Compression (Air)
4	2*	15	25	80	240	Hardness, Compression (Air, Ethanol)
4	3*	15	25	80	240	Hardness, Compression (Air, Ethanol, Desiccated)
4	1*	5	10	50	230	Compression (Air, Ethanol)
4	2*	15	10	50	230	Hardness, Compression (Air)
5	4**	2	unreinforced	-	240	Hardness
5	5**	2	unreinforced	-	240	Compression (Air)
5	6**	2	unreinforced	-	240	Compression (Air)
6	9**	5	5	40	260	Compression (Air)
6	12**	2	5	40	260	Hardness
6	14**	2	10	40	190	Hardness
6	15**	6	10	40	190	Compression (Air)
7	5**	7	25	40	190	Hardness, Compression (Air)
7	6**	7	25	40	190	Hardness, Compression (Air)
7	7**	6	25	40	190	Hardness, Compression (Air)
7	14**	1	10	80	330	Hardness
7	16**	10	10	80	330	Hardness, Compression (Air)
7	17**	7	10	80	330	Hardness, Compression (Air)
7	35**	6	5	80	320	Hardness, Compression (Air)
7	2**	1	25	40	190	Tension
7	24**	2	10	80	330	Tension
7	27**	2	10	80	330	Tension
7	33**	2	25	80	240	Tension
7	34**	1	25	80	240	Tension
7	38**	1 •	5	80	320	Tension
7	18**	1	10	80	330	Shear
7	19**	1	10	80	330	Shear
7	21**	1	10	80	330	Shear
7	28**	1	10	80	330	Shear
7	29**	1	10	80	330	Shear
7	31**	1	25	80	240	Shear

* Parmenter & Milstein Numbering System

** NASA Numbering System

2. TESTING PROCEDURES

2.1 Hardness Tests

Hardness tests were the first type of material testing technique initiated because of the non-destructive nature and, for many materials, the ease of application of such tests. Generally hardness tests yield pertinent information about the response of a material at the expense of only a few indents on the material's surface, compared with the complete destruction of specimens often associated with tensile and compression tests.

Traditional Methods of Indentation

Initially, traditional indentation methods such as Vickers and Knoop were employed for hardness determination. Unfortunately, these methods failed to work on the silica aerogel specimens. At even very small loads ($\leq$ 0.245 N), the indentation pressure was too large for these fragile materials, and resulted in cracks and surface cave-ins. In addition, because the aerogels absorb and transmit light more readily than they reflect it, it was difficult to obtain enough contrast in the magnified images of the indents to make accurate measurements of indent size. This was particularly true for very low loads, and for the more opaque (fiber-reinforced) aerogels. Attempts to use dyes to improve the contrast of the magnified images were unsuccessful because the dyes caused cracks on the surfaces of the aerogels (see Section 2.5). Examples of indents made in semi-transparent (unreinforced) aerogels are provided in the following two figures. Figure 2.1 is a photograph of an indent made with a Vickers microindenter at a load of 0.981 N. Figure 2.2 is a series of photographs of an indent made with a Knoop microindenter at a load of 1.961 N.

Alternative Indentation Approach

Results of experiments with Vickers and Knoop hardness tests demonstrated the need to substantially reduce indentation pressure in order to deform the aerogels plastically without creating cracks. In an alternative approach, the indents were made with a 19.05

mm diameter steel ball, at loads of 18.2 N and smaller. The ball and socket fixture was secured to the crosshead of a displacement-controlled *Instron 1123* testing machine. The load was measured with a compression load cell (range = 0 to 981 N), and the crosshead displacement was measured with a linear variable differential transformer (LVDT) (range = ± 1.27 mm). All tests were conducted under ambient conditions. An initial preload of 2.02 N was applied to minimize surface effects. The load was subsequently applied to the "full-loading" value and then reduced to the preload value where the net indentation value, δ, was determined. The indent surface area, A, was approximated from the indent depth and ball diameter, D, with the following relation:

$$A = \pi D \delta . \tag{2.1}$$

The hardness, H, was defined as the maximum load, L, divided by the indent surface area:

$$H = \frac{L}{A} . \tag{2.2}$$

Test Parameters

The influences of three testing parameters on the hardness were investigated. First, the duration of time at maximum displacement was varied to see if the aerogels were prone to stress relaxation, or creep. During these tests, specimens were loaded at a rate of 0.102 mm/min until a force of approximately 14 N was reached, and then the displacement was held constant for a specified period of time before the load was reduced. The time at maximum displacement ranged from 0 to 60 minutes. Second, the maximum load was varied to see how load sensitive the hardness tests were. The peak loads ranged from 10.2 to 18.3 N. Loads higher than 18.3 N tended to crack the specimens and loads smaller than 10.2 N tended to yield indecernible results. Third, the rate dependence of the hardness was studied by varying the crosshead speed from 0.025 to 0.203 mm/min.

Photoelasticity

Tests were performed to determine whether the transparent, unreinforced, aerogels would exhibit birefringence (photoelasticity) when indented; this is of interest because such birefringence could be used as a means of characterizing internal stresses in the material. For these tests, a polarizing lens was placed behind the specimen, an analyzing lens was placed in front of the specimen, and a fiber-optic white light source was used for illumination. The aerogels were then viewed and filmed with a video camera while being indented with the steel ball.

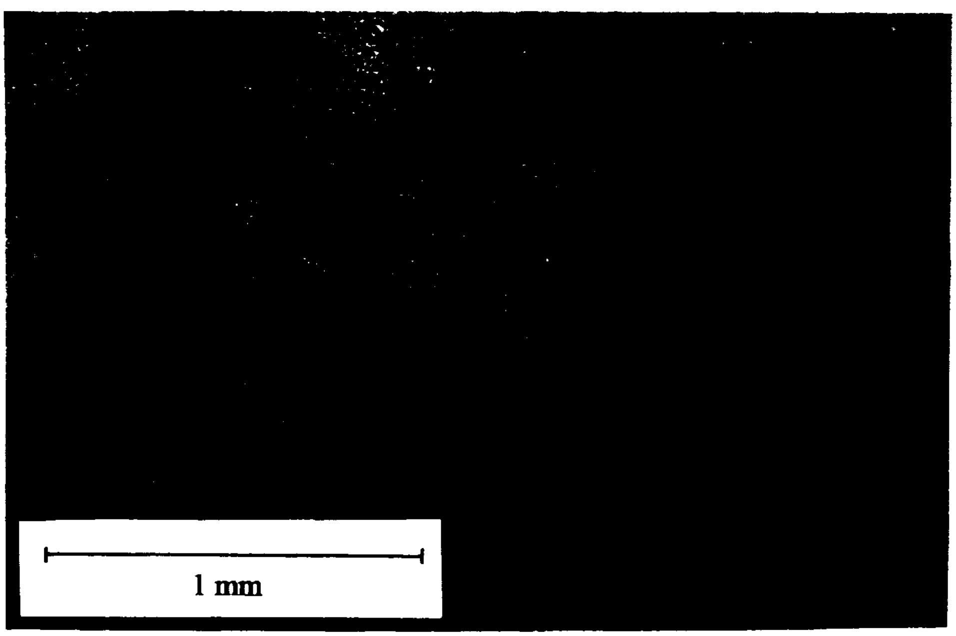

Figure 2.1
Vickers Indentation at 0.981 N Load

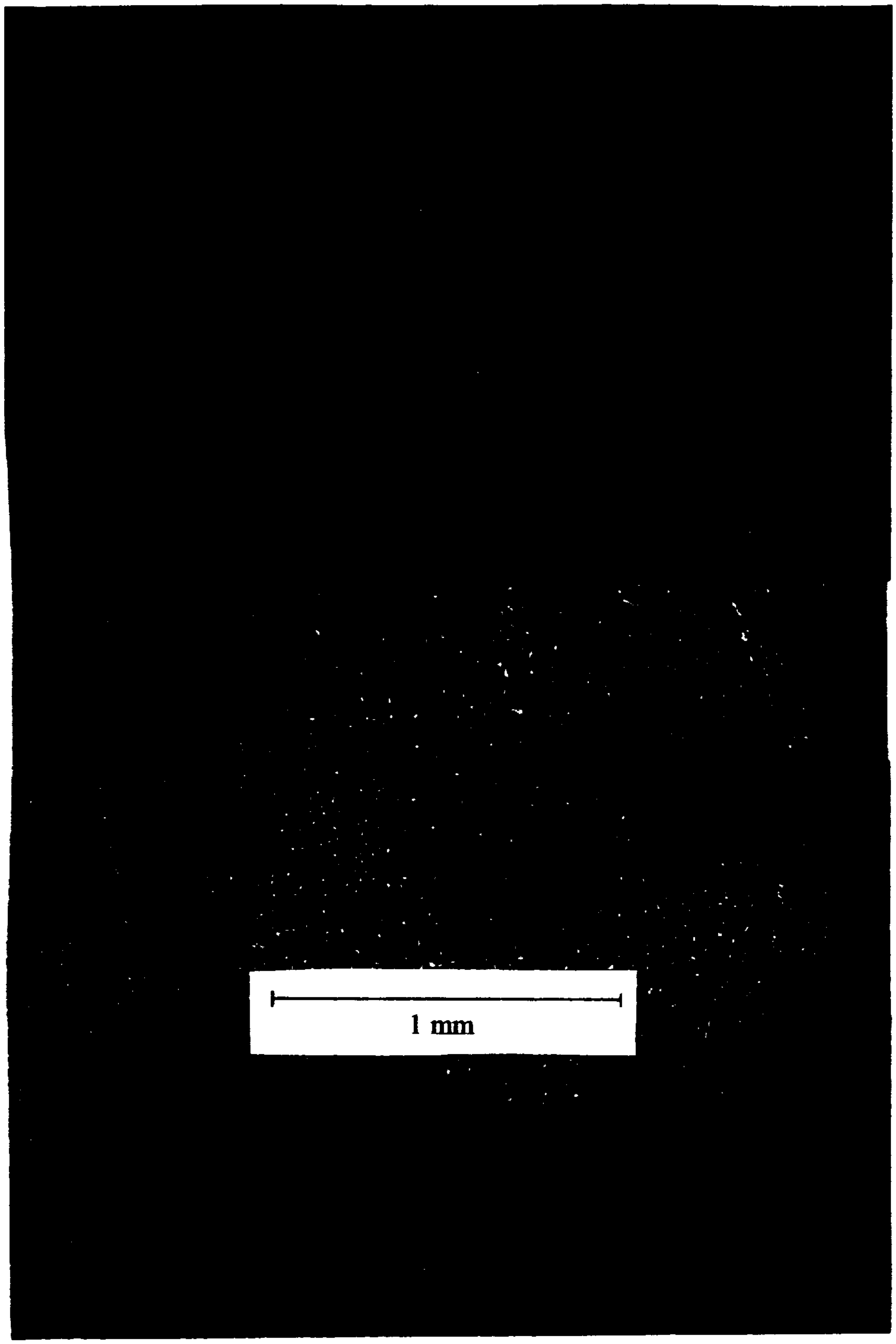

Figure 2.2
Knoop Indentation at 1.961 N Load

2.2 Compression Tests

Compression tests were performed with the same displacement-controlled *Instron 1123* testing machine used for hardness tests. Compression specimens were machined from raw material into rectangular blocks. The blocks had square cross sections and heights equal to twice the length of a side (see Appendix A for dimensions). The specimens were placed, one at a time, between the top and bottom portions of a compression fixture, and were loaded at a rate of 0.102 mm/min by lowering the top portion of the fixture (which was secured to the crosshead) until they fractured macroscopically. The bottom portion of the compression fixture was a stationary flat plate whereas the top portion consisted of a "frictionless" hemisphere secured into a socket with vacuum grease. The top portion was thus self-aligning. The load was measured with a compression load cell (range = 0 to 981 N), and the crosshead displacement was measured with a LVDT (range = ± 6.35 mm). The majority of tests were conducted under ambient conditions.

The Load-Displacement curves were converted to Stress-Strain curves by dividing the loads by the original cross-sectional areas of the specimens, and the displacements by the original heights of the specimens. The compressive strength, the strain at fracture, and two secant moduli were determined from the Stress-Strain data.

Tests in Ethanol

Tests were conducted in a liquid ethanol environment at ambient temperatures to determine ethanol's applicability for use in future cryogenic experiments. If compression results in ethanol matched compression results in air, then ethanol would be a potential medium in which to cool specimens to cryogenic temperatures. For these tests, the specimens were submerged in a petri dish full of ethanol, and tested with the procedure for compression tests described above.

Effects of Age and Storage Environment

The influences of age and storage environment on aerogel compression results were quantified by comparing Stress-Strain curves for aerogels that had different storage histories. Two types of aerogels were investigated. The first type of aerogel was manufactured with a target density of 50 kg/m^3 and a fiber percentage of 10%. Tests were performed on compression specimens machined from two different batches of bulk material. Specimens from one batch were tested within one week of being machined, and specimens from the other batch were stored in an air environment, under ambient conditions, for 2 months before being tested. The second type of aerogel studied was manufactured with a target density of 80 kg/m^3 and a fiber percentage of 25%. For this type of aerogel, all tests were done on specimens machined from the same batch of bulk material. Some compression specimens were tested within a week of being machined, some were tested after being stored in an air environment, under ambient conditions, for approximately 2 months, and the remaining were tested after being stored in the same air environment for two months and then in a desiccator at ambient temperature for 10 days. The dessicator's purpose was to remove any absorbed moisture from the specimens.

2.3 Tensile Tests

Tensile tests were performed with the displacement-controlled *Instron 1123* testing machine described previously. The aerogel specimens were machined from bulk material into "dog-bone" shapes with the dimensions provided in Appendix A. The specimens were inserted and held with pins between the top and bottom portions of a tension fixture, and were then loaded by raising the top portion at a rate of 0.102 mm/min until they fractured macroscopically. The bottom portion was stationary, while the top portion was secured to the load cell with a universal coupling. The load cell's range was 0 to 981 N. The crosshead displacement was determined from the Instron's internal displacement gage. Strain gages were not used to measure the actual strain within the gage length of the specimens because of the extreme difficulty in adhering gages without damaging or altering the mechanical properties of the aerogels. All tensile tests were conducted under ambient conditions.

2.4 Shear Tests

Tests were conducted on the *Instron 1123* with notched beam specimens (commonly referred to as Iosipescu specimens) in antisymmetric four point bending. Figure 2.3 shows a diagram of the loading arrangement. The dimensions of an Iosipescu specimen are provided in Appendix A.

Under the appropriate conditions, a specimen tested in this way will have virtually pure shear within the section of the notch-root axis [Iosipescu, 1963]. Since brittle materials fail in tension before they fail in shear, this type of test will yield the lower bound of the shear strength (i.e., the actual shear strength will be greater than the indicated shear strength at failure) rather than the ultimate shear strength if the specimens tested behave as truly brittle materials. The load was measured with a compression load cell (range = 0 to 981 N), and the displacement was determined from the Instron's internal displacement gage. The crosshead speed was set at 0.102 mm/min, and all experiments were conducted under ambient conditions.

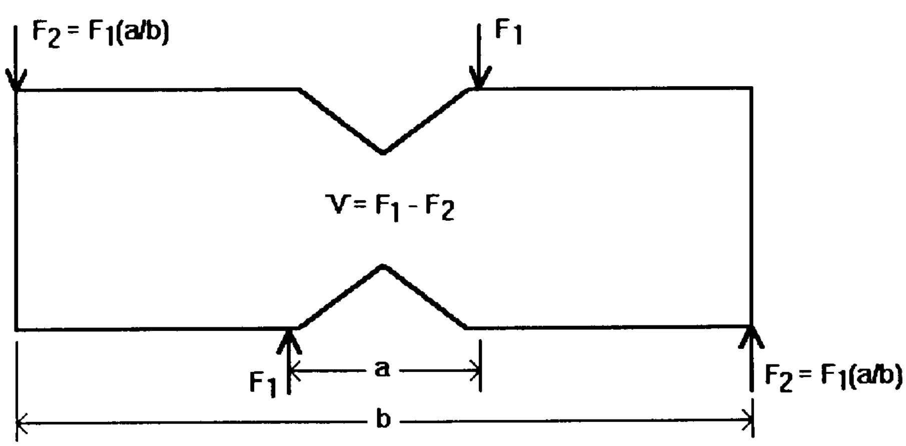

Figure 2.3
Antisymmetric Four Point Bending Arrangement

2.5 Special Handling

It was observed that the aerogels are soluble in water (hydrophobic) and other liquids. In addition, perspiration from fingers and hands can cause micro-cracks to form on surfaces that have been handled without gloves. To prevent this from occurring, all test specimens were handled with gloves. Moreover, special care was taken to degrease and dry all equipment that came in contact with the specimens.

3. RESULTS

3.1 Hardness Tests

A summary of the hardness results for each different type of aerogel tested is provided in Table 3.1. In addition, plots depicting the relationships between target density and hardness and target density and final density, as well as a representative Load-Displacement curve are shown in Figures 3.1 through 3.3, respectively. The Load-Displacement curve is from an experiment with an unreinforced aerogel specimen. The bulk of the hardness tests were carried out with a maximum load of approximately 14 N, a crosshead speed of 0.102 mm/min, and no time delay at maximum load. For the aerogel manufactured with a target density of 40 kg/m^3 and a fiber percentage of 10%, the maximum load was lowered to approximately 10 N because of the extreme softness of the material. Appendix B contains detailed hardness results and representative Load-Displacement curves for each type of specimen tested.

The results in Table 3.1 and Figures 3.1 and 3.2 indicate that the hardness is a strong function of fiber percentage and target density. The hardness tends to increase with an increase in target density for a given fiber percentage, and decrease with an increase of fiber percentage for a given target density. However, an exception to the second trend is found with specimens of target density equal to 40 kg/m^3. For these specimens, the hardness of the 10% fiber-reinforced material is smaller than the hardness of the 25% fiber-reinforced material.

Results of the three investigations of the influence of testing parameters are depicted graphically in Figures 3.4 through 3.6. Detailed hardness results are provided in Appendix C. Figure 3.4 shows the variation of hardness with time at maximum displacement. Each datum point reflects a separate indentation. The displacement was held constant for time periods ranging from 0 to 60 minutes. The results indicate that the load relaxed, the indentation depth increased, and therefore, the hardness decreased, with an increase in time at maximum displacement. The amount of relaxation was rapid at first, and then gradually leveled off. These results are indicative of a creeping material. Figure 3.5

shows the influence of maximum applied load upon hardness. The important result here is that hardness is not sensitive to load, within the scatter due to material inhomogeneities found in many of the materials. Figure 3.6 depicts the influence of cross-head speed (or loading rate) on the measured hardness. Again, the important conclusion is that crosshead speed is not a significant variable in the range of ~ 0.05 to 0.2 mm/min.

Table 3.1
Summary of Hardness Results

Fiber Percentage (%)	Target Density (kg/m^3)	Final Density (kg/m^3)	Number of Indents	Mean Hardness (MPa*)	Standard Deviation, σ (MPa)
0	-	240	12	5.37	0.47
5	40	260	10	2.20	0.26
5	80	320	6	5.67	1.84
10	40	190	7	0.97	0.04
10	50	230	6	3.71	0.55
10	80	330	12	5.37	2.71
25	40	190	14	1.54	0.06
25	50	200	24	2.02	0.24
25	80	240	10	2.11	0.21

* 9.8066 MPa = 1 kg/mm^2

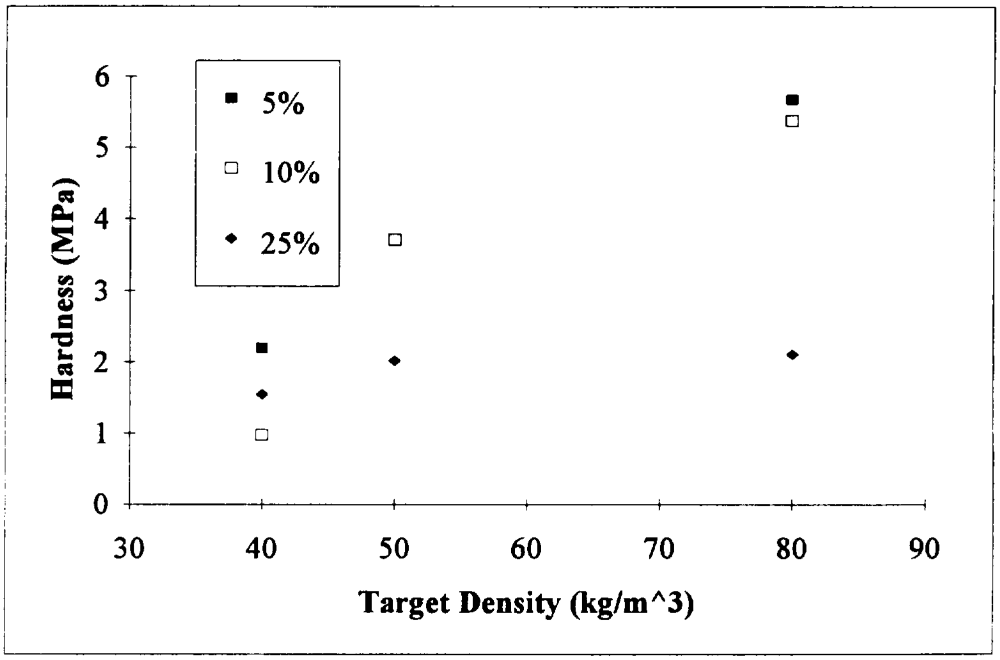

Figure 3.1
Hardness vs. Target Density
with Fiber Percentage as a Parameter

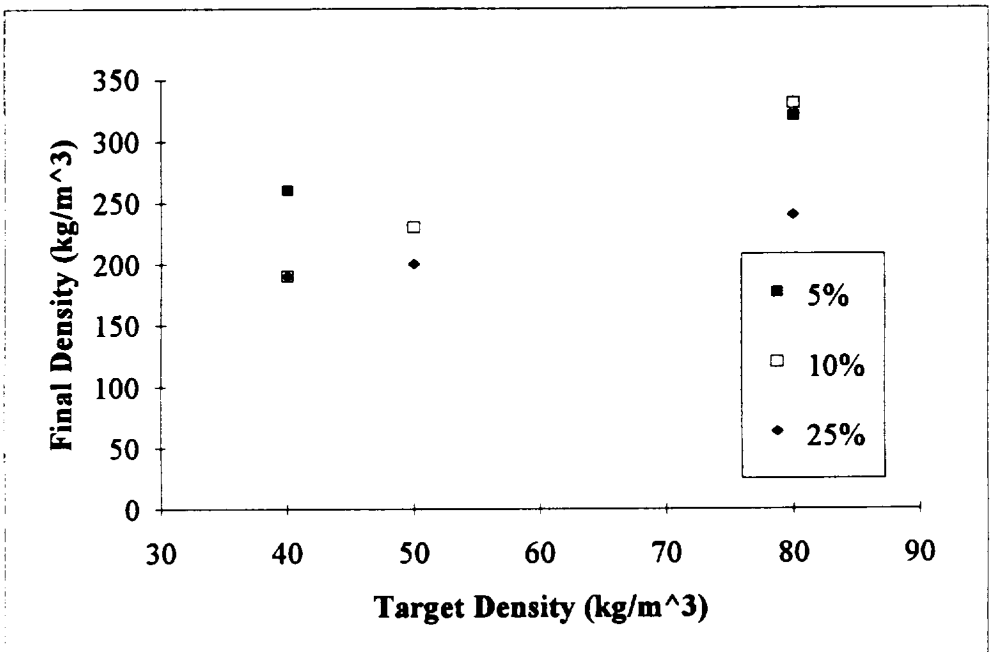

Figure 3.2
Final Density vs. Target Density
with Fiber Percentage as a Parameter

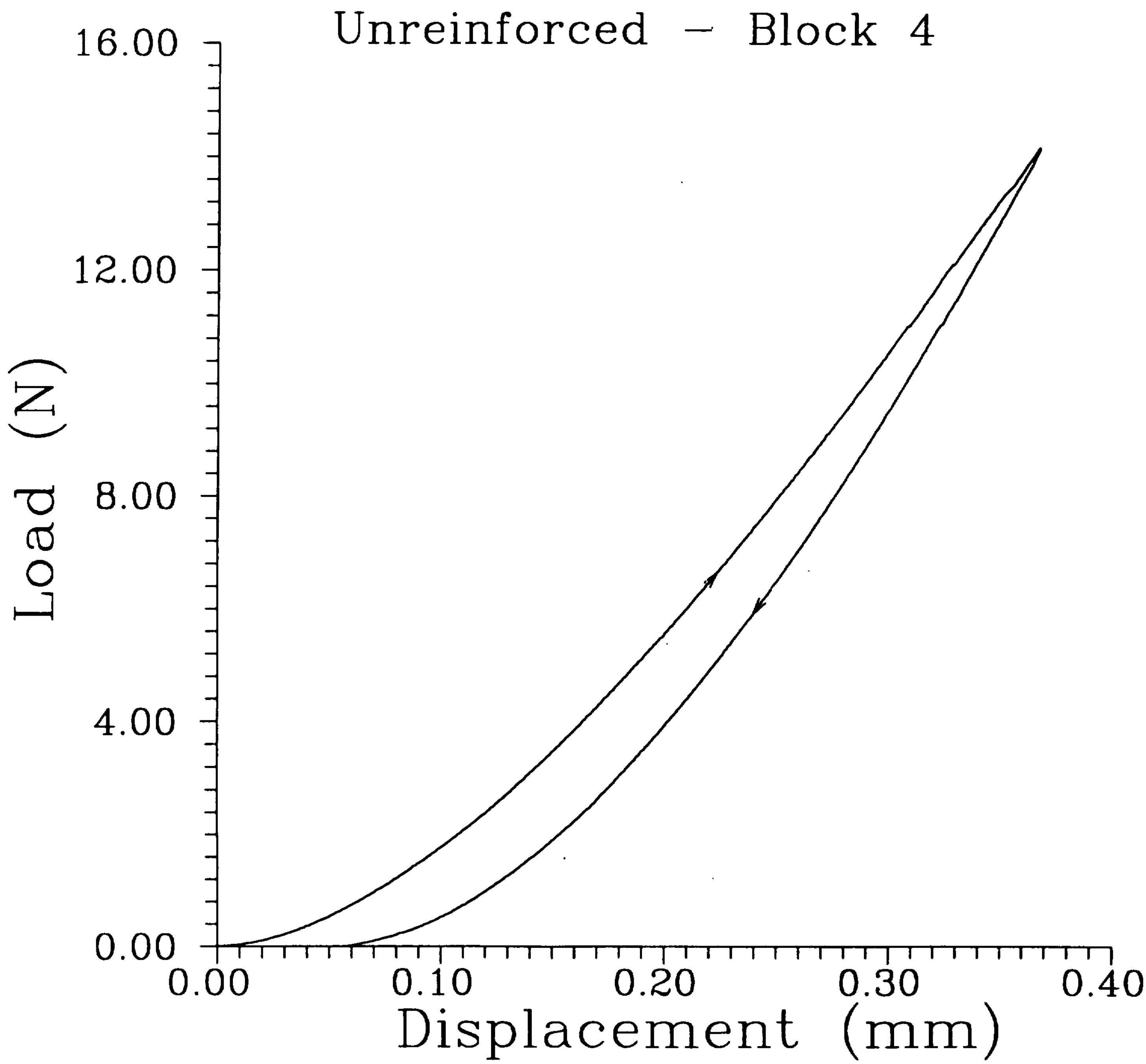

Figure 3.3
Load vs. Displacement Curve for Unreinforced Silica Aerogel using Hardness Measurement

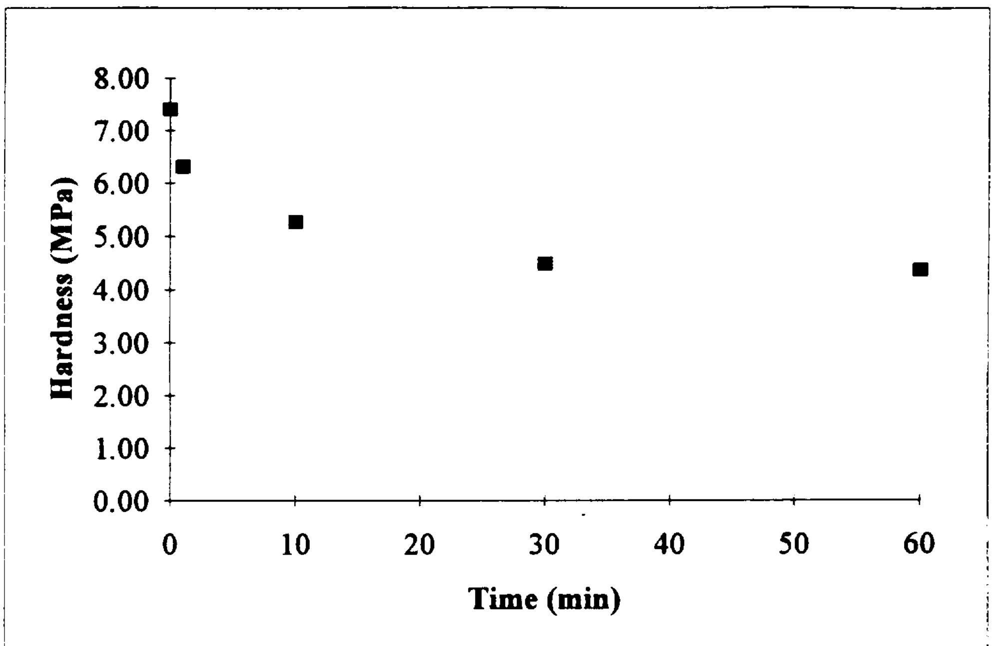

Figure 3.4 - Relaxation Test
Hardness vs. Time at Maximum Displacement

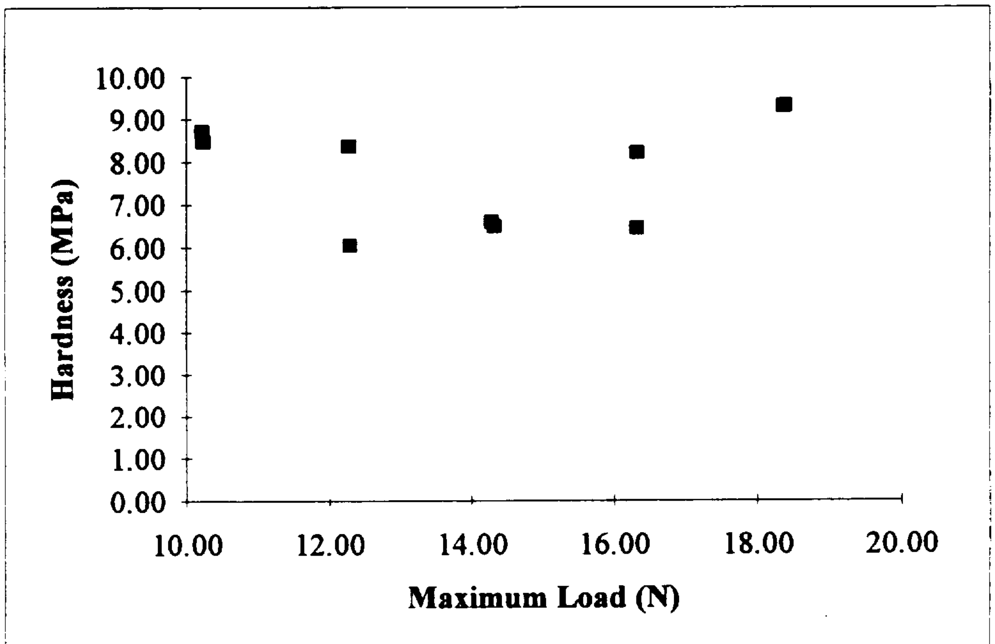

Figure 3.5 - Load Variation Test
Hardness vs. Maximum Load

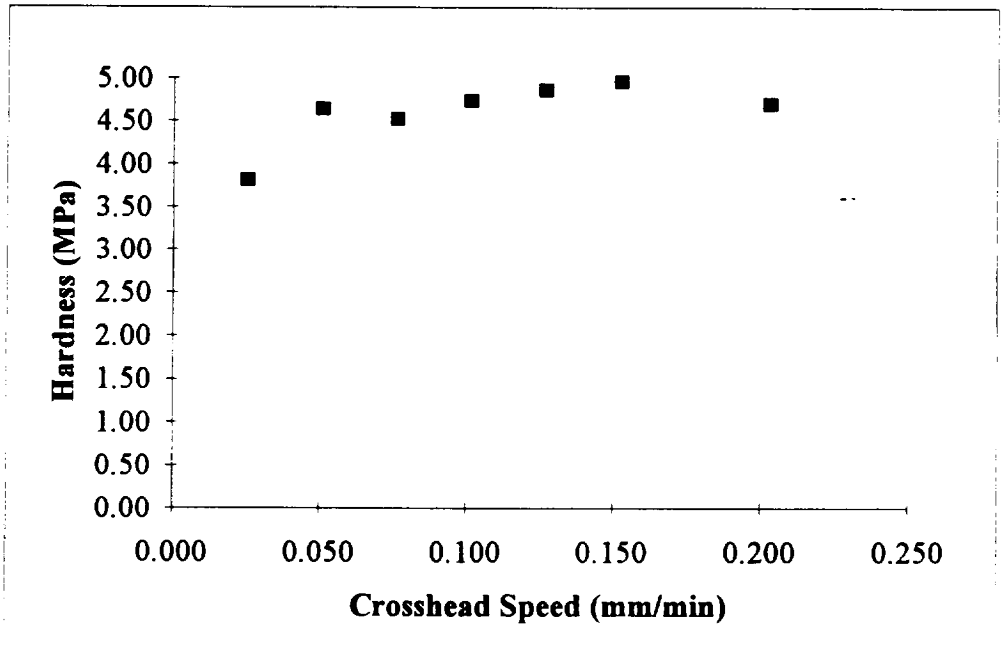

Figure 3.6 - Rate Test
Hardness vs. Crosshead Speed

Photoelasticity

Photographs depicting the state of stress of unreinforced aerogel during indentation are provided in Figures 3.7a,b,c. The applied load increases from Figure 3.7a to Figure 3.7c. Although the images lack clarity because of the poor quality of the transparent specimens provided for testing, birefringence is clearly present. Thus photoelasticity techniques may indeed be used to study internal stresses in transparent aerogel specimens. The scratches on the surface of the present specimen, through which the fringe patterns were observed, resulted in scattering of incoming light and, therefore, reduced clarity. More tests are anticipated if transparent samples of reasonable quality are made available.

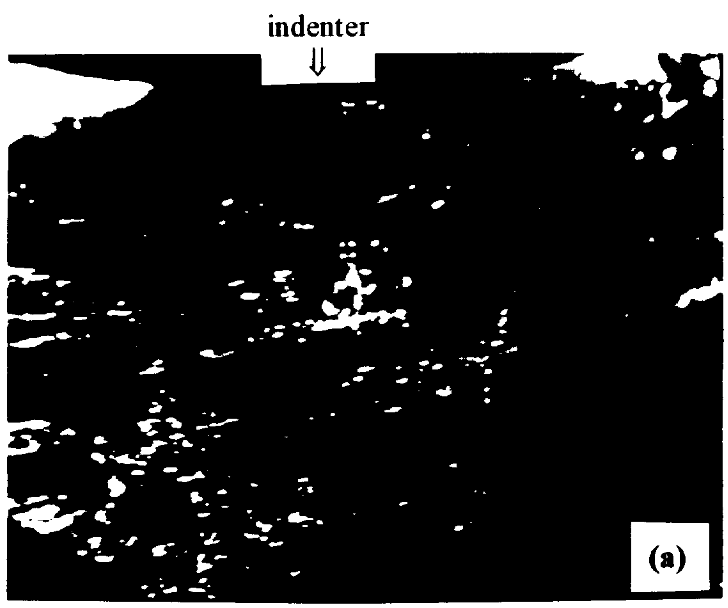

Figure 3.7
Stress Distributions in a Photoelastic Specimen During Indentation. Load Increases from Fig. 3.7a to Fig.'3.7c.

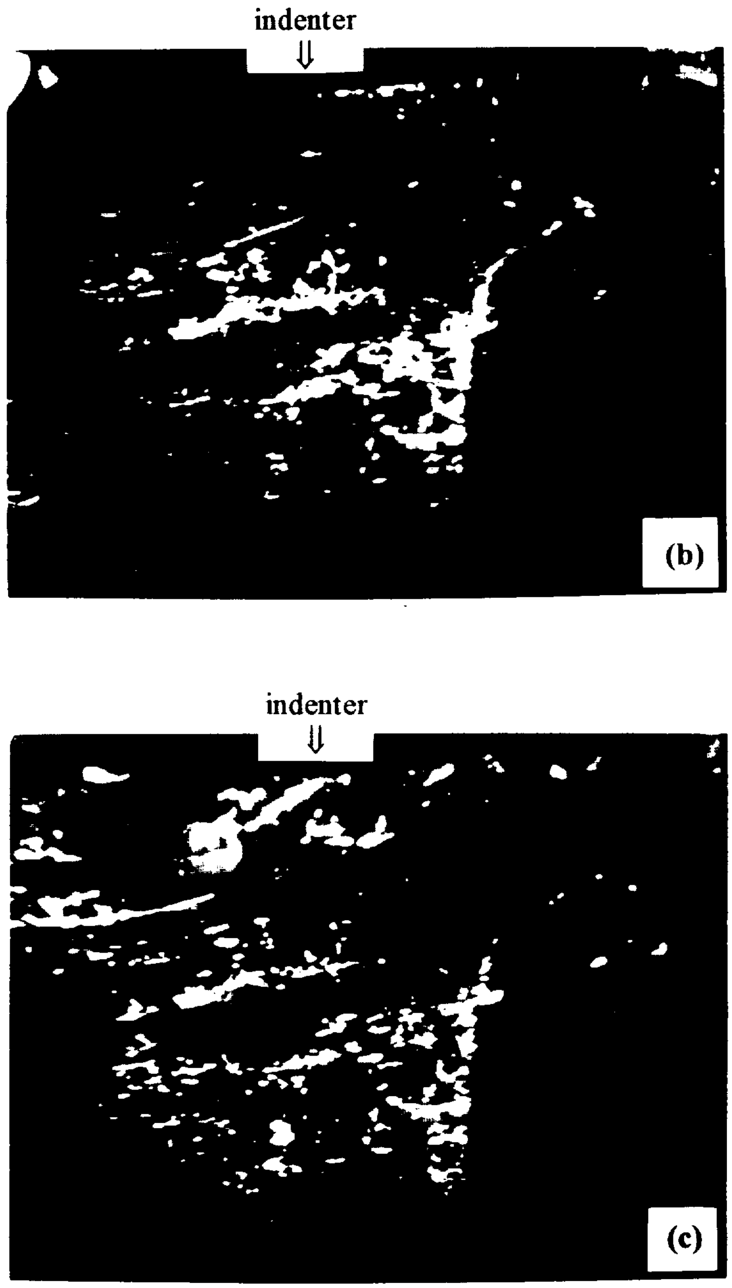

Figure 3.7, continued
Stress Distributions in a Photoelastic Specimen During Indentation. Load Increases from Fig. 3.7a to Fig. 3.7c.

3.2 Compression Tests

A summary of compression results for the various aerogels tested is provided in Table 3.2. The compressive strength is defined as the maximum stress carried by the specimens during a test, and the strain at fracture is the strain at which macroscopic failure of the specimen occurred. Each secant modulus is determined by measuring the slope between two points on the Stress-Strain curves. For $E_{50\%}$, the slope is calculated between the point of stress equal to 0.040 MPa and the point where the stress is 50% of the compressive strength. For $E_{90\%}$, the slope is calculated between the point of stress equal to 0.040 MPa and the point where the stress is 90% of the compressive strength. The slopes are referenced to the 0.040 MPa value to eliminate effects of any surface irregularities. Representative stress-strain curves for each type of material tested are shown in Figure 3.8, and the relationship between compressive strength and target density is depicted in Figure 3.9. Appendix D contains detailed compression results and Stress-Strain curves for every experiment conducted.

The data in Table 3.2 and Figures 3.8 and 3.9 indicate that the compressive strength, the strain at fracture, and the secant moduli are all dependent on target density and fiber percentage. The compressive strength increased with an increase in target density for a given fiber percentage, and decreased with an increase in fiber percentage for a given target density. There was one exception to the second trend: the compressive strength of the aerogel manufactured with 25% fibers and a target density of 40 kg/m^3 exceeded that of the aerogel manufactured with 10% fibers and a target density of 40 kg/m^3. This result is consistent with the results from hardness experiments. Furthermore, the strain at fracture tended to decrease with an increase in target density for a given fiber percentage, but did not follow a discernible trend with fiber percentage. Finally, the secant moduli increased with an increase in target density for a given fiber percentage, and decreased (for the most part) with an increase in fiber percentage for a given target density. Again, the exception to this was found for the specimens of target density equal to 40 kg/m^3, and fiber percentages of 10% and 25%.

It is possible that the exceptions mentioned above are the result of inconsistant production and storage histories of the specimens before shipment to our labs. It has been found that age and storage environment have appreciable influences on the compression results of aerogel specimens, as is demonstrated in subsequent paragraphs.

Table 3.2

Summary of Compression Results

Fiber Percentage (%)	Target Density (kg/m^3)	Final Density (kg/m^3)	Number of Specimens	Compressive Strength, S (MPa)	Strain at Fracture, ε_f (mm/mm)	Secant Modulus @ 50% of S (MPa)	Secant Modulus @ 90% of S (MPa)
0	-	204	3	$S = 1.01$	$\varepsilon_f = 0.100$	$E_{50\%} = 16.4$	$E_{90\%} = 14.1$
				$\sigma = 0.03$	$\sigma = 0.009$	$\sigma = 1.8$	$\sigma = 0.6$
5	40	260	3	$S = 1.00$	$\varepsilon_f = 0.071$	$E_{50\%} = 20.4$	$E_{90\%} = 18.3$
				$\sigma = 0.08$	$\sigma = 0.010$	$\sigma = 3.2$	$\sigma = 3.2$
5	80	320	4	$S = 1.45$	$\varepsilon_f = 0.053$	$E_{50\%} = 36.0$	$E_{90\%} = 33.9$
				$\sigma = 0.18$	$\sigma = 0.004$	$\sigma = 3.4$	$\sigma = 2.5$
10	40	190	6	$S = 0.34$	$\varepsilon_f = 0.069$	$E_{50\%} = 8.1$	$E_{90\%} = 6.1$
				$\sigma = 0.03$	$\sigma = 0.007$	$\sigma = 1.6$	$\sigma = 0.9$
10	50	230	9	$S = 1.01$	$\varepsilon_f = 0.067$	$E_{50\%} = 23.4$	$E_{90\%} = 18.0$
				$\sigma = 0.05$	$\sigma = 0.004$	$\sigma = 1.4$	$\sigma = 0.7$
10	80	330	15	$S = 1.27$	$\varepsilon_f = 0.051$	$E_{50\%} = 30.4$	$E_{90\%} = 31.8$
				$\sigma = 0.14$	$\sigma = 0.003$	$\sigma = 4.4$	$\sigma = 3.2$
25	40	190	16	$S = 0.55$	$\varepsilon_f = 0.142$	$E_{50\%} = 8.6$	$E_{90\%} = 5.3$
				$\sigma = 0.03$	$\sigma = 0.015$	$\sigma = 0.7$	$\sigma = 0.5$
25	80	240	15	$S = 0.79$	$\varepsilon_f = 0.077$	$E_{50\%} = 22.3$	$E_{90\%} = 15.0$
				$\sigma = 0.02$	$\sigma = 0.010$	$\sigma = 3.1$	$\sigma = 2.1$

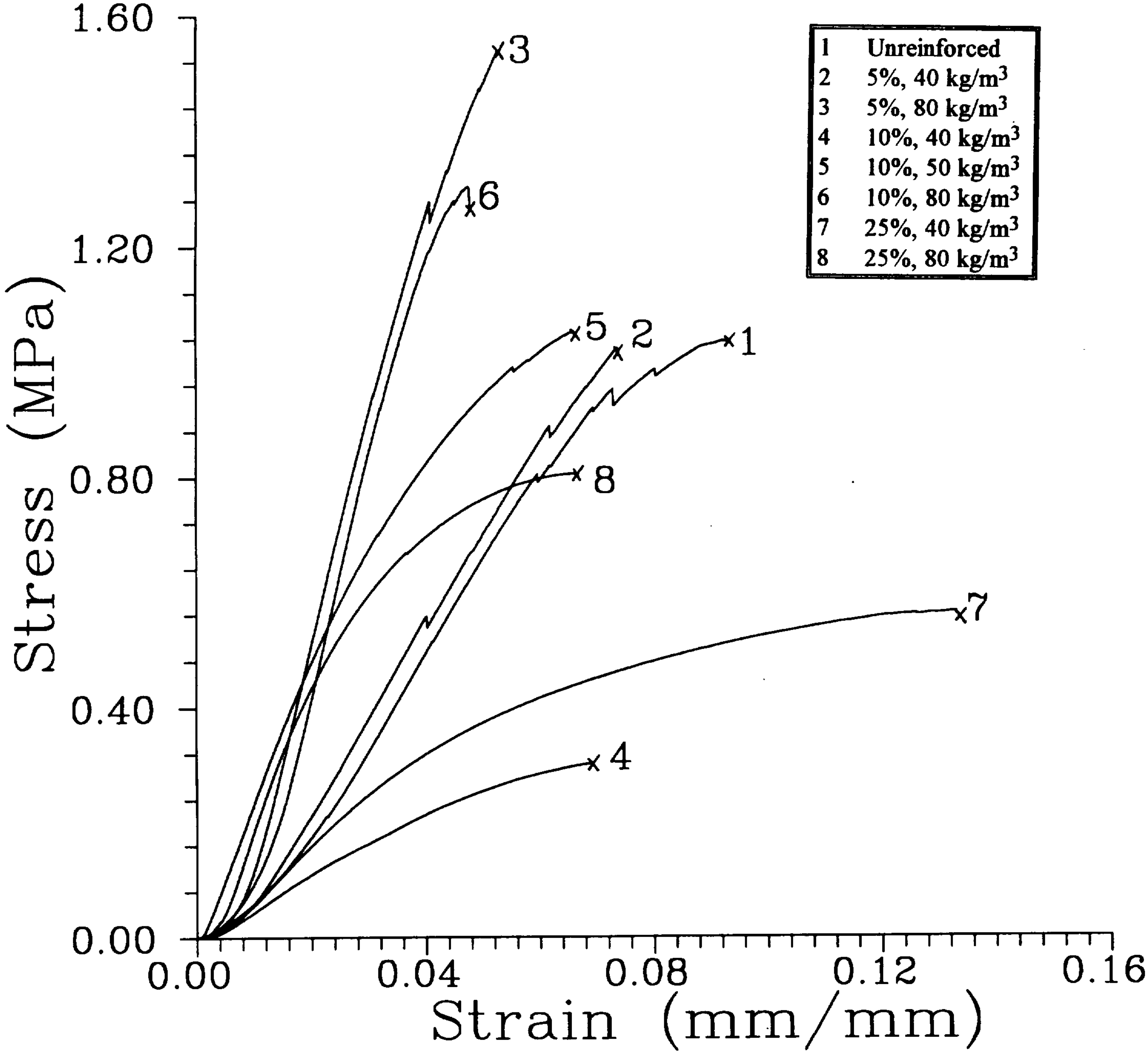

Figure 3.8
Representative Stress-Strain Data

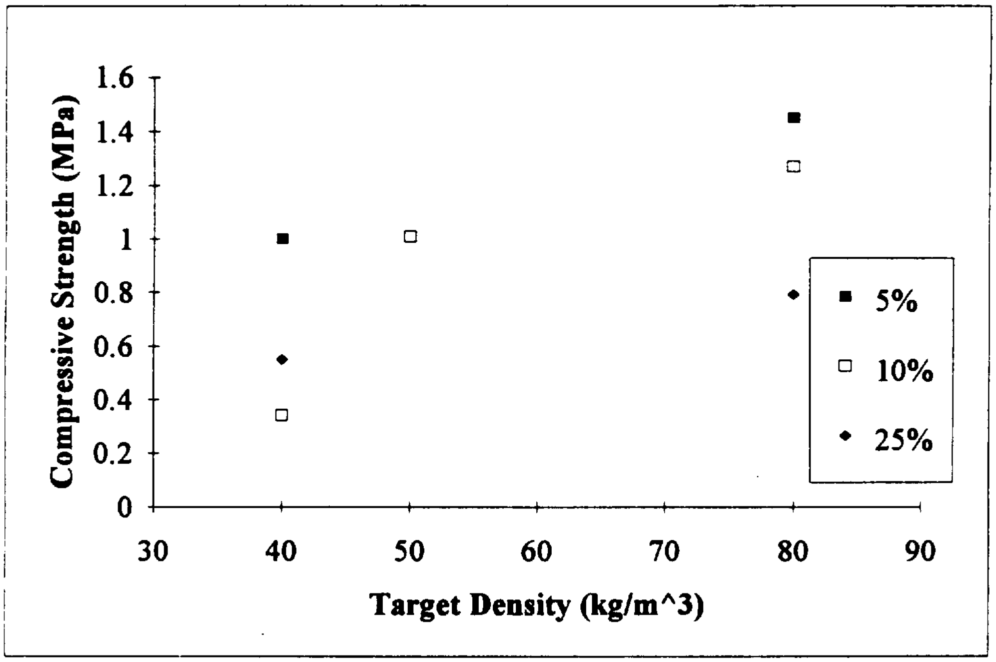

Figure 3.9
Compressive Strength vs. Target Density
with Fiber Percentage as a Parameter

Tests in Ethanol

The compressive results of experiments in ethanol are compared with results of experiments in air in Table 3.3 and in Figures 3.10 through 3.12. All specimens were stored in air, under ambient conditions, for approximately two months before being tested. For both types of material, the compression results for tests in ethanol are not consistent, and show a considerably greater amount of scatter (larger σ values in Table 3.3), than results for tests in air. The average compressive strength is smaller in ethanol than in air by 43% for the 10% fibers case, and by 16% for the 25% fibers case. The calculated moduli are also higher in air than in ethanol. In addition, the compression specimens appeared to crack and begin to dissolve upon exposure to the ethanol solution. Therefore, ethanol is not a desirable medium in which to conduct cryogenic tests. Detailed compression results and stress-strain curves are provided in Appendices E and F, for tests done in ethanol and air, respectively.

Table 3.3

Summary of Compression Results for Tests in Air and Ethanol

Fiber Percentage (%)	Target Density (kg/m^3)	Final Density (kg/m^3)	Environment	Number of Specimens	Compressive Strength, S (MPa)	Secant Modulus @ 50% of S (MPa)	Secant Modulus @ 90% of S (MPa)
10	50	250	Air	2	S = 1.07 σ = 0.05	$E_{50\%}$ = 34.2 σ = 0.2	$E_{90\%}$ = 28.4 σ = 0.1
10	50	250	Ethanol	3	S = 0.61 σ = 0.21	$E_{50\%}$ = 20.5 σ = 6.4	$E_{90\%}$ = 18.1 σ = 6.9
25	80	250	Air	3	S = 0.78 σ = 0.05	$E_{50\%}$ = 29.5 σ = 3.0	$E_{90\%}$ = 23.9 σ = 1.4
25	80	250	Ethanol	4	S = 0.65 σ = 0.08	$E_{50\%}$ = 24.3 σ = 5.1	$E_{90\%}$ = 20.9 σ = 4.1

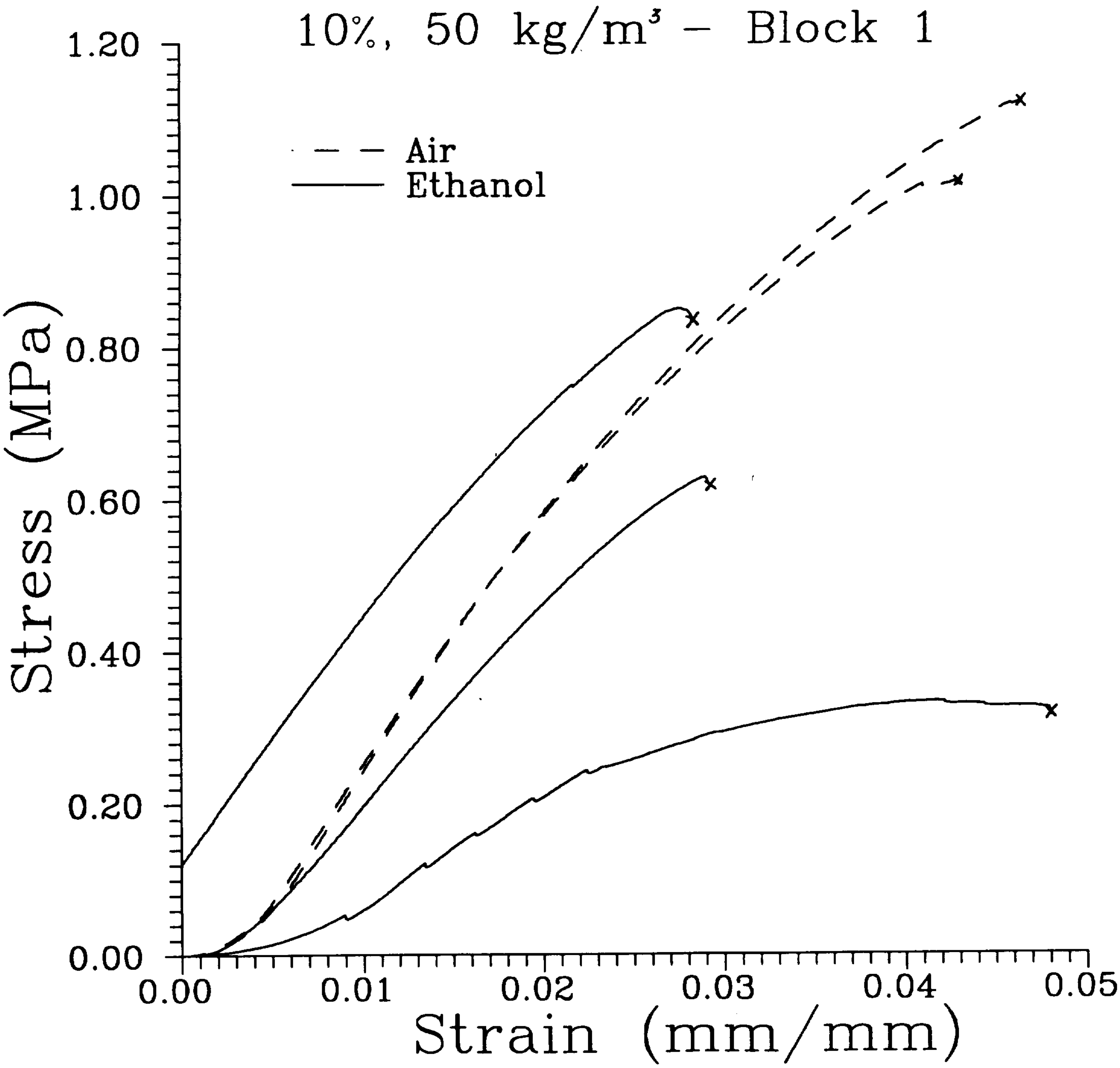

Figure 3.10

Comparison of Stress-Strain Curves for Tests in Ethanol and Air.

Target Density = 50 kg/m^3, Fiber Percentage = 10%.

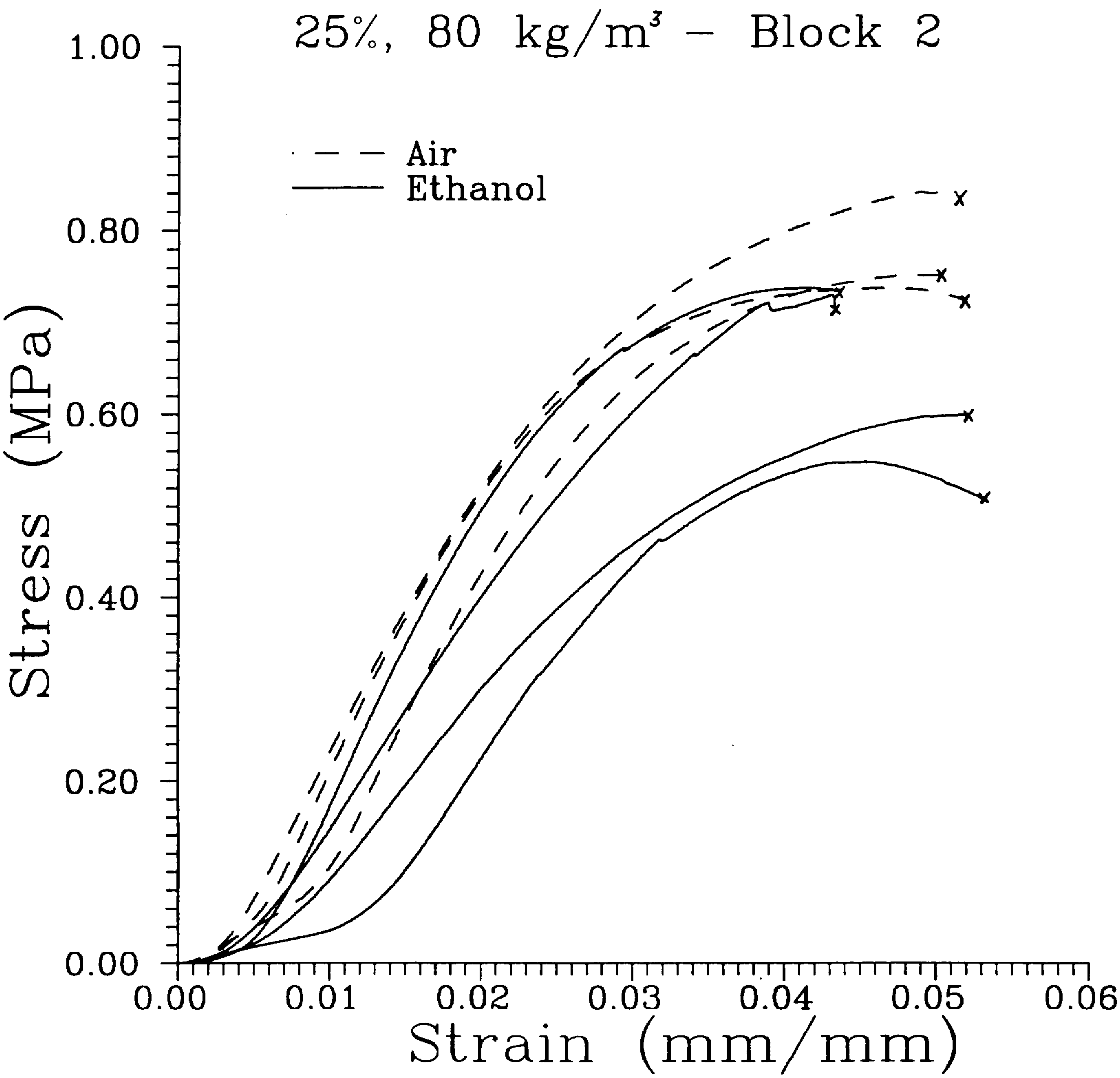

Figure 3.11

Comparison of Stress-Strain Curves for Tests in Ethanol and Air.

Target Density = 80 kg/m^3, Fiber Percentage = 25%.

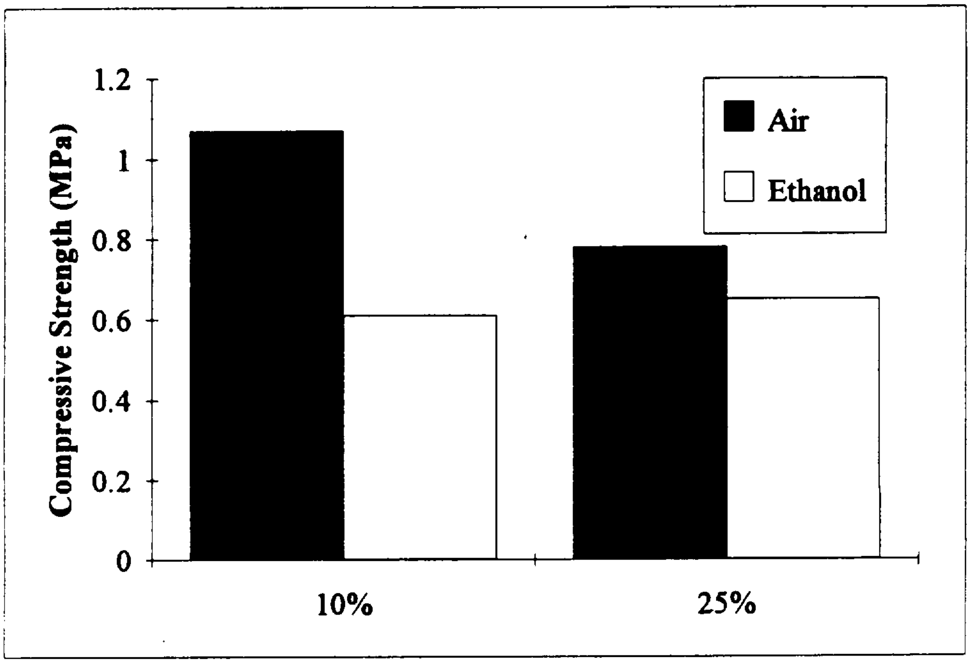

Figure 3.12
Comparison of Compressive Strengths for Tests in Ethanol and Air for 10% and 25% Fiber Reinforced Specimens

Effects of Age and Storage Environment

The influences of age and storage environment are tabulated in Table 3.4 and depicted in Figures 3.13 through 3.15. Figure 3.13 is a comparison of the compressive responses of specimens (10% fibers, target density = 50 kg/m^3) aged for 2 months in air with specimens tested within a week of being machined. Figure 3.14 is a comparison of the compressive responses of specimens (25% fibers, target density = 80 kg/m^3) aged for 2 months in air, with specimens aged for 2 months in air and then stored in a desiccator for ten days, and with specimens tested within a week of being machined. Figure 3.15 is a comparison of the strains at fracture for the various materials tested. The results indicate that the aging process tends to increase the compressive strength and secant moduli, while decreasing the strain at fracture for both types of materials. Therefore, the toughness decreases and the specimens seem to become more brittle with age. Furthermore, although the density decreases noticeably after desiccation, the compressive results for desiccated specimens agree well with the results for specimens aged in air alone. The results may also indicate a slight increase in strength occurring during desiccation, but since the increase is of the same order as experimental scatter, a solid conclusion cannot be drawn. Detailed compression results and Stress-Strain curves are included in Appendix D for freshly machined specimens, Appendix F for specimens aged in air, and Appendix G for specimens aged in air and then desiccated.

Table 3.4

Summary of Compression Results for Specimens Freshly Machined, Aged in Air, and Aged in Air and Desiccated

Fiber Percent (%)	Target Density (kg/m^3)	Final Density (kg/m^3)	Storage	Number of Specimens	Compressive Strength, S (MPa)	Strain at Fracture, ε_f (mm/mm)	Modulus @ 50% of S (MPa)	Modulus @ 90% of S (MPa)
10	50	230	Fresh	9	$S = 1.01$ $\sigma = 0.05$	$\varepsilon_f = 0.067$ $\sigma = 0.004$	$E_{50\%} = 23.4$ $\sigma = 1.4$	$E_{90\%} = 18.0$ $\sigma = 0.7$
10	50	250	Aged	2	$S = 1.07$ $\sigma = 0.05$	$\varepsilon_f = 0.045$ $\sigma = 0.002$	$E_{50\%} = 34.2$ $\sigma = 0.2$	$E_{90\%} = 28.4$ $\sigma = 0.1$
25	80	240	Fresh	3	$S = 0.77$ $\sigma = 0.02$	$\varepsilon_f = 0.073$ $\sigma = 0.007$	$E_{50\%} = 23.9$ $\sigma = 1.4$	$E_{90\%} = 16.1$ $\sigma = 0.8$
25	80	250	Aged	3	$S = 0.77$ $\sigma = 0.09$	$\varepsilon_f = 0.045$ $\sigma = 0.004$	$E_{50\%} = 28.9$ $\sigma = 5.9$	$E_{90\%} = 25.1$ $\sigma = 3.8$
25	80	240	Des-iccated	4	$S = 0.90$ $\sigma = 0.05$	$\varepsilon_f = 0.047$ $\sigma = 0.004$	$E_{50\%} = 30.6$ $\sigma = 2.1$	$E_{90\%} = 26.9$ $\sigma = 1.5$

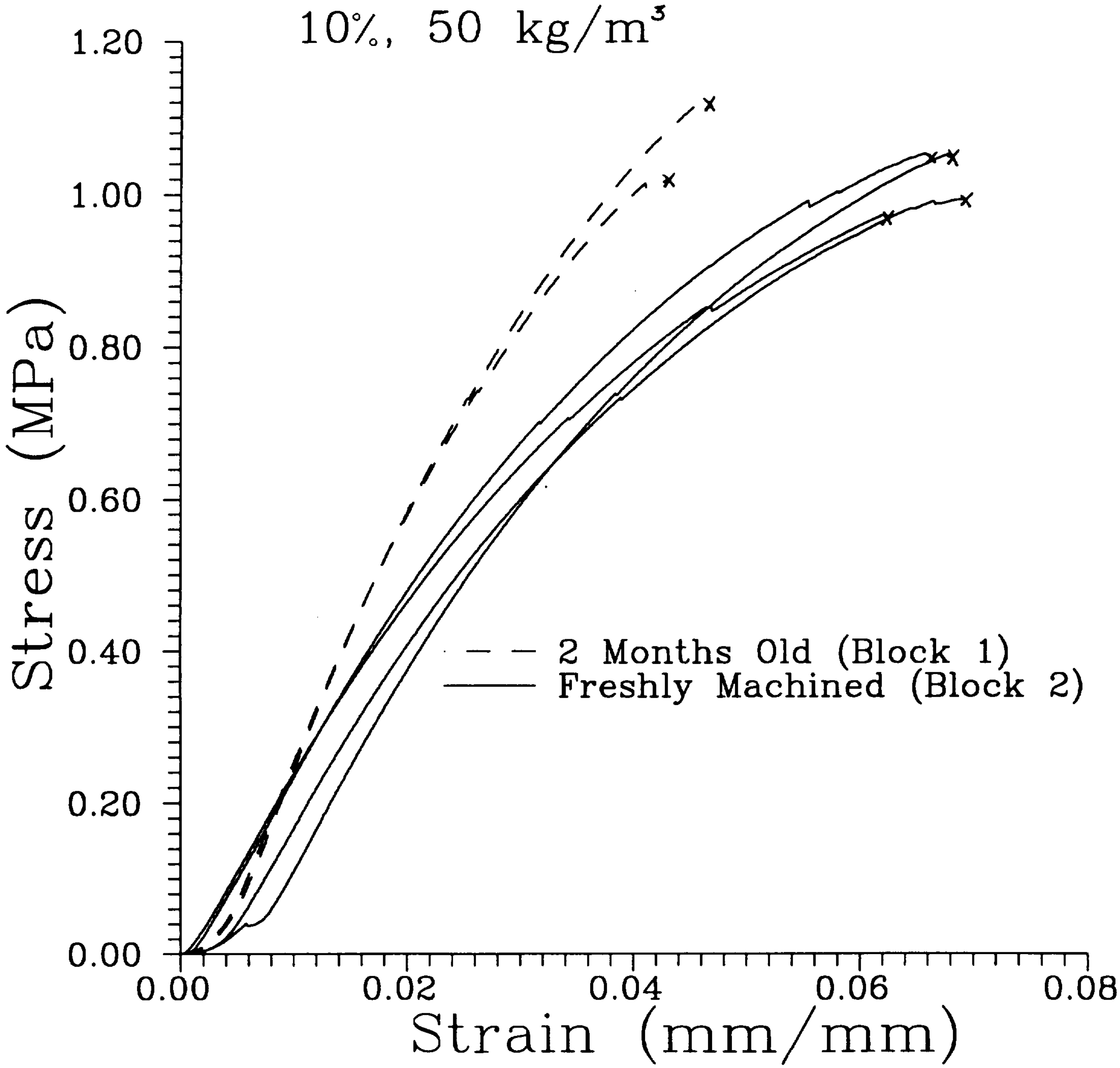

Figure 3.13
Comparison of Stress-Strain Curves for Freshly Machined Specimens and Specimens Aged in Air for 2 Months.
Target Density = 50 kg/m^3, Fiber Percentage = 10%.

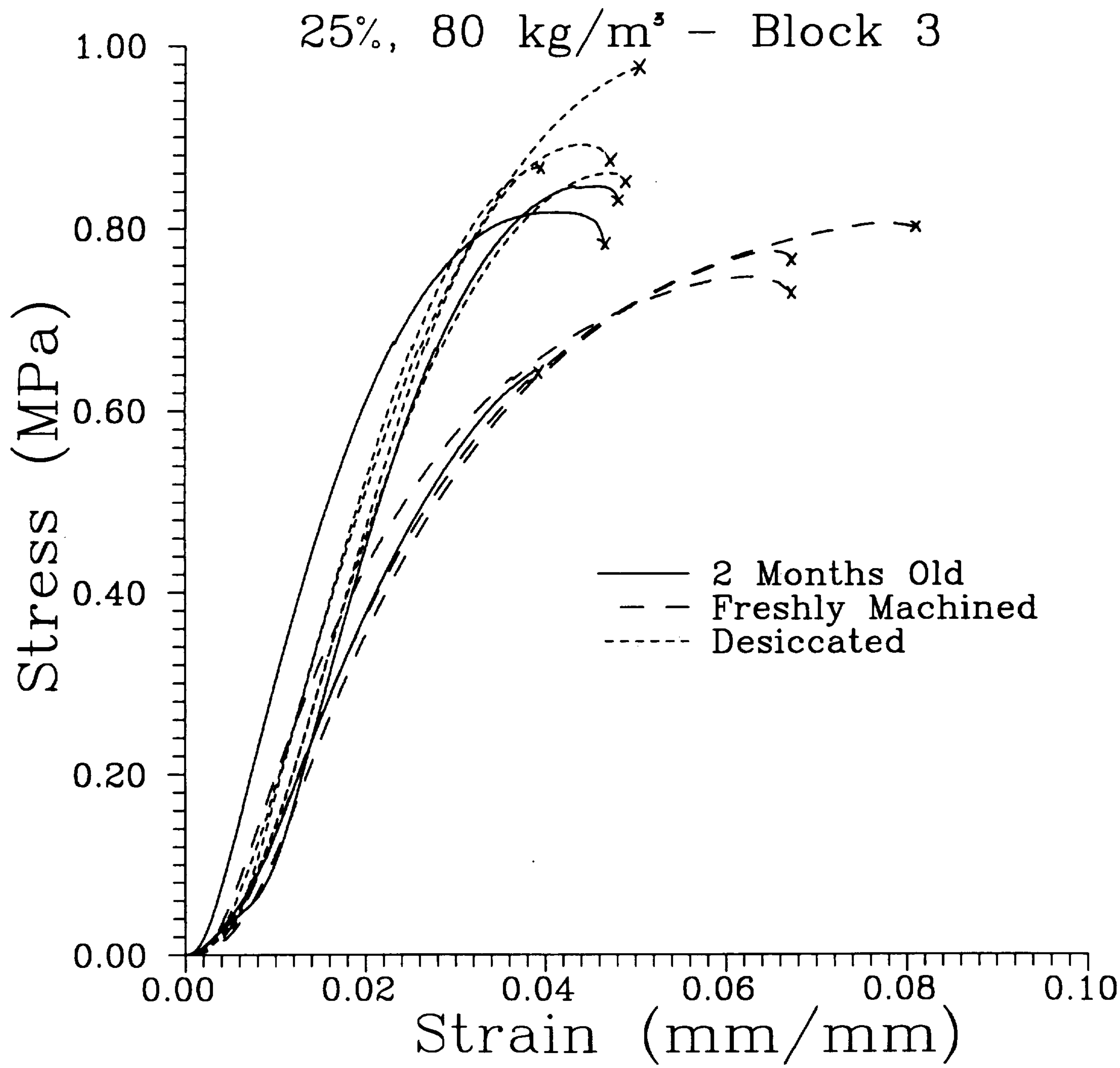

Figure 3.14

Comparison of Stress-Strain Curves for Freshly Machined Specimens, Specimens Aged in Air for 2 Months, and Specimens Aged in Air for Two Months and Desiccated for 10 Days. Target Density = 80 kg/m^3, Fiber Percentage = 25%.

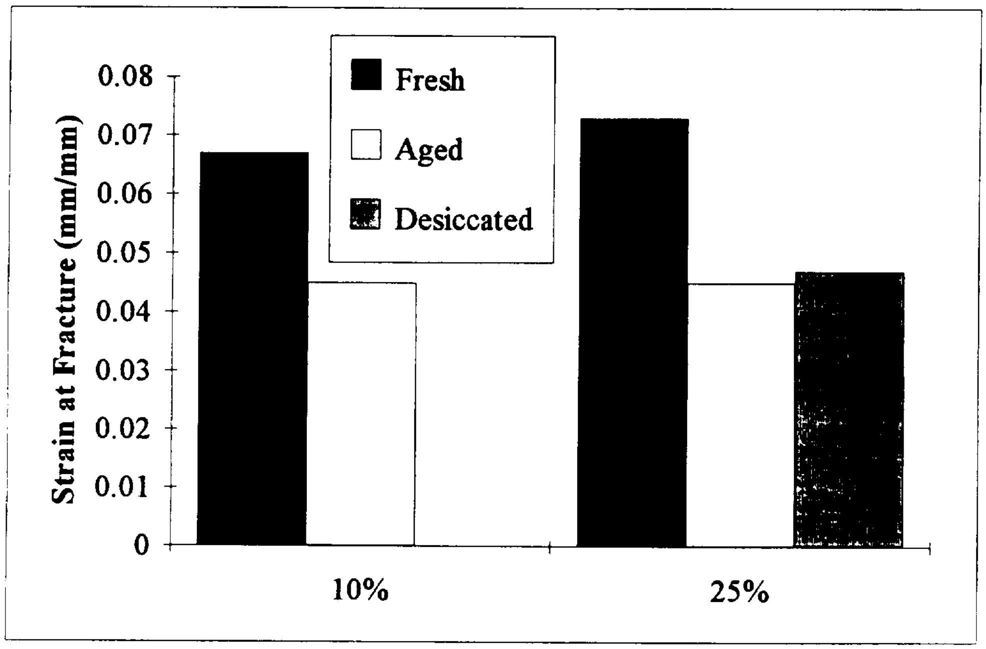

Figure 3.15
Comparison of Strains at Fracture for Fresh, Aged, and Desiccated Specimens

3.3 Correlation of Compressive Strength and Hardness

The relationship between hardness, H, and compressive strength, S, is plotted in Figure 3.16. It is worthwhile to relate hardness to compressive strength, since the former is a measure of the resistance to the local compressive strength in the neighborhood of the indenter, but is less destructive than traditional compression tests. Considering the wide range of processing parameters investigated, there is reasonably good correlation between the compressive strength and the hardness.

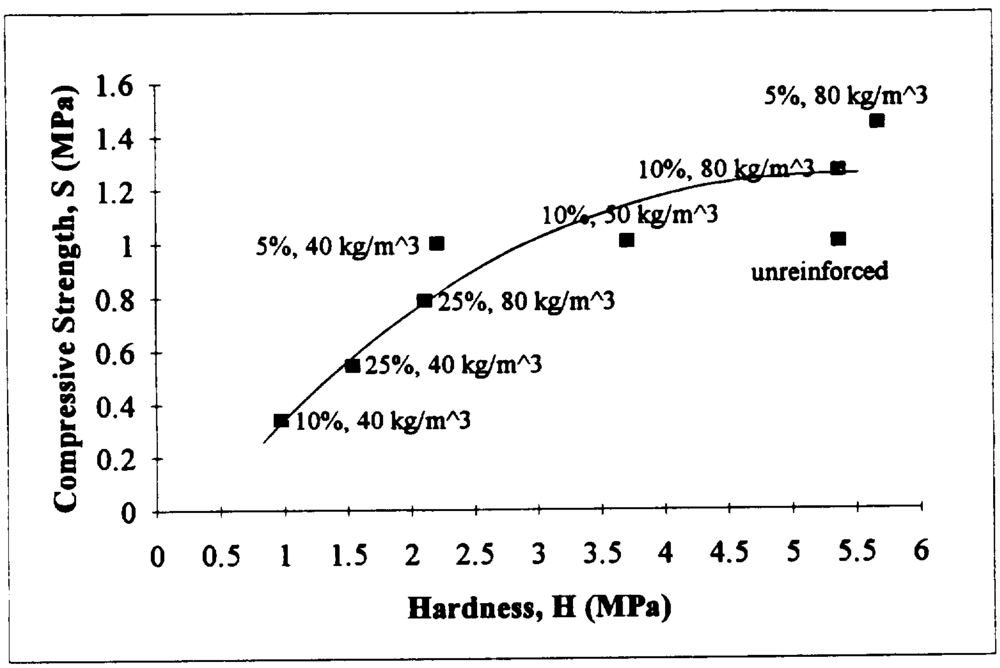

Figure 3.16
Compressive Strength vs. Hardness

3.4 Tensile Tests

The tensile tests proved to be very challenging due to practical difficulties machining and handling specimens with such small cross-sectional areas within the gage length. In addition, there was only a limited amount of bulk aerogel material to work with of sufficient size and quality. As a result, only three of ten specimens machined remained in-tack up to the point of load application. The majority of specimens broke in the process of mounting them into the test fixture. Two of the specimens tested consisted of 25% fibers, and had a target density of 80 kg/m^3; one specimen consisted of 5% fibers and had a target density of 80 kg/m^3. The results of the three experiments are summarized in Table 3.5, and their stress-strain curves are provided in Figures 3.17 and 3.18.

The results show a significant discrepancy between the stress-strain responses of the two specimens manufactured with 25% fibers and a target density of 80 kg/m^3. Their initial slopes (i.e., Young's moduli) agree well, with values approximately equal to 13 MPa, but then diverge at a strain of approximately 0.005 mm/mm. Furthermore, the ultimate tensile strength of the weaker specimen is 44% less than that of the stronger specimen. The Young's modulus of the 5%, 80 kg/m^3 specimen is significantly larger, with a value of approximately 23 MPa. However, since the ultimate tensile strength of this specimen falls between that of the previous two specimens, no conclusions about the relative strengths of the two types of material can be made on the basis of these tests.

Table 3.5
Summary of Tensile Results

Fiber Percentage (%)	Target Density (kg/m^3)	Final Density (kg/m^3)	Block #	Ultimate Tensile Strength (MPa)	Strain at Fracture, ε_f (mm/mm)	Young's Modulus (MPa)
5	80	320	38	0.25	0.012	23.2
25	80	240	33	0.32	0.017	13.5*
25	80	240	34	0.18	0.016	13.1*

* Initial Young's Modulus

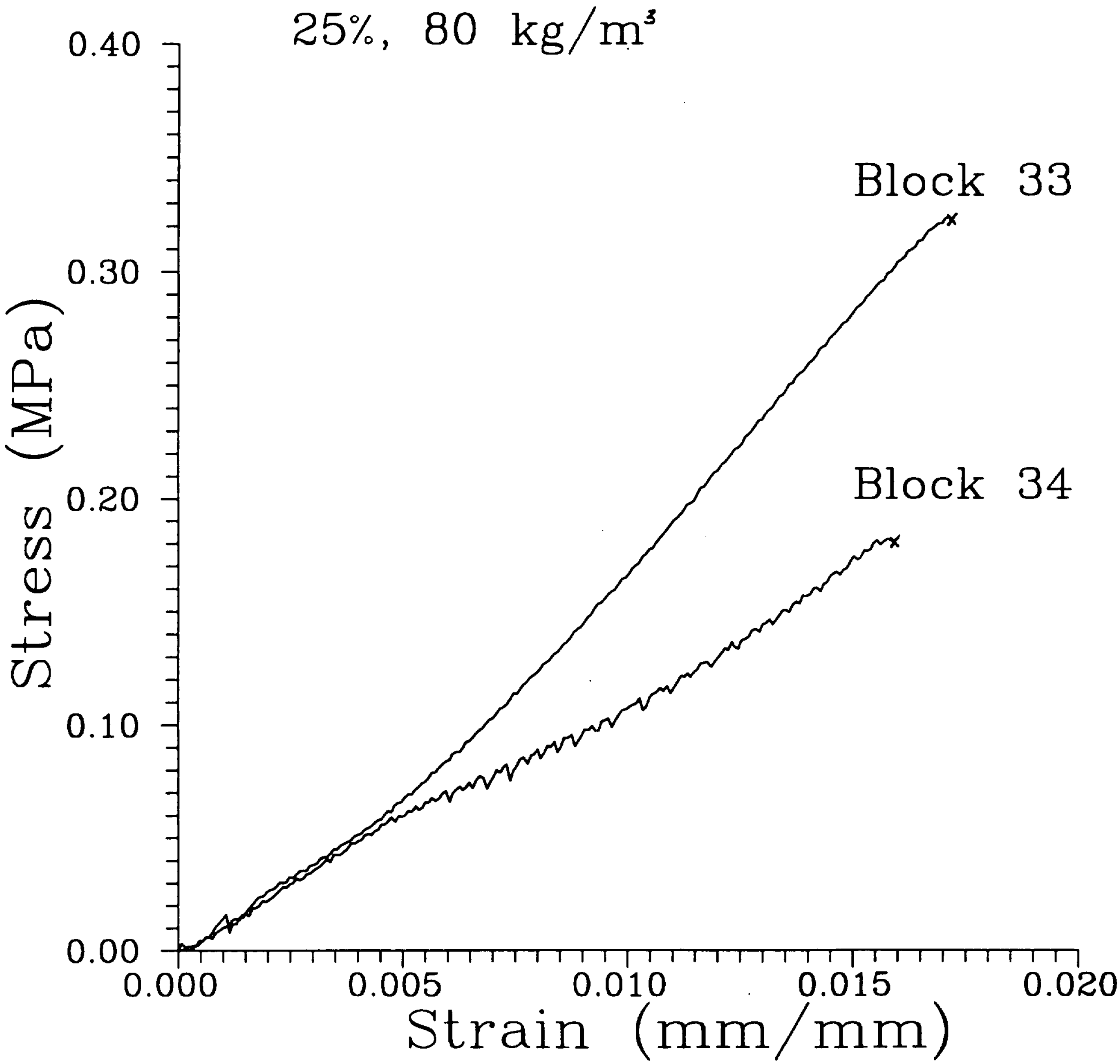

Figure 3.17

Stress-Strain Curve for Tensile Specimens.

Target Density = 80 kg/m^3, Fiber Percentage = 25%

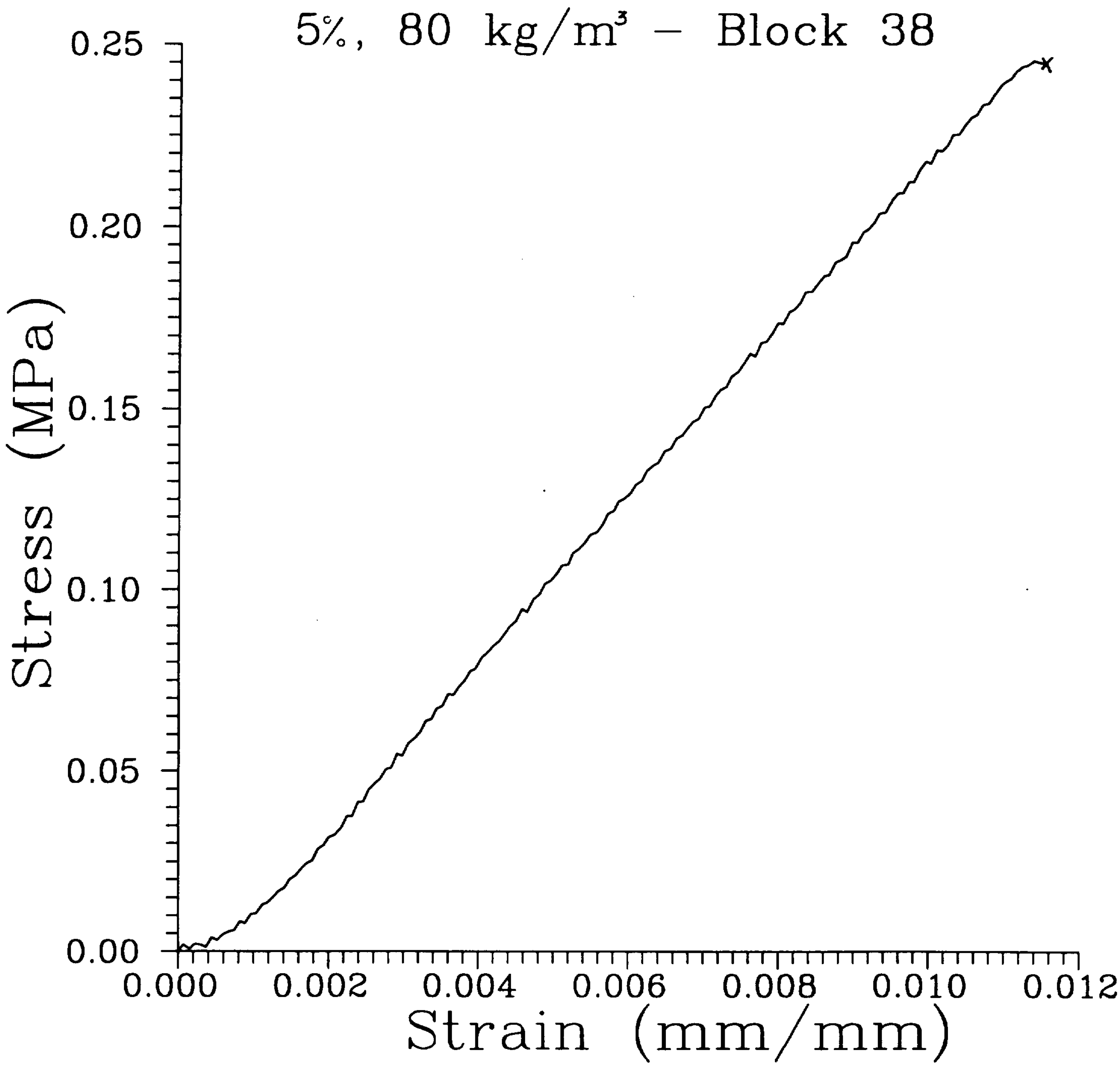

Figure 3.18

Stress-Strain Curve for Tensile Specimen.

Target Density = 80 kg/m^3, Fiber Percentage = 5%

3.5 Shear Tests

Shear tests were attempted on six Iosipescu specimens. Five specimens had a target density of 80 kg/m^3 and 10% fibers, and one specimen had a target density of 80 kg/m^3 and 25% fibers. Tests were limited to these six specimens because of insufficient quality and quantity of material to machine a larger amount and variety of specimens. All but one specimen failed in tension rather than in shear. The exception to this trend failed under mixed-mode conditions. These findings are consistent with brittle material behavior. Brittle materials are stronger in shear than they are in tension, and thus preferentially fail by tension. As a result, only the lower bound of shear strength, equal to approximately 0.1 MPa for both types of material, could be obtained from these tests. Diagrams depicting Iosipescu specimens failing by pure shear and by tension are provided in Figure 3.19.

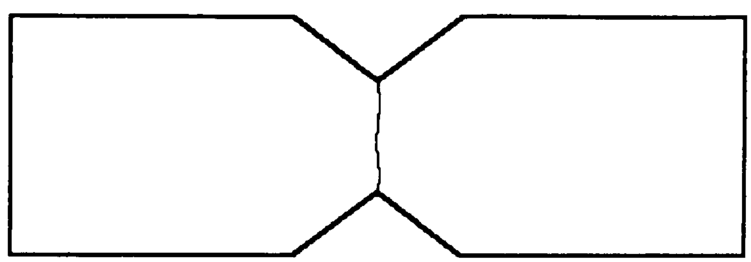

(a)

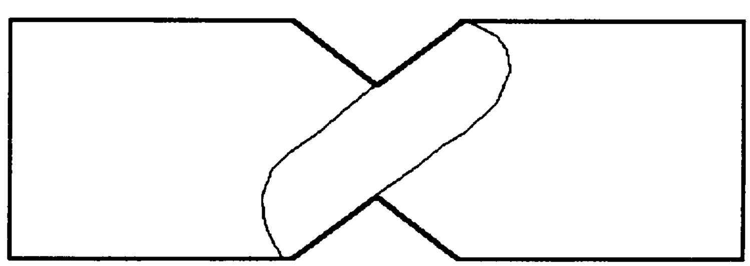

(b)

Figure 3.19
Diagrams of a) an Iosipescu specimen failing by pure shear, and b) and Iosipescu specimen failing by tension.

4. SUMMARY & CONCLUSIONS

Mechanical tests of unreinforced and fiber-reinforced silica aerogels have yielded several interesting findings. Most significantly, the aerogels generally exhibited lower compressive strengths, increased softness, and decreased elastic moduli when reinforced with fibers. This is partly due to the larger final densities observed for unreinforced and slightly reinforced aerogels relative to highly reinforced aerogels. During the supercritical drying process, the fibers support the matrix, reducing the amount of overall shrinkage. Without the fibers, or with smaller numbers of fibers, the matrix more readily shrinks resulting in a larger density. However, it is likely that density is not the only factor contributing to the lower strengths observed in reinforced aerogels. It is also possible that the fiber arrangement and the fiber-matrix bonding play a role in weakening the composite. The fibers do, nevertheless, offer at least one benefit: they seem to improve the aerogels' toughness.

The results of various qualitative tests indicate that the aerogels are: 1) sensitive to moisture absorption from handling and storage, 2) exhibit birefringence, and 3) may exhibit stress relaxation (or creep) under certain conditions. In addition, good correlation between hardness and compressive strength was found over a wide range of processing parameters. Finally, initial tensile and shear test results suggest that the aerogels have low tensile strengths relative to their compressive and shear strengths. This behavior is typical of brittle materials.

Future experiments should focus on detailed room temperature tensile tests, as well as on compression, hardness, and tensile tests at cryogenic temperatures. Cryogenic compression tests have been made in a gaseous helium environment by Arvidson and Scull [1986]. Modification of their technique may be applicable to other mecahnical testing on reinforced aerogels, as well. Moreover, before the mechanical response of reinforced aerogels can be fully understood, more tests of unreinforced aerogels are necessary. Unreinforced aerogels are of particular use because their birefringent nature allows for visual determination of stress fields during mechanical testing. In addition, the creep response of aerogels should be investigated in detail by the use of traditional techniques along with acoustic emission tests to record the sound of the composites cracking. Also of interest would be scanning electron microscope visualization of aerogel microstructure, cracks, and fiber pullout. Finally, fatigue, bending and load cycling tests should be initiated.

REFERENCES

Arvidson, J. M., and L. L. Scull, "Compressive Properties of Silica Aerogel at 295, 76, and 20 K," Advances in Cryogenic Engineering Materials, R. P. Reed and A. F. Clark (eds.), vol. 32, National Bureau of Standards, Boulder Colorado, 1986.

Cross, J., R. Goswin, R. Gerlach, and J. Fricke, "Mechanical Properties of SiO_2 - Aerogels," *Revue de Physique Appliquee, C4-4*, 24, 185-190, 1989.

Fricke, J., "Aerogels and their Applications," *Journal of Non-Crystalline Solids*, 147&148, 356-362, 1992.

Gronauer, M., A. Kadur, and J. Fricke, "Mechanical and Acoustic Properties of Silica Aerogel," Aerogels, J. Fricke (ed.), Springer, Berlin, 1986.

Gross, J. and J. Fricke, "Ultrasonic Velocity Measurements in Silica, Carbon, and Organic Aerogels," *Journal of Non-Crystalline Solids*, 145, 217-222, 1992.

Gross, J., J. Fricke, R. W. Pekala, and L. W. Hrubesh, "Elastic Nonlinearity of Aerogels," *Physical Review B*, 45(22), 12774-12777, 1992.

Iosipescu, N., "Photoelastic Investigations on an Accurate Procedure for the Pure Shear Testing of Materials," *Rev. de Mec. Appl.*, 1, 147-164, 1963.

Teichner, S. J., G. A. Nicolaon, M. A. Vicarini, and G. E. E. Gardes, "Inorganic Oxide Aerogels," *Advances in Colloid and Interface Science*, 5, 245-273, 1976.

Woignier, T. and J. Phalippou, "Scaling Law Variation of the Mechanical Properties of Silica Aerogels," *Revue de Physique Appliquee, C4-4*, 24, 179-184, 1989.

APPENDIX A
Specimen Dimensions

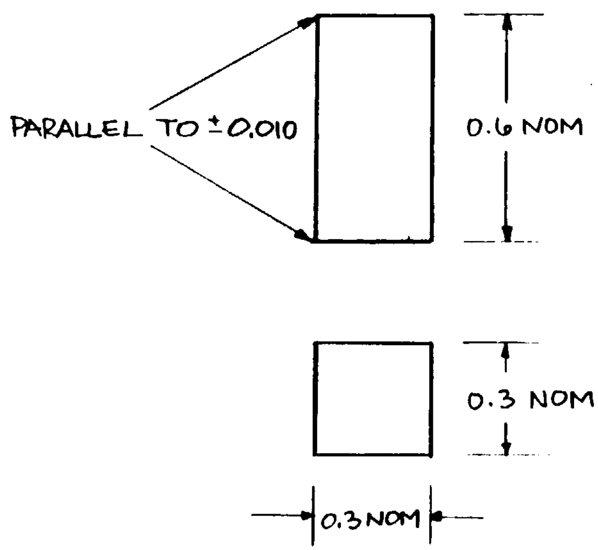

NOTES:
1) ALL DIMENSIONS IN INCHES

DRAWN BY: KELLY PARMENTER
SCALE: 2 X

COMPRESSION SPECIMEN

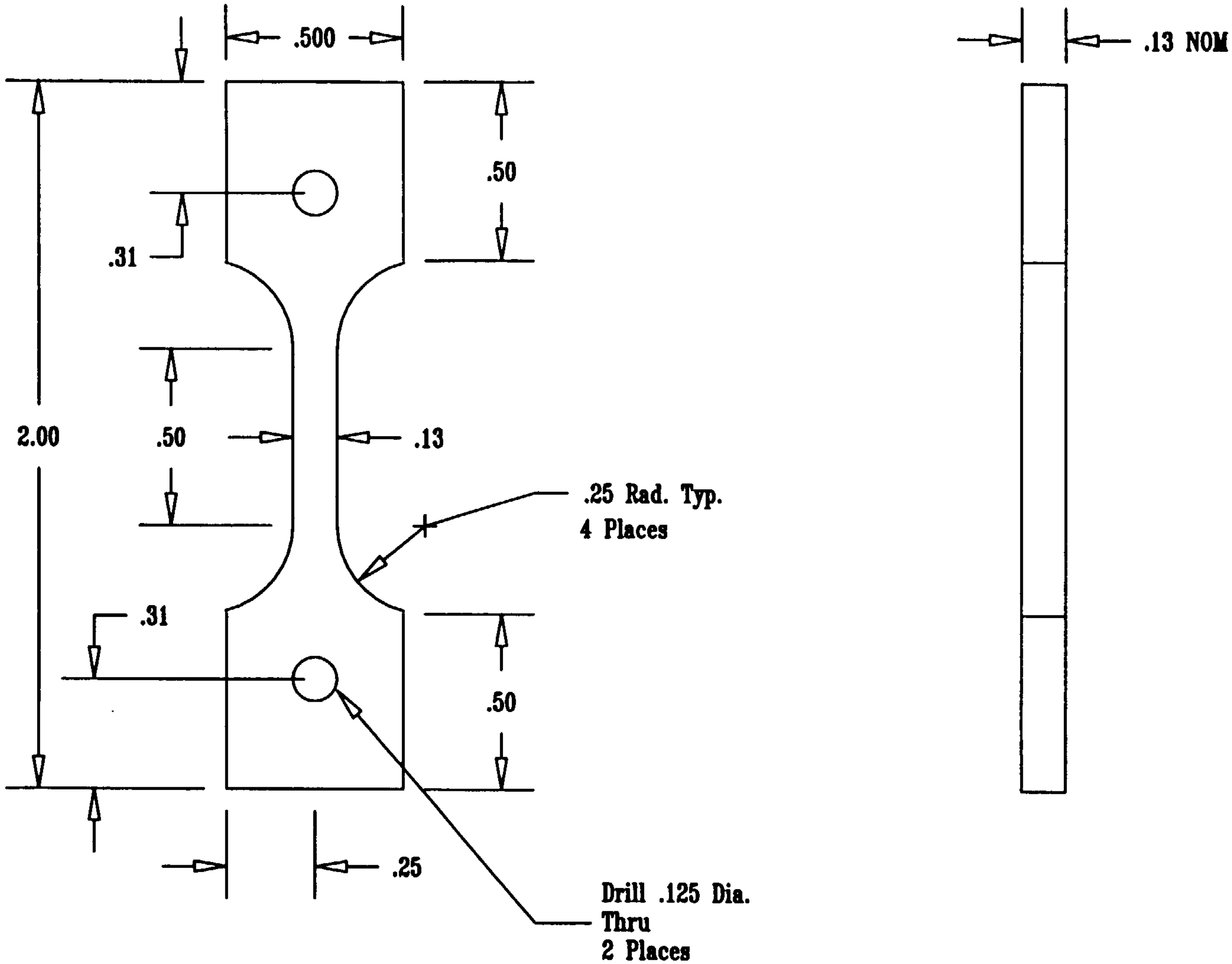

NOTES:
1. Material:
2. Tolerances: +/- .010
3. Quantity:
4. Account:

Drawn: K.A.Fields 6.9.95	Pin-Loaded Tensile Specimen
Scale: 2X	SA-1010

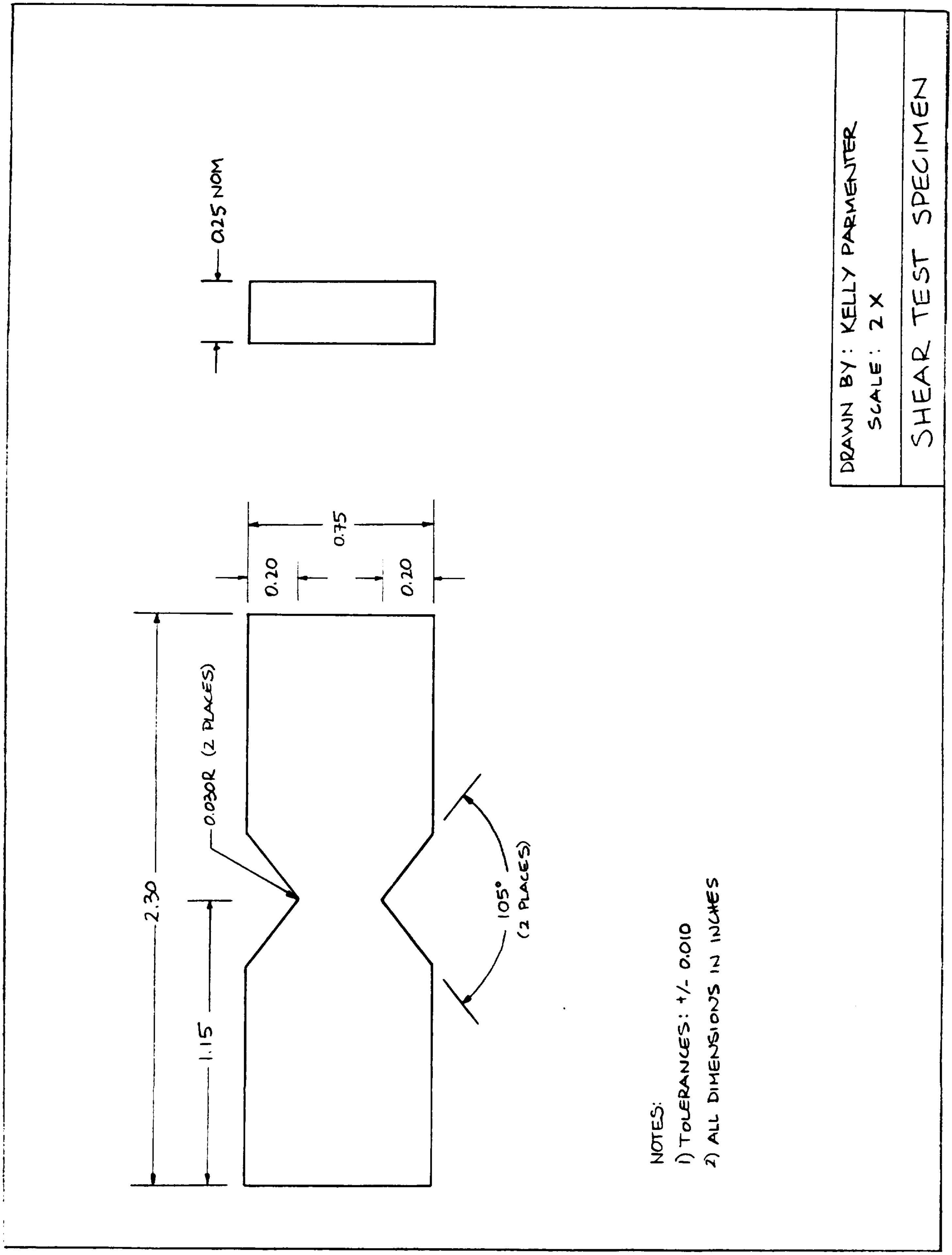
DRAWN BY: KELLY PARMENTER
SCALE: 2 X
SHEAR TEST SPECIMEN
0.25 NOM
0.75
0.20
0.20
2.30
1.15
0.030R (2 PLACES)
105°
(2 PLACES)
NOTES:
1) TOLERANCES: +/- 0.010
2) ALL DIMENSIONS IN INCHES

APPENDIX B

Hardness Results

Hardness

Block #4, Unreinforced

3/21/95

Avg. Density = 240 kg/m^3

Depth (mm)	Max. Load (N)	Hardness (MPa)
0.042	14.22	5.67
0.041	14.24	5.78
0.046	14.20	5.15
0.054	14.21	4.38
0.051	14.20	4.68
0.043	14.25	5.50
0.045	14.22	5.25
0.042	14.23	5.63
0.048	14.22	4.94
0.041	14.22	5.76
0.040	14.23	5.98
0.042	14.22	5.68
	Average	5.37
	Standard Deviation	0.47

Notes:

Ball Diameter = 19.05 mm

Hardness is based on depth at 2.02 N load

H = Max. Load/(pi * ball diam. * depth)

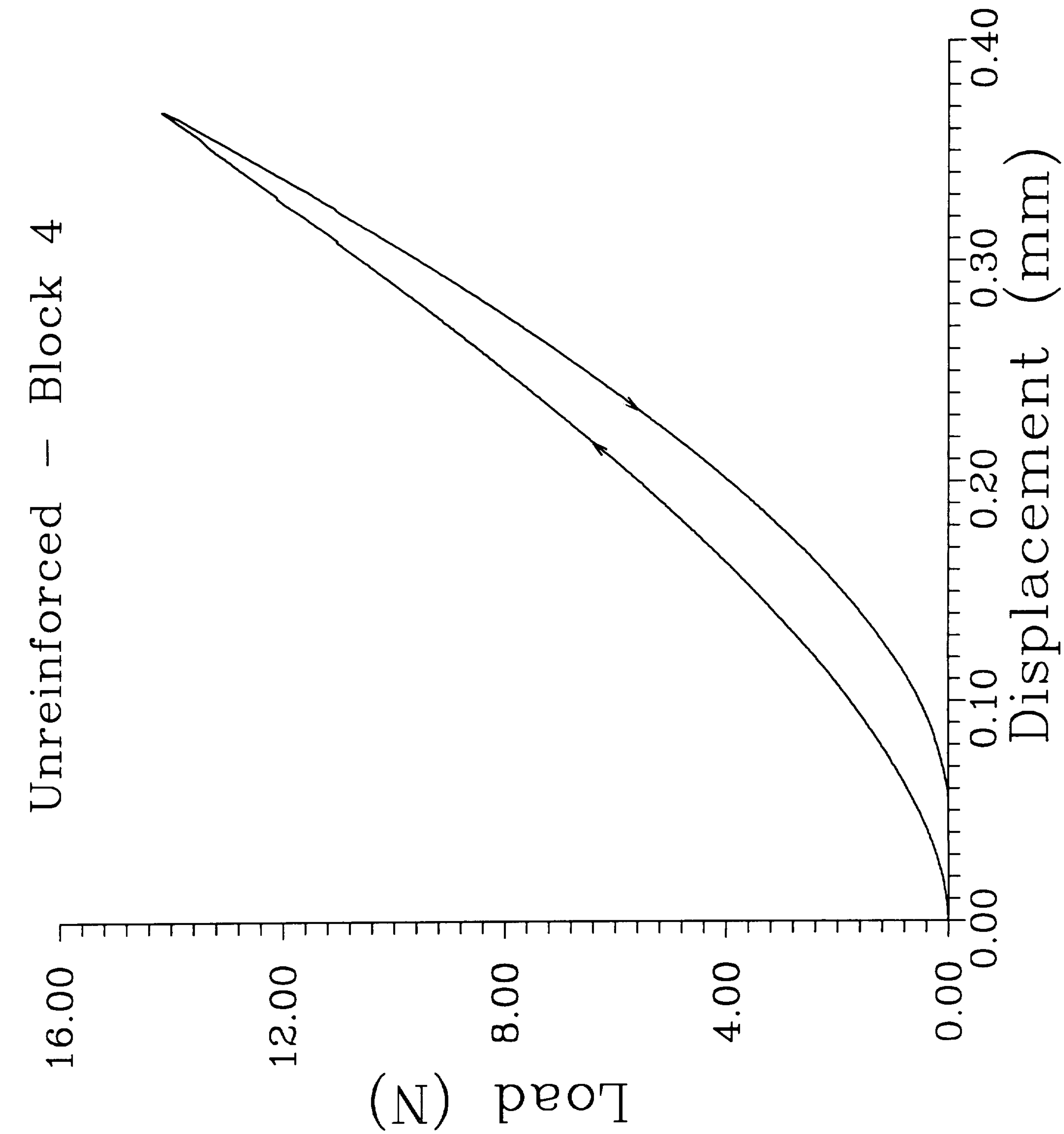
Unreinforced - Block 4
Load (N)
16.00
12.00
8.00
4.00
0.00
Displacement (mm)
0.00
0.10
0.20
0.30
0.40

Hardness

Block #12, 5% Fibers, Target Density = 40 kg/m^3

3/22/95

Avg. Density = 260 kg/m^3

Depth (mm)	Max. Load (N)	Hardness (MPa)
0.138	14.02	1.70
0.090	14.23	2.64
0.099	14.24	2.39
0.124	14.22	1.91
0.107	14.21	2.21
0.119	14.21	1.99
0.106	14.23	2.24
0.096	14.23	2.47
0.103	14.22	2.30
0.110	14.20	2.15
	Average	2.20
	Standard Deviation	0.26

Notes:
Ball Diameter = 19.05 mm
Hardness is based on depth at 2.02 N load
H = Max. Load/(pi * ball diam. * depth)

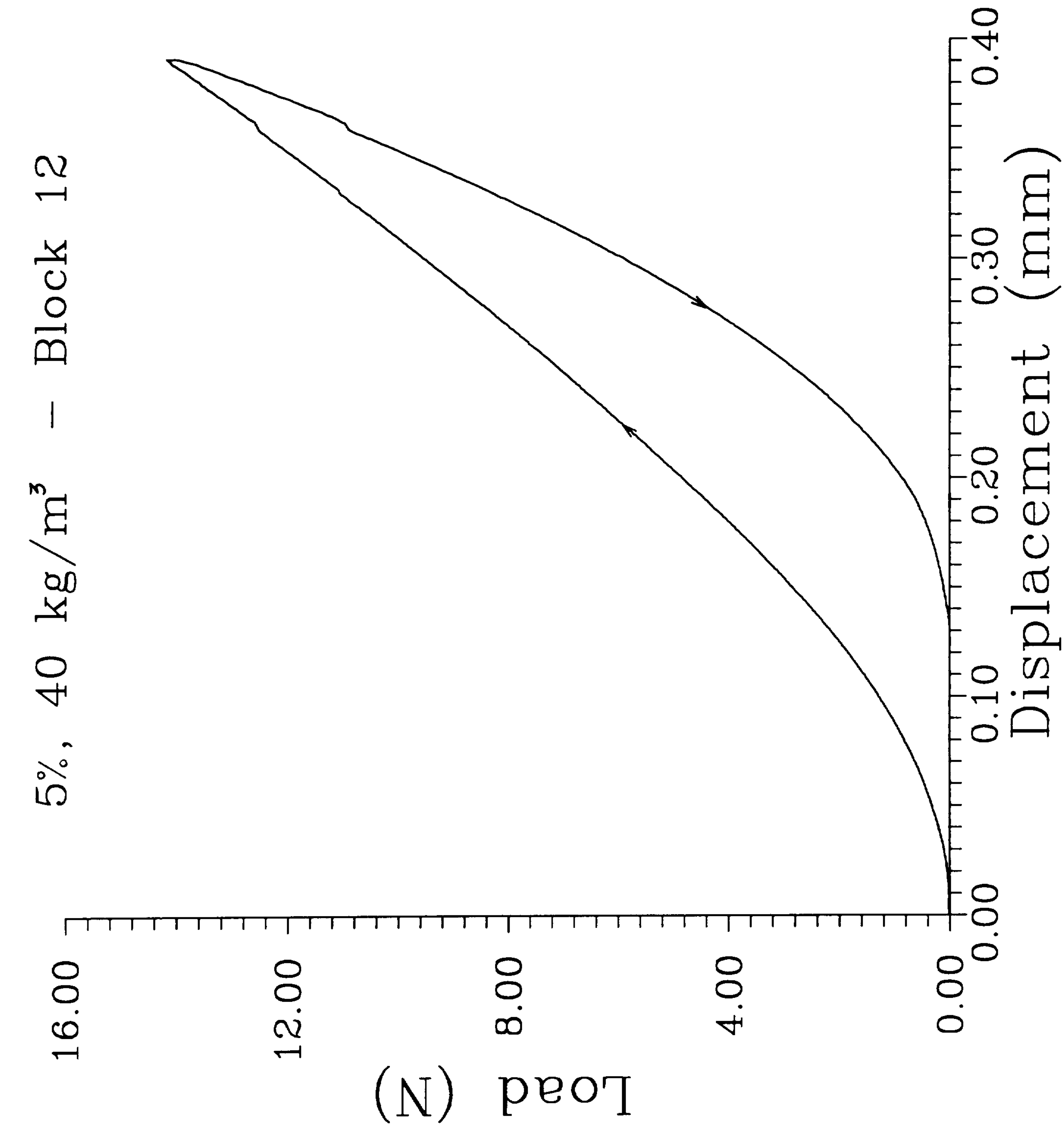

5%, 40 kg/m³ – Block 12
Load (N)
16.00
12.00
8.00
4.00
0.00
Displacement (mm)
0.00
0.10
0.20
0.30
0.40

Hardness

Block #35, 5% Fibers, Target Density = 80 kg/m^3

5/22/95

Avg. Density = 320 kg/m^3

Depth (mm)	Max. Load (N)	Hardness (MPa)
0.052	14.25	4.55
0.058	14.25	4.09
0.047	14.27	5.05
0.028	14.25	8.51
0.030	14.26	7.91
0.061	14.27	3.90
	Average	5.67
	Standard Deviation	1.84

Notes:
Ball Diameter = 19.05 mm
Hardness is based on depth at 2.02 N load
H = Max. Load/(pi * ball diam. * depth)

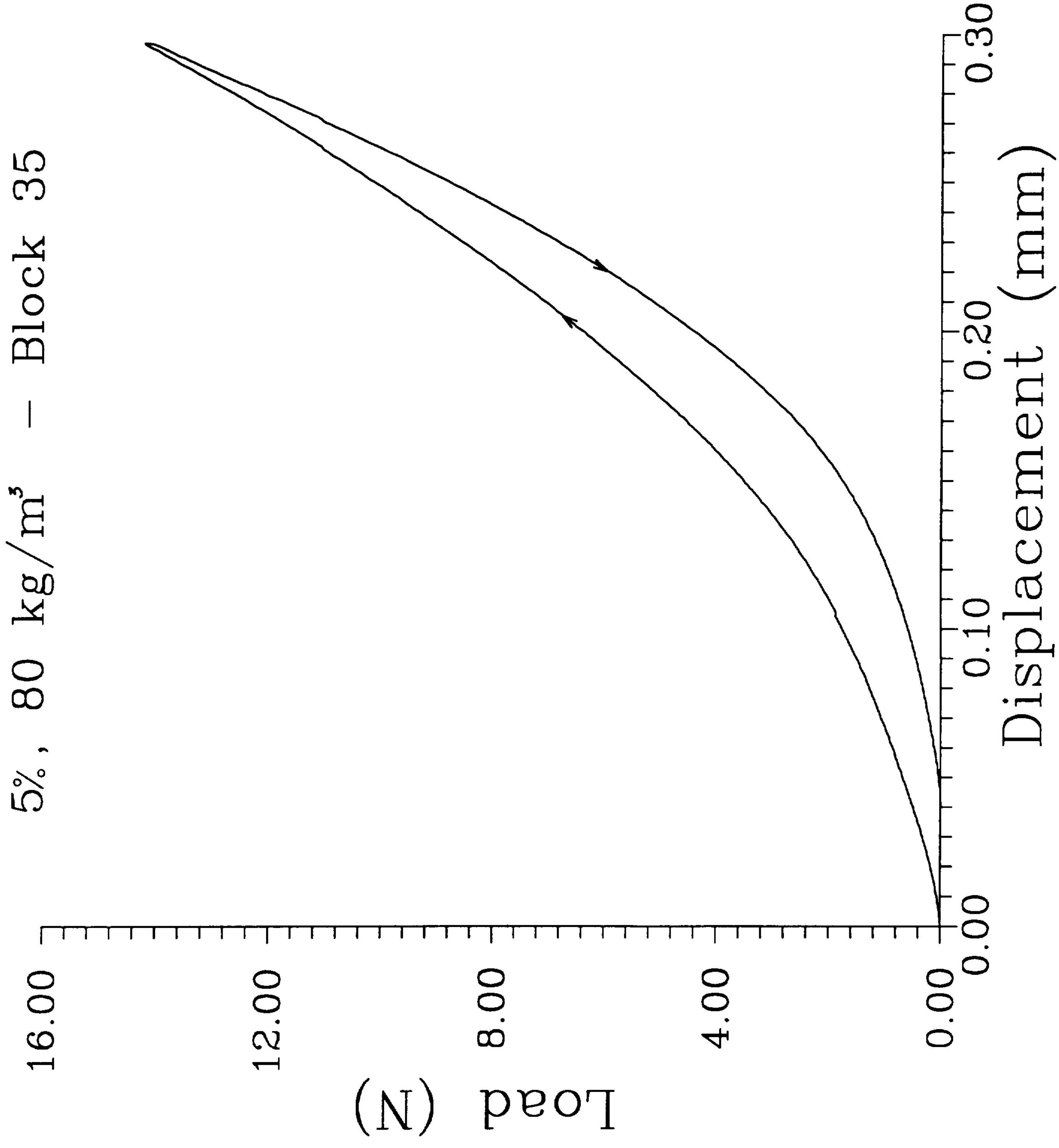
5%, 80 kg/m³ — Block 35
Load (N)
Displacement (mm)
0.00
4.00
8.00
12.00
16.00
0.00
0.10
0.20
0.30

Hardness

Block #14, 10% Fibers, Target Density = 40 kg/m^3

3/23/95

Avg. Density = 190 kg/m^3

Depth (mm)	Max. Load (N)	Hardness (MPa)
0.174	10.12	0.97
0.187	10.13	0.91
0.176	10.14	0.96
0.173	10.14	0.98
0.185	10.15	0.92
0.163	10.15	1.04
0.167	10.13	1.01
	Average	0.97
	Standard Deviation	0.04

Notes:

Ball Diameter = 19.05 mm

Hardness is based on depth at 2.02 N load

H = Max. Load/(pi * ball diam. * depth)

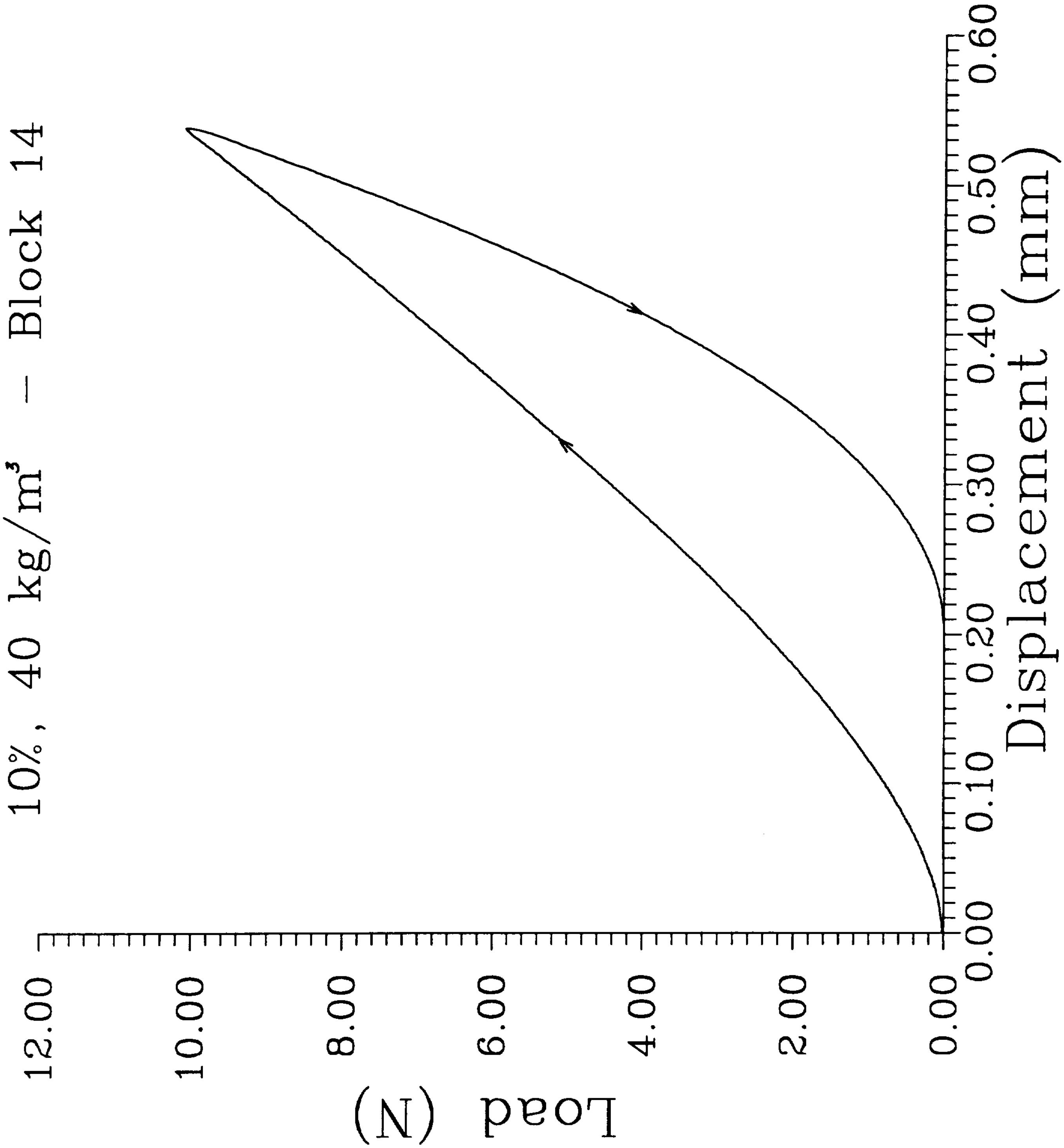
10%, 40 kg/m³ — Block 14
Load (N)
Displacement (mm)
0.00
2.00
4.00
6.00
8.00
10.00
12.00
0.00
0.10
0.20
0.30
0.40
0.50
0.60

Hardness

Block #2, 10% Fibers, Target Density = 50 kg/m^3

3/13/95

Avg. Density = 230 kg/m^3

Depth (mm)	Max. Load (N)	Hardness (MPa)
0.080	14.20	2.97
0.053	14.43	4.54
0.070	14.23	3.38
0.073	14.20	3.25
0.061	14.23	3.93
0.057	14.20	4.17
	Average	3.71
	Standard Deviation	0.55

Notes:
Ball Diameter = 19.05 mm
Hardness is based on depth at 2.02 N load
H = Max. Load/(pi * ball diam. * depth)

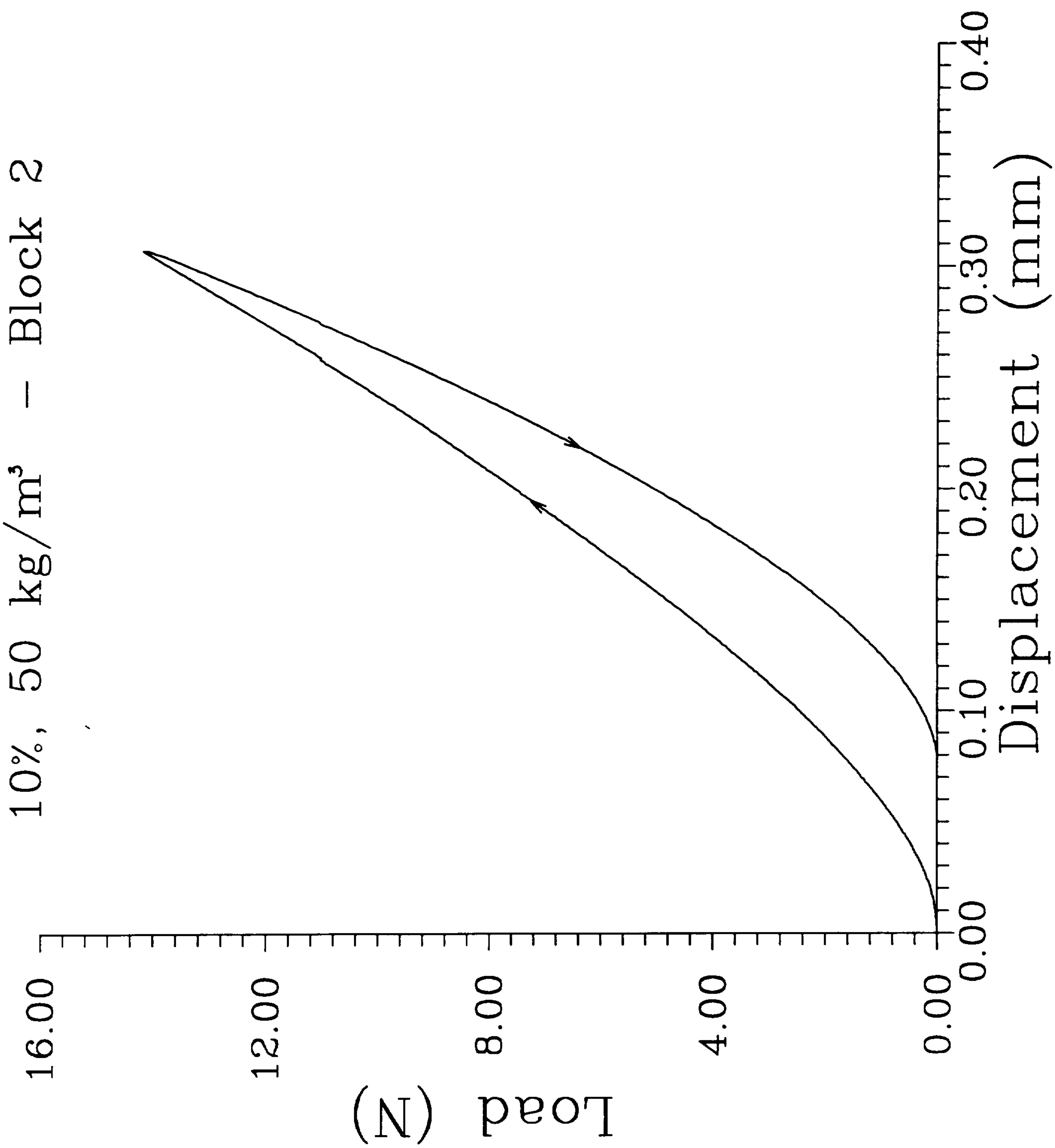

10%, 50 kg/m³ – Block 2
Load (N)
0.00
4.00
8.00
12.00
16.00
Displacement (mm)
0.00
0.10
0.20
0.30
0.40

Hardness

Blocks#16 & 17, 10% Fibers, Target Density = 80 kg/m^3

5/22/95

Avg. Density = 330 kg/m^3

Depth (mm)	Max. Load (N)	Hardness (MPa)	Block #
0.116	14.29	2.06	17
0.114	14.24	2.08	17
0.121	14.26	1.97	17
0.121	14.27	1.96	17
0.025	14.27	9.37	17
0.039	14.24	6.05	16
0.040	14.34	5.99	16
0.035	14.26	6.82	16
0.050	15.00	5.03	16
0.024	14.27	9.87	16
0.039	14.26	6.15	16
0.034	14.26	7.11	16
	Average	5.37	
	Standard Deviation	2.71	

Notes:
Ball Diameter = 19.05 mm
Hardness is based on depth at 2.02 N load
H = Max. Load/(pi * ball diam. * depth)

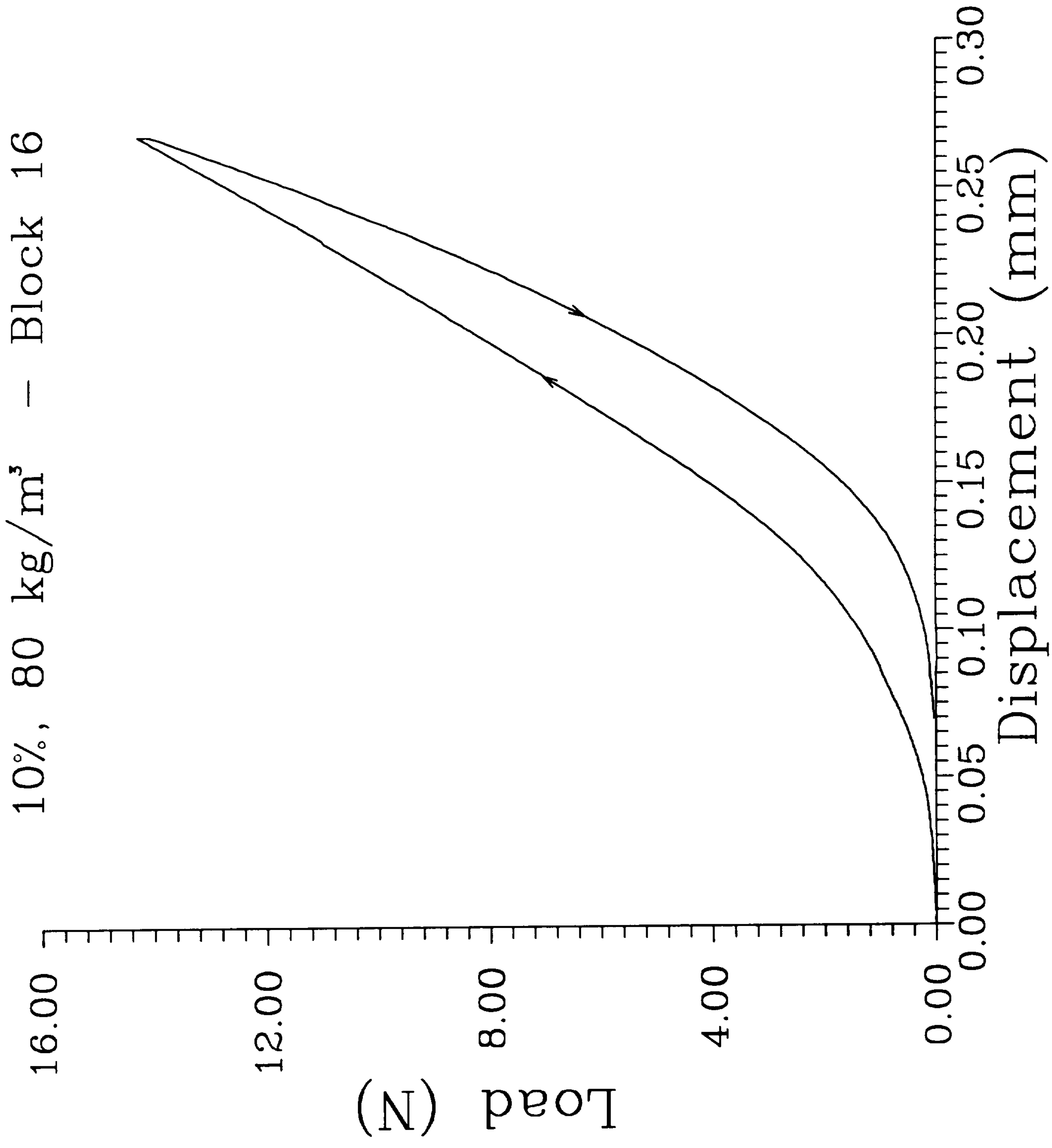
10%, 80 kg/m³ – Block 16
Displacement (mm)
Load (N)
0.00
0.05
0.10
0.15
0.20
0.25
0.30
0.00
4.00
8.00
12.00
16.00

Hardness

Blocks #5, 6 & 7, 25% Fibers, Target Density = 40 kg/m^3

5/18/95 - 5/19/95

Avg. Density = 190 kg/m^3

Depth (mm)	Max. Load (N)	Hardness (MPa)	Block #
0.165	14.19	1.44	5
0.164	14.19	1.45	5
0.152	14.33	1.58	5
0.148	14.20	1.61	5
0.155	14.20	1.53	6
0.155	14.23	1.53	6
0.157	14.20	1.51	6
0.159	14.19	1.50	6
0.159	14.20	1.49	6
0.146	14.21	1.63	7
0.153	14.21	1.56	7
0.147	14.20	1.62	7
0.150	14.19	1.58	7
0.158	14.20	1.51	7
	Average	1.54	
	Standard Deviation	0.06	

Notes:
Ball Diameter = 19.05 mm
Hardness is based on depth at 2.02 N load
H = Max. Load/(pi * ball diam. * depth)

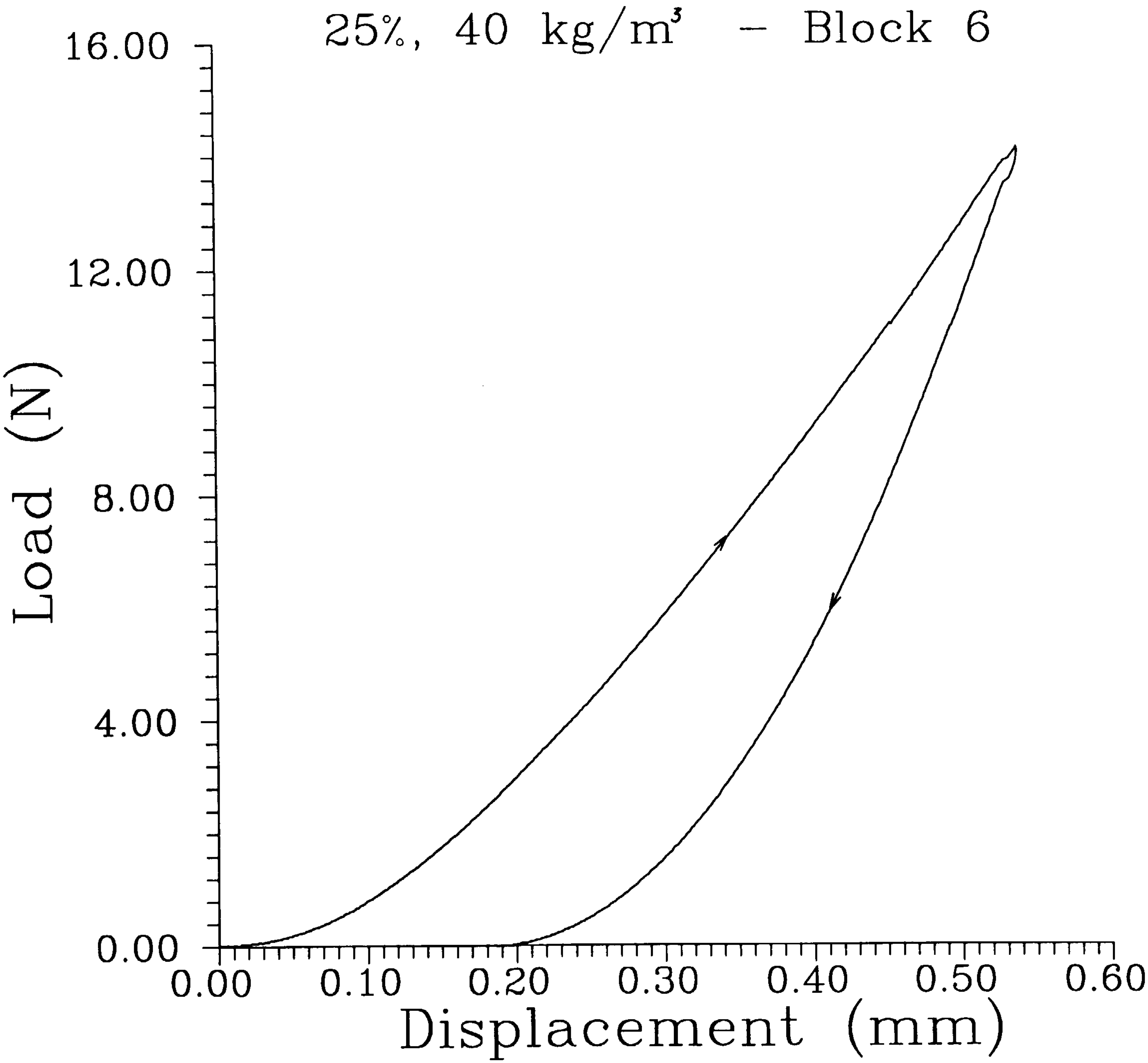

25%, 40 kg/m³ – Block 6
16.00
12.00
8.00
4.00
0.00
Load (N)
0.00
0.10
0.20
0.30
0.40
0.50
0.60
Displacement (mm)

Hardness

Block A, 25% Fibers, Target Density = 50 kg/m^3

Avg. Density = 200 kg/m^3

Depth (mm)	Max. Load (N)	Hardness (MPa)
0.133	14.19	1.78
0.101	14.18	2.34
0.113	14.19	2.10
0.115	14.20	2.07
0.104	14.21	2.29
0.112	14.21	2.13
0.118	14.18	2.00
0.107	14.21	2.22
0.105	14.20	2.26
0.099	14.20	2.39
0.109	14.19	2.17
0.128	13.99	1.83
0.150	14.25	1.59
0.119	14.23	2.00
0.122	14.23	1.95
0.104	14.21	2.28
0.103	14.22	2.31
0.120	14.19	1.98
0.158	14.20	1.50
0.118	14.23	2.01
0.117	14.24	2.03
0.130	14.18	1.83
0.142	14.20	1.68
0.135	14.19	1.75
	Average	**2.02**
	Standard Deviation	**0.24**

Notes:
Ball Diameter = 19.05 mm
Hardness is based on depth at 2.02 N load
H = Max. Load/(pi * ball diam. * depth)

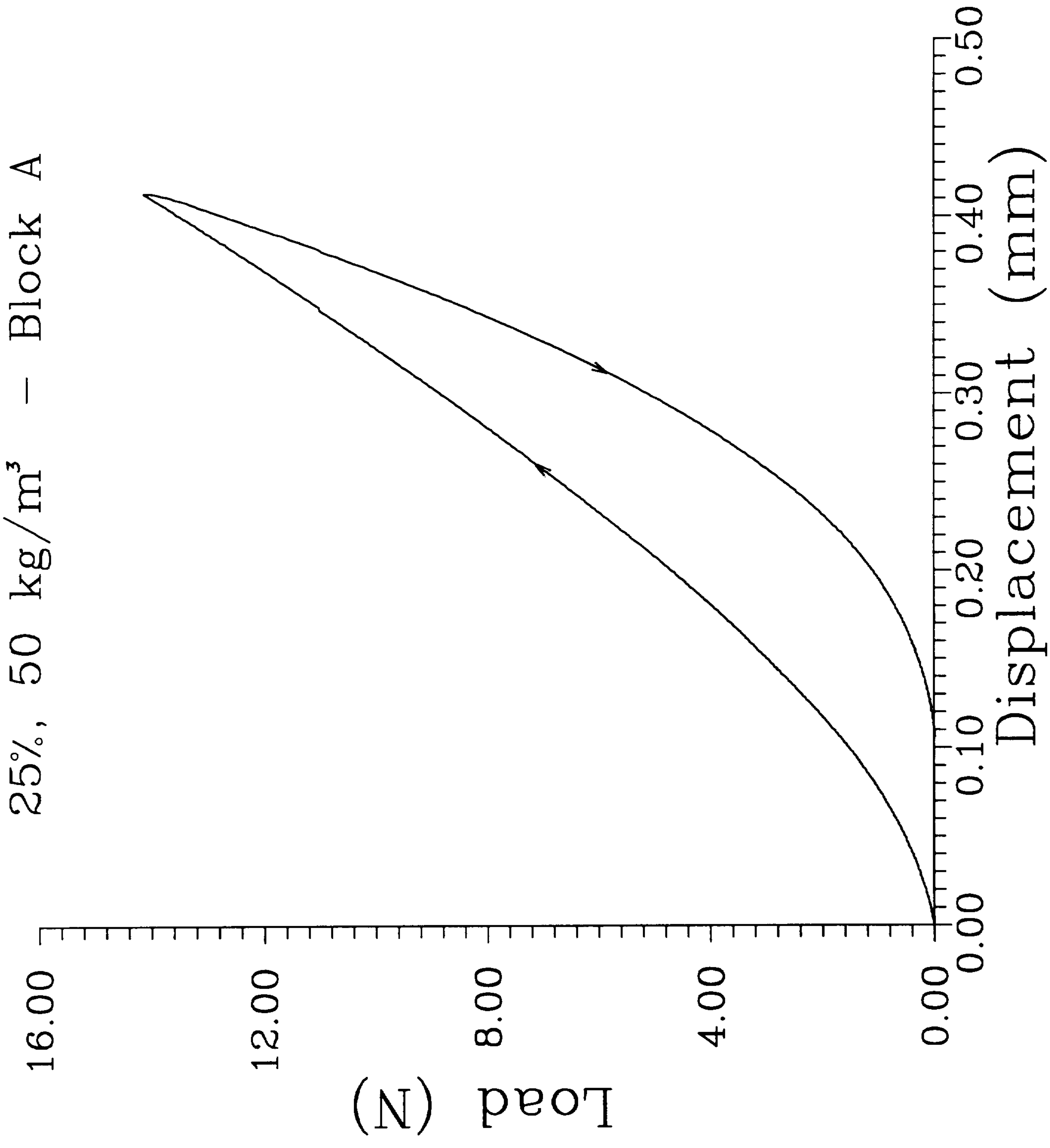
25%., 50 kg/m³ - Block A
Displacement (mm)
Load (N)
0.00
0.10
0.20
0.30
0.40
0.50
0.00
4.00
8.00
12.00
16.00

Hardness

Blocks #2 and 3, 25% Fibers, Target Density = 80 kg/m^3

3/9/95 & 3/13/95

Avg. Density = 240 kg/m^3

Depth (mm)	Max. Load (N)	Hardness (MPa)	Block #
0.130	14.19	1.82	2
0.115	14.21	2.07	2
0.143	14.61	1.71	2
0.111	14.01	2.10	2
0.110	14.24	2.17	2
0.115	14.18	2.05	3
0.110	14.21	2.16	3
0.100	14.22	2.37	3
0.097	14.22	2.46	3
0.107	14.20	2.21	3
	Average	2.11	
	Standard Deviation	0.21	

Notes:

Ball Diameter = 19.05 mm

Hardness is based on depth at 2.02 N load

H = Max. Load/(pi * ball diam. * depth)

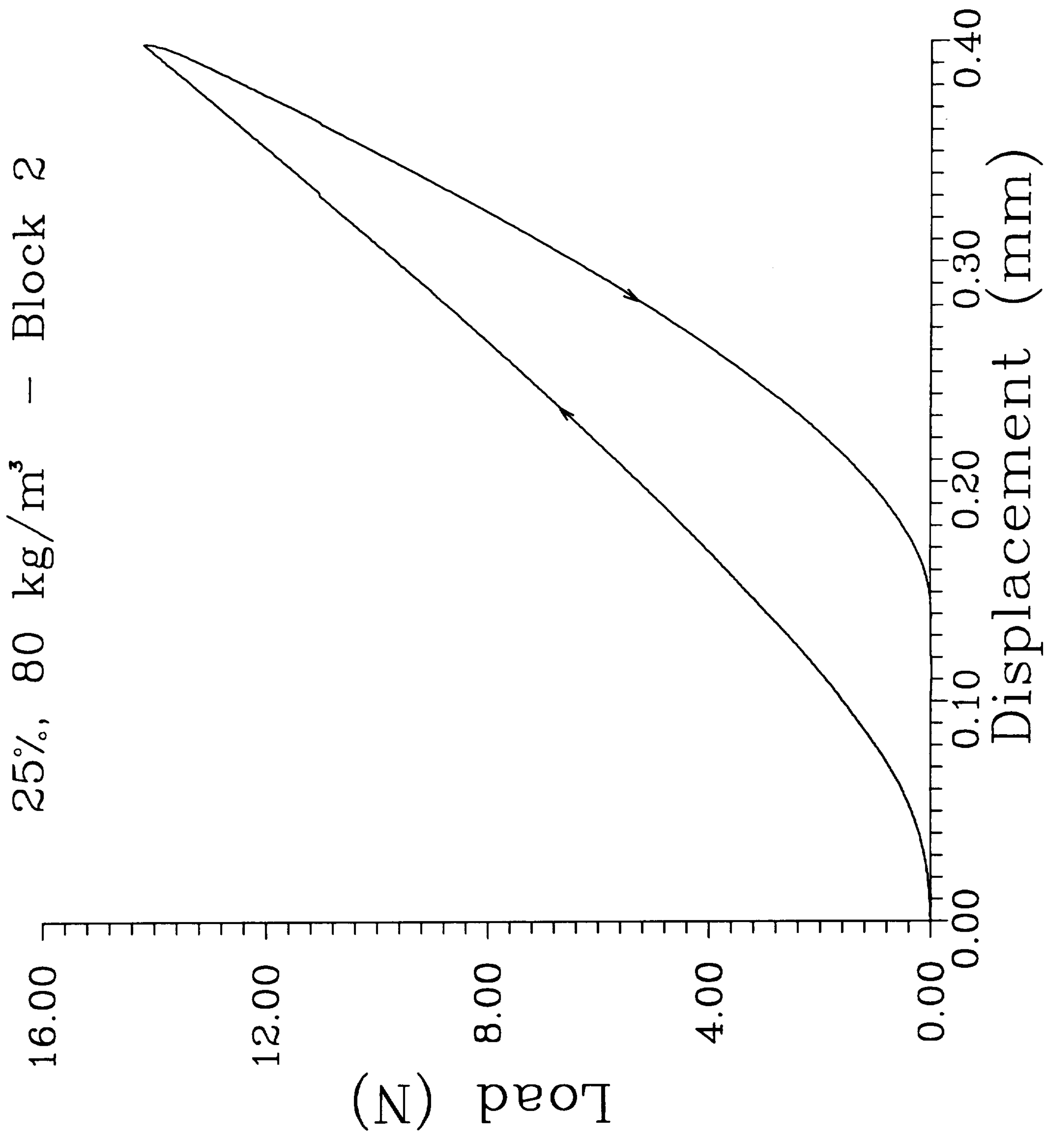
25%, 80 kg/m³ – Block 2
Load (N)
0.00
4.00
8.00
12.00
16.00
Displacement (mm)
0.00
0.10
0.20
0.30
0.40

APPENDIX C

Hardness Trend Data

Relaxation Test

Avg. Density = 250 kg/m^3

1/5/95

Max. Load (N)	Depth (mm)	Time	Hardness (MPa)	Load Drop (N)
14.28	0.032	0	7.40	0.00
14.30	0.038	1	6.31	0.51
14.30	0.045	10	5.27	1.19
14.27	0.053	30	4.49	1.67
14.26	0.055	60	4.36	2.04

Notes:
Ball Diameter = 19.05 mm
Hardness is based on depth at 2.02 N load
H = Max. Load/(pi * ball diam. * depth)

Hardness vs. Maximum Load Test

Avg. Density = 300 kg/m^3

1/4/95

Depth (mm)	Max. Load (N)	Hardness (MPa)
0.020	10.23	8.48
0.034	12.28	6.05
0.036	14.28	6.60
0.042	16.30	6.45
0.033	18.35	9.33
0.020	10.21	8.72
0.024	12.27	8.38
0.037	14.31	6.51
0.033	16.32	8.23
0.033	18.37	9.34

Notes:

Ball Diameter = 19.05 mm

Hardness is based on depth at 2.02 N load

H = Max. Load/(pi * ball diam. * depth)

Hardness vs. Crosshead Speed

Avg. Density = 210 kg/m^3

12/28/95

Max. Load (N)	Depth (mm)	Crosshead Speed (mm/min)	Hardness (MPa)
14.19	0.062	0.025	3.82
14.21	0.051	0.051	4.65
14.23	0.053	0.076	4.53
14.25	0.050	0.102	4.74
14.25	0.049	0.127	4.87
14.25	0.048	0.152	4.96
14.33	0.051	0.203	4.70

Notes:

Ball Diameter = 19.05 mm

Hardness is based on depth at 2.02 N load

H = Max. Load/(pi * ball diam. * depth)

APPENDIX D

Compression Results: Tests in Air

Summary of Compression Results

Unreinforced - 5th block

4/17/95 - Tests in Air

Avg Density = 240 kg/m^3

Expt. #	Compressive Strength (MPa)	Compressive Strain at Fracture (mm/mm)	E(50%) (MPa)	E(90%) (MPa)
1	0.97	0.093	16.7	13.4
2	1.01	0.113	18.5	14.9
3	1.04	0.093	14.1	14.1
Average	**1.01**	**0.100**	**16.4**	**14.1**
Std. Dev.	**0.03**	**0.009**	**1.8**	**0.6**

Notes:

1) The crosshead speed was 0.1016 mm/min
2) E(50%) is the secant modulus between the point A, of stress = 0.04 MPa, and point B, of stress = 50% of the compressive strength
3) E(90%) is the secant modulus between the point A, of stress = 0.04 MPa, and point C, of stress = 90% of the compressive strength
4) The specimens were unreinforced
5) Tests were done at room temperature in air, with no prior desiccation

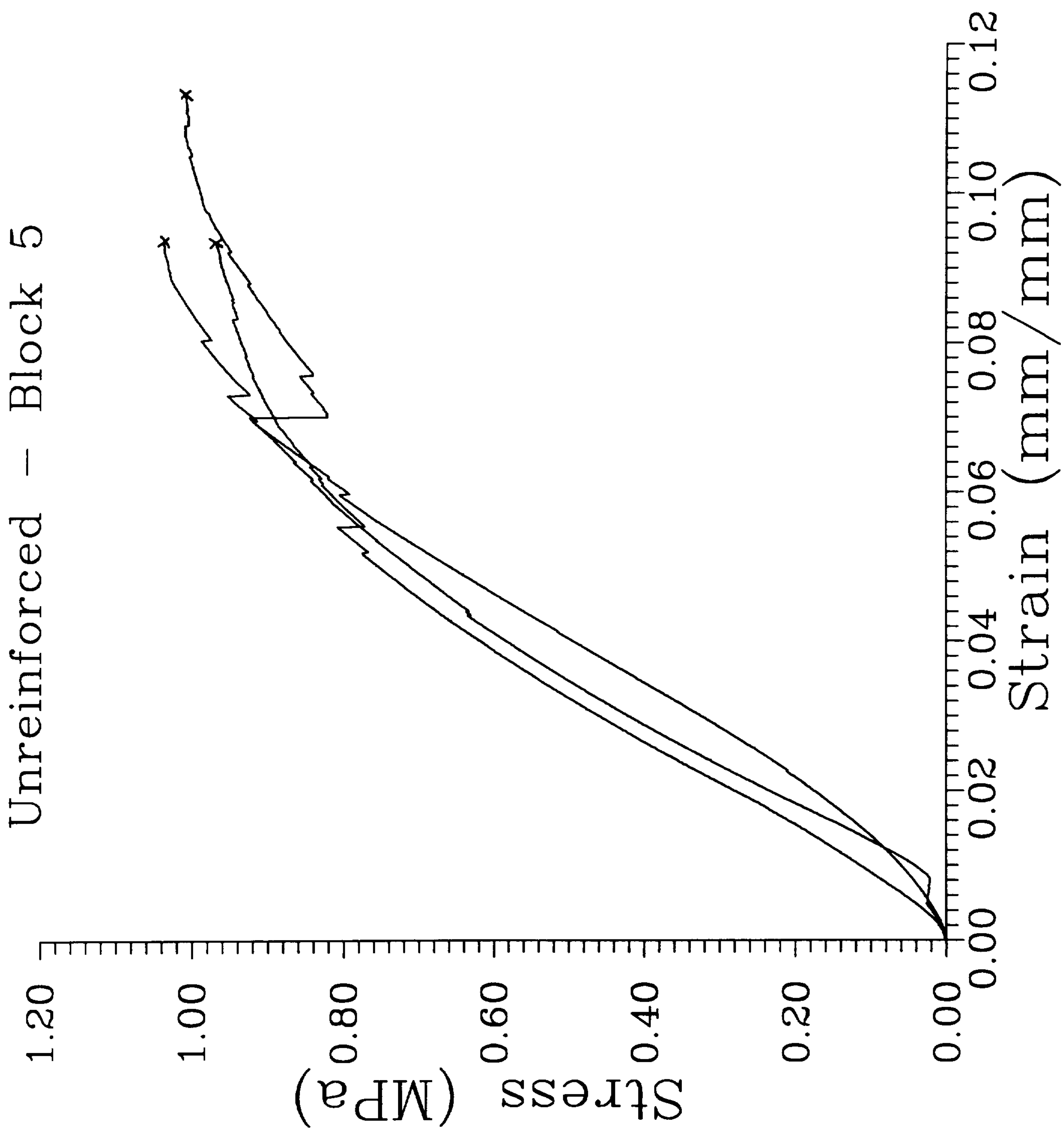

Unreinforced - Block 5
Stress (MPa)
0.00
0.20
0.40
0.60
0.80
1.00
1.20
Strain (mm/mm)
0.00
0.02
0.04
0.06
0.08
0.10
0.12

Summary of Compression Results

5%, 40 kg/m^3 - 9th block

3/31/95 - Tests in Air

Avg Density = 260 kg/m^3

Expt. #	Compressive Strength (MPa)	Compressive Strain at Fracture (mm/mm)	E(50%) (MPa)	E(90%) (MPa)
1	1.09	0.058	21.4	22.7
2	0.89	0.082	23.7	17.2
3	1.02	0.074	16.1	15.0
Average	**1.00**	**0.071**	**20.4**	**18.3**
Std. Dev.	**0.08**	**0.010**	**3.2**	**3.2**

Notes:

1) The crosshead speed was 0.1016 mm/min
2) E(50%) is the secant modulus between the point A, of stress = 0.04 MPa, and point B, of stress = 50% of the compressive strength
3) E(90%) is the secant modulus between the point A, of stress = 0.04 MPa, and point C, of stress = 90% of the compressive strength
4) The specimens were 5% fiber loaded, target density = 40 kg/m^3
5) Tests were done at room temperature in air, with no prior desiccation

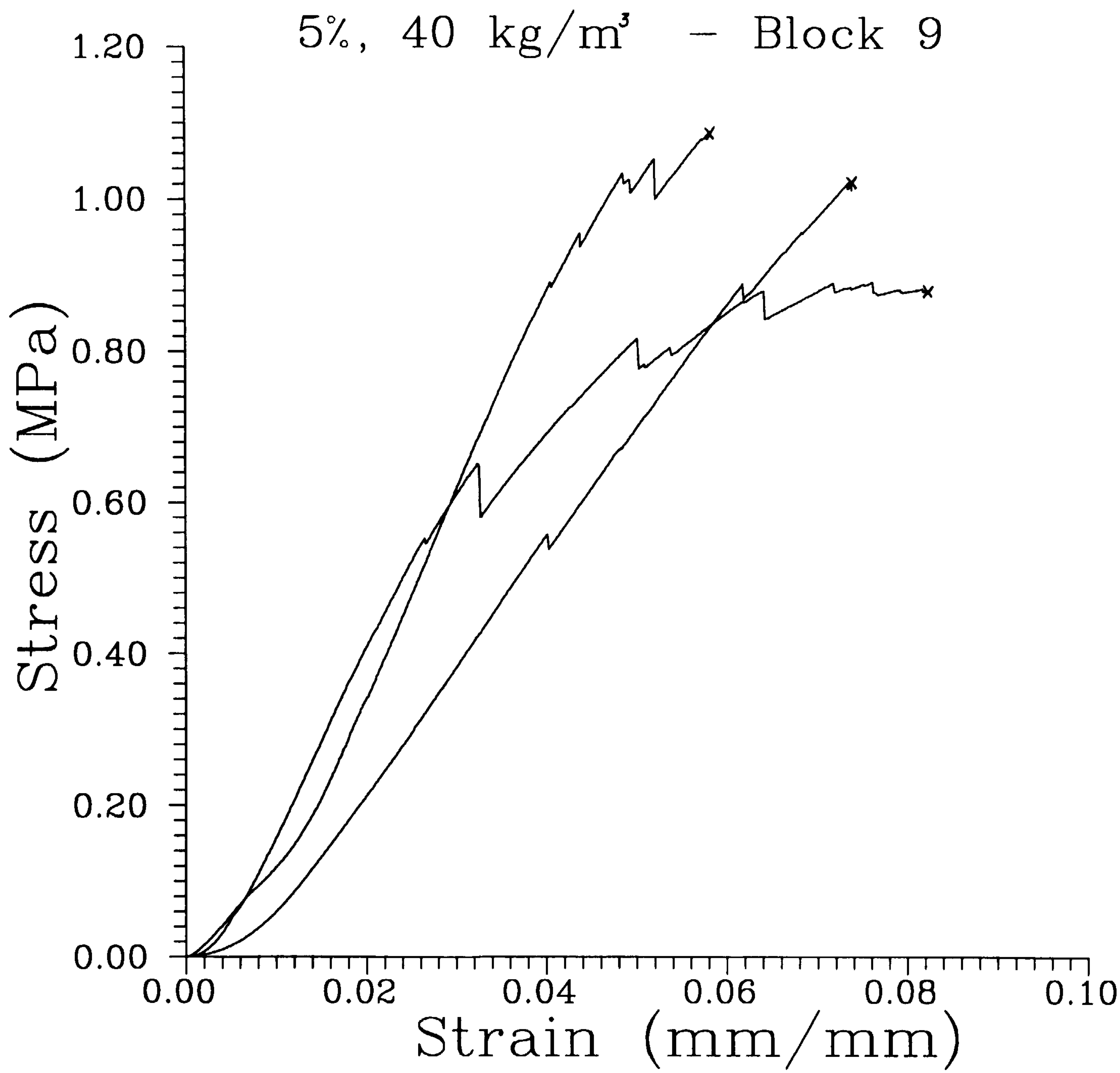

5%, 40 kg/m³ – Block 9
Stress (MPa)
Strain (mm/mm)
0.00
0.20
0.40
0.60
0.80
1.00
1.20
0.00
0.02
0.04
0.06
0.08
0.10

Summary of Compression Results

5%, 80 kg/m^3 - 35th block

6/2/95 - Tests in Air

Avg Density = 320 kg/m^3

Expt. #	Compressive Strength (MPa)	Compressive Strain at Fracture (mm/mm)	E(50%) (MPa)	E(90%) (MPa)
1	1.21	0.046	30.3	29.9
2	-	-	-	-
3	1.37	0.058	37.4	35.8
4	1.54	0.053	36.6	33.8
5	1.68	0.053	39.5	36.2
Average	**1.45**	**0.053**	**36.0**	**33.9**
Std. Dev.	**0.18**	**0.004**	**3.4**	**2.5**

Notes:

1) The crosshead speed was 0.1016 mm/min
2) E(50%) is the secant modulus between the point A, of stress = 0.04 MPa, and point B, of stress = 50% of the compressive strength
3) E(90%) is the secant modulus between the point A, of stress = 0.04 MPa, and point C, of stress = 90% of the compressive strength
4) The specimens were 5% fiber loaded, target density = 80 kg/m^3
5) Tests were done at room temperature in air, with no prior desiccation

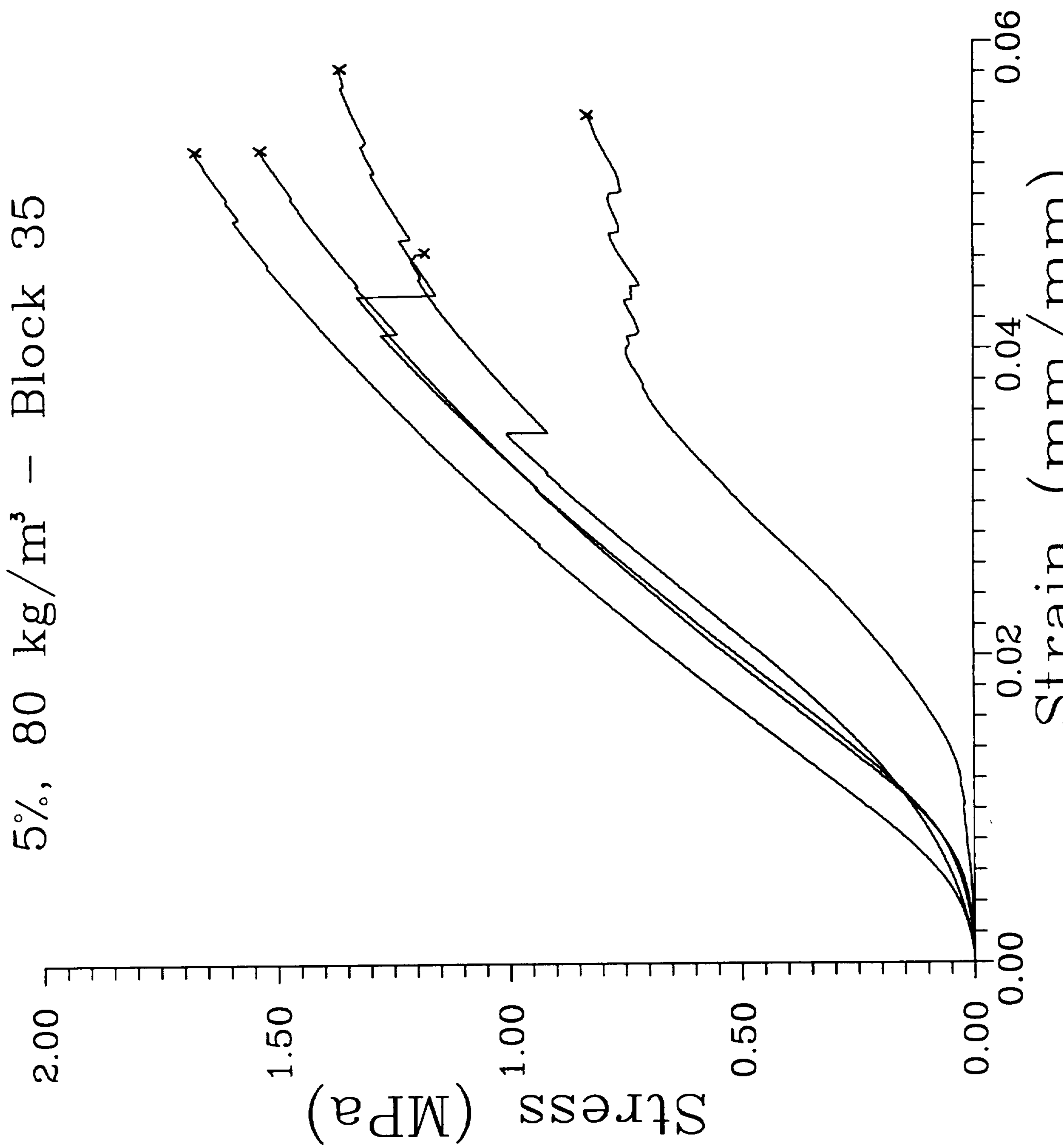

5%, 80 kg/m³ – Block 35
Stress (MPa)
2.00
1.50
1.00
0.50
0.00
0.00
0.02
0.04
0.06
Strain (mm/mm)

Summary of Compression Results

10%, 40 kg/m^3 - 15th block

3/31/95 - Tests in Air

Avg Density = 190 kg/m^3

Expt. #	Compressive Strength (MPa)	Compressive Strain at Fracture (mm/mm)	E(50%) (MPa)	E(90%) (MPa)
1	0.30	0.069	6.11	5.08
2	0.38	0.064	10.14	7.24
3	0.30	0.063	7.49	5.60
4	0.36	0.061	9.97	7.34
5	0.35	0.079	8.44	6.25
6	0.35	0.078	6.45	5.32
Average	**0.34**	**0.069**	**8.10**	**6.14**
Std. Dev.	**0.03**	**0.007**	**1.57**	**0.89**

Notes:

1) The crosshead speed was 0.1016 mm/min
2) E(50%) is the secant modulus between the point A, of stress = 0.04 MPa, and point B, of stress = 50% of the compressive strength
3) E(90%) is the secant modulus between the point A, of stress = 0.04 MPa, and point C, of stress = 90% of the compressive strength
4) The specimens were 10% fiber loaded, target density = 40 kg/m^3
5) Tests were done at room temperature in air, with no prior desiccation

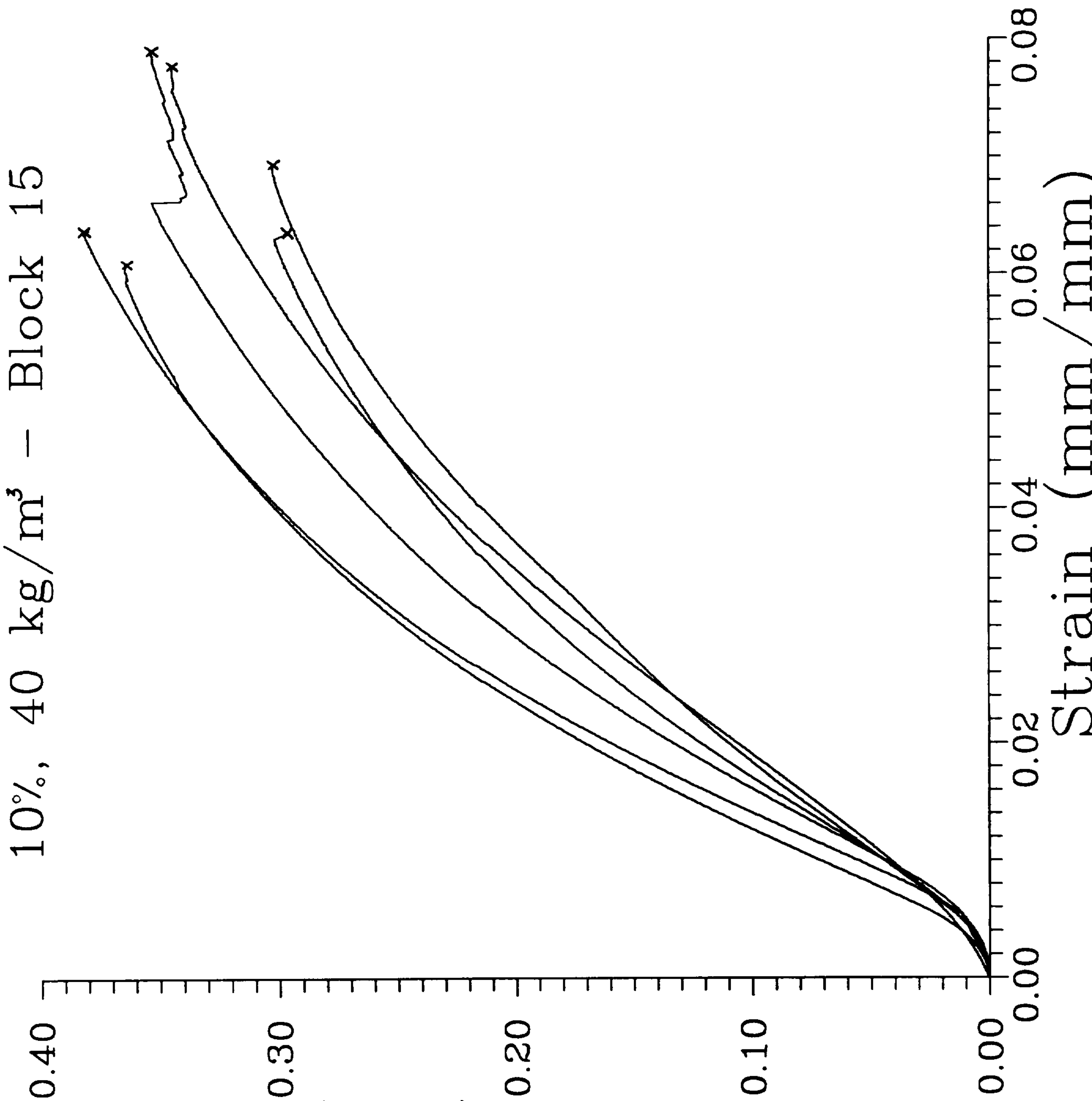
10%, 40 kg/m³ – Block 15
Stress (MPa)
0.00
0.10
0.20
0.30
0.40
Strain (mm/mm)
0.00
0.02
0.04
0.06
0.08

Summary of Compression Results

10%, 50 kg/m^3 - 2nd block

3/14/95 - Tests in Air

Avg Density = 230 kg/m^3

Expt. #	Compressive Strength (MPa)	Compressive Strain at Fracture (mm/mm)	E(50%) (MPa)	E(90%) (MPa)
1	1.05	0.066	24.7	18.9
2	0.97	0.062	23.9	17.6
3	0.99	0.069	23.5	17.7
4	1.05	0.068	24.3	18.8
5	1.05	0.070	23.9	18.3
6	1.07	0.070	24.5	18.7
7	1.02	0.073	23.1	16.9
8	0.89	0.062	19.6	16.9
9	0.97	0.064	23.3	18.1
Average	**1.01**	**0.067**	**23.4**	**18.0**
Std. Dev.	**0.05**	**0.004**	**1.4**	**0.7**

Notes:

1) The crosshead speed was 0.1016 mm/min
2) E(50%) is the secant modulus between the point A, of stress = 0.04 MPa, and point B, of stress = 50% of the compressive strength
3) E(90%) is the secant modulus between the point A, of stress = 0.04 MPa, and point C, of stress = 90% of the compressive strength
4) The specimens were 10% fiber loaded, target density = 50 kg/m^3
5) Tests were done at room temperature in air, with no prior desiccation

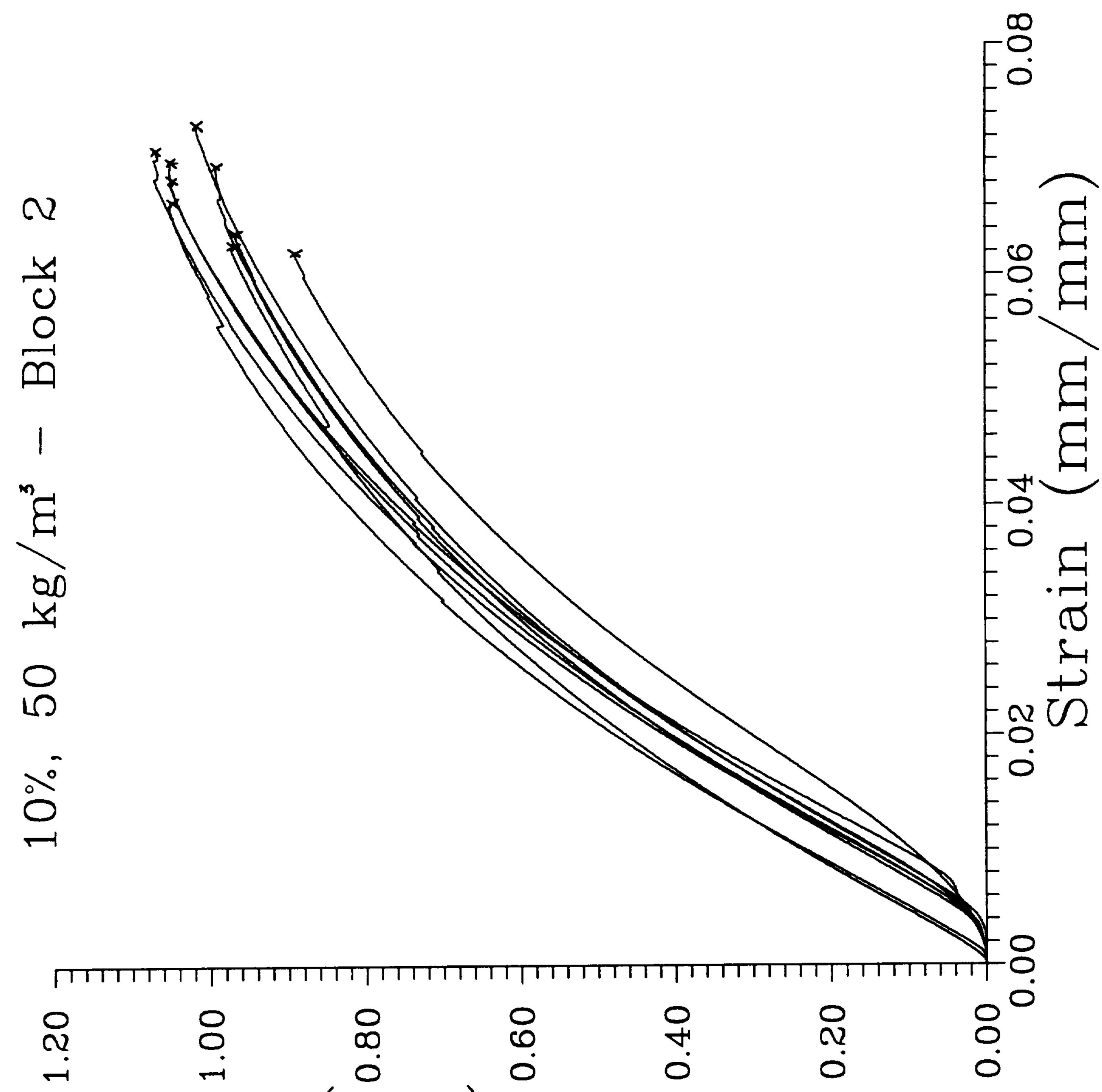
10%, 50 kg/m³ – Block 2
Stress (MPa)
Strain (mm/mm)
0.00
0.20
0.40
0.60
0.80
1.00
1.20
0.00
0.02
0.04
0.06
0.08

Summary of Compression Results

10%, 80 kg/m^3 - 16th & 17th block

6/1/95 - 6/2/95 - Tests in Air

Avg Density = 330 kg/m^3

Expt. #	Compressive Strength (MPa)	Compressive Strain at Fracture (mm/mm)	E(50%) (MPa)	E(90%) (MPa)
16-1	1.05	0.051	26.5	29.1
16-2	1.18	0.057	22.9	25.9
16-3	1.23	0.054	26.3	28.7
16-4	1.19	0.051	26.3	28.9
16-5	1.52	0.052	34.8	37.8
16-6	1.48	0.050	35.2	34.6
16-7	1.31	0.057	29.7	31.0
16-8	1.10	0.049	26.1	29.3
16-9	1.24	0.050	30.6	31.4
17-1	1.30	0.048	31.8	33.6
17-2	1.49	0.053	34.8	34.0
17-3	1.29	0.046	38.4	35.6
17-4	1.14	0.049	26.3	28.3
17-5	1.24	0.048	34.0	34.8
17-6	1.33	0.049	32.8	33.4
Average	**1.27**	**0.051**	**30.4**	**31.8**
Std. Dev.	**0.14**	**0.003**	**4.4**	**3.2**

Notes:

1) The crosshead speed was 0.1016 mm/min
2) E(50%) is the secant modulus between the point A, of stress = 0.04 MPa, and point B, of stress = 50% of the compressive strength
3) E(90%) is the secant modulus between the point A, of stress = 0.04 MPa, and point C, of stress = 90% of the compressive strength
4) The specimens were 10% fiber loaded, target density = 80 kg/m^3
5) Tests were done at room temperature in air, with no prior desiccation

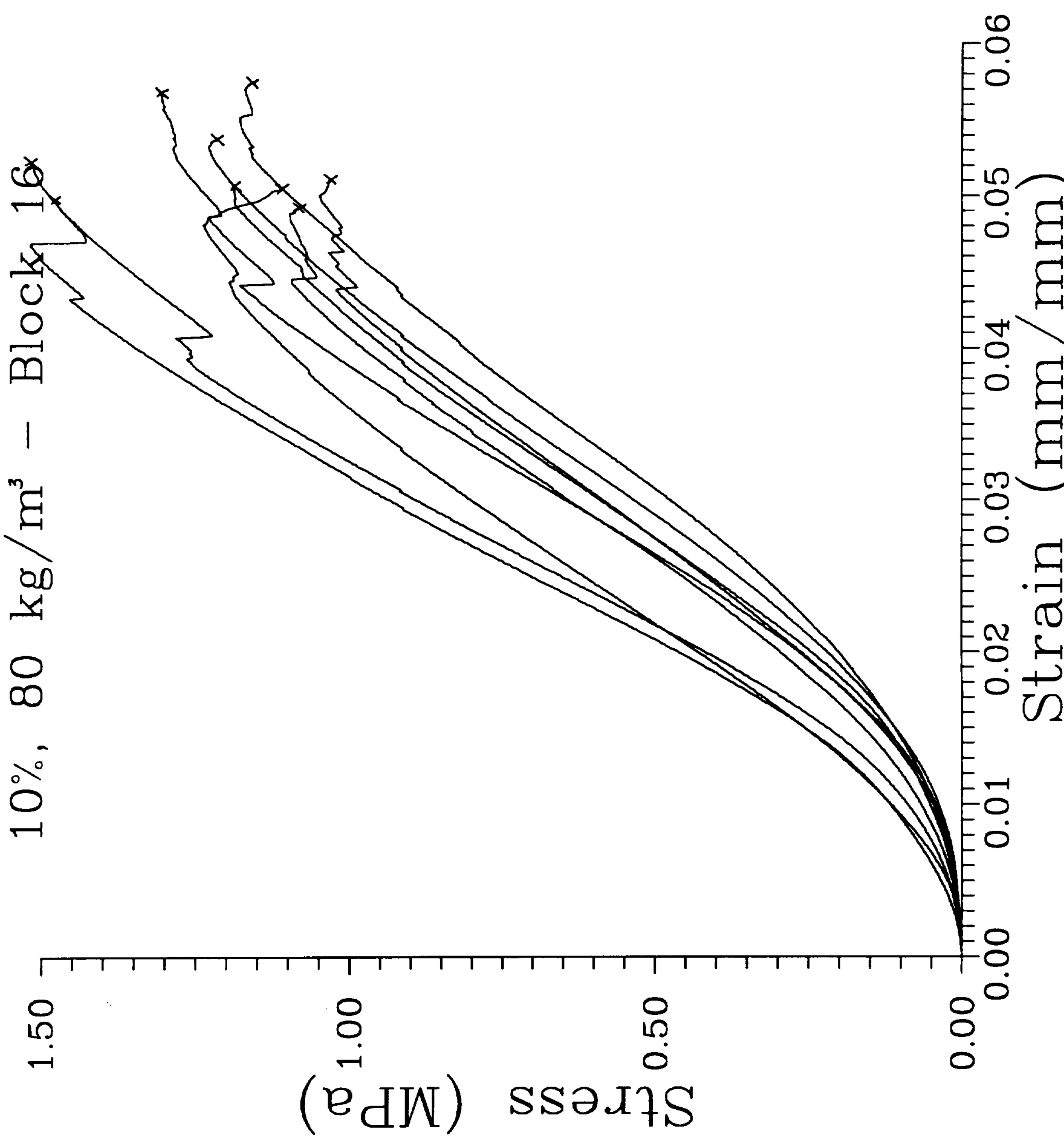
10%, 80 kg/m³ – Block 16
Stress (MPa)
0.00
0.50
1.00
1.50
Strain (mm/mm)
0.00
0.01
0.02
0.03
0.04
0.05
0.06

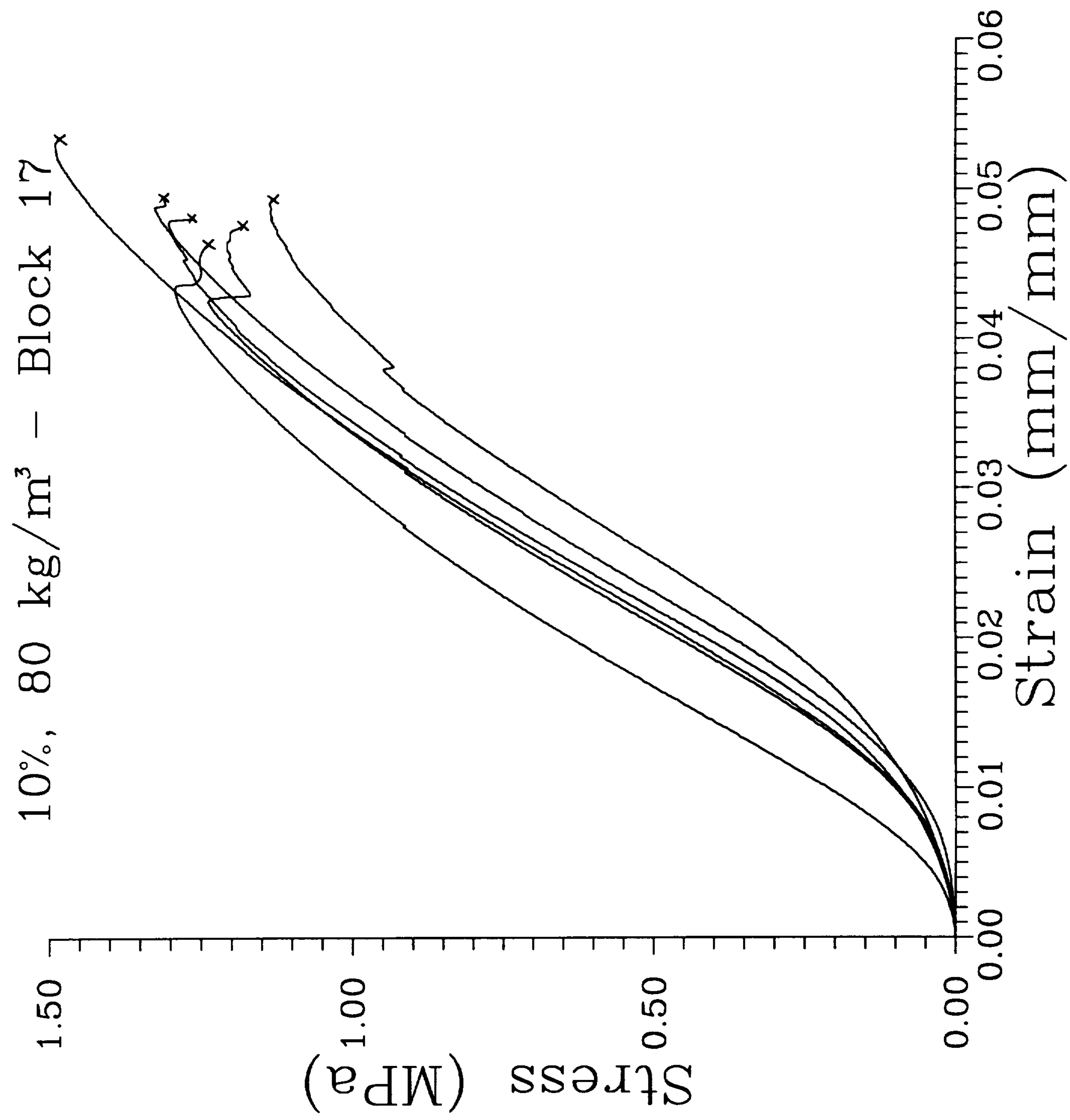

10%, 80 kg/m³ – Block 17
Stress (MPa)
Strain (mm/mm)
0.00
0.50
1.00
1.50
0.00
0.01
0.02
0.03
0.04
0.05
0.06

Summary of Compression Results

25%, 40 kg/m^3 - 5th, 6th & 7th block

5/23/95 - 5/31/95 - Tests in Air

Avg Density = 190 kg/m^3

Expt. #	Compressive Strength (MPa)	Compressive Strain at Fracture (mm/mm)	E(50%) (MPa)	E(90%) (MPa)
7-1	0.59	0.154	8.4	5.0
7-2	0.57	0.151	9.3	5.5
7-3	0.57	0.134	9.2	5.6
7-4	0.55	0.146	7.3	5.3
7-5	0.50	0.106	9.6	6.4
6-1	0.49	0.134	9.1	5.5
6-2	0.57	0.164	8.4	4.7
6-3	0.56	0.156	9.0	4.9
6-4	0.49	0.125	9.4	6.0
6-5	0.54	0.135	9.2	5.3
5-1	0.58	0.156	8.0	4.6
5-2	0.54	0.149	7.3	4.8
5-3	0.58	0.155	7.7	4.7
5-4	0.53	0.120	8.9	5.7
5-5	0.54	0.148	8.6	5.2
5-6	0.56	0.139	8.5	5.0
Average	**0.55**	**0.142**	**8.6**	**5.3**
Std. Dev.	**0.03**	**0.015**	**0.7**	**0.5**

Notes:

1) The crosshead speed was 0.1016 mm/min
2) E(50%) is the secant modulus between the point A, of stress = 0.04 MPa, and point B, of stress = 50% of the compressive strength
3) E(90%) is the secant modulus between the point A, of stress = 0.04 MPa, and point C, of stress = 90% of the compressive strength
4) The specimens were 25% fiber loaded, target density = 40 kg/m^3
5) Tests were done at room temperature in air, with no prior desiccation

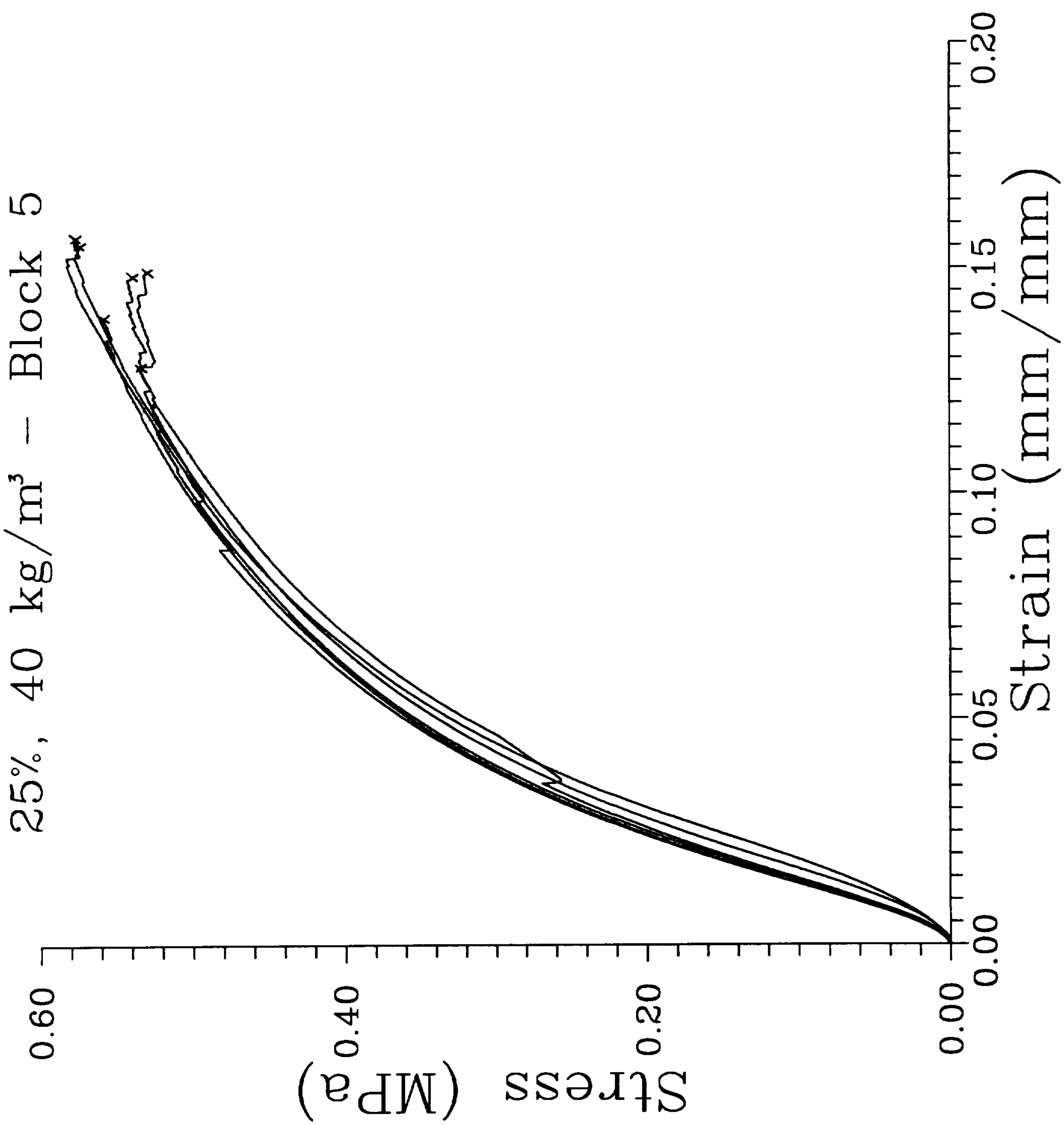

25%, 40 kg/m³ – Block 5
Stress (MPa)
0.00
0.20
0.40
0.60
Strain (mm/mm)
0.00
0.05
0.10
0.15
0.20

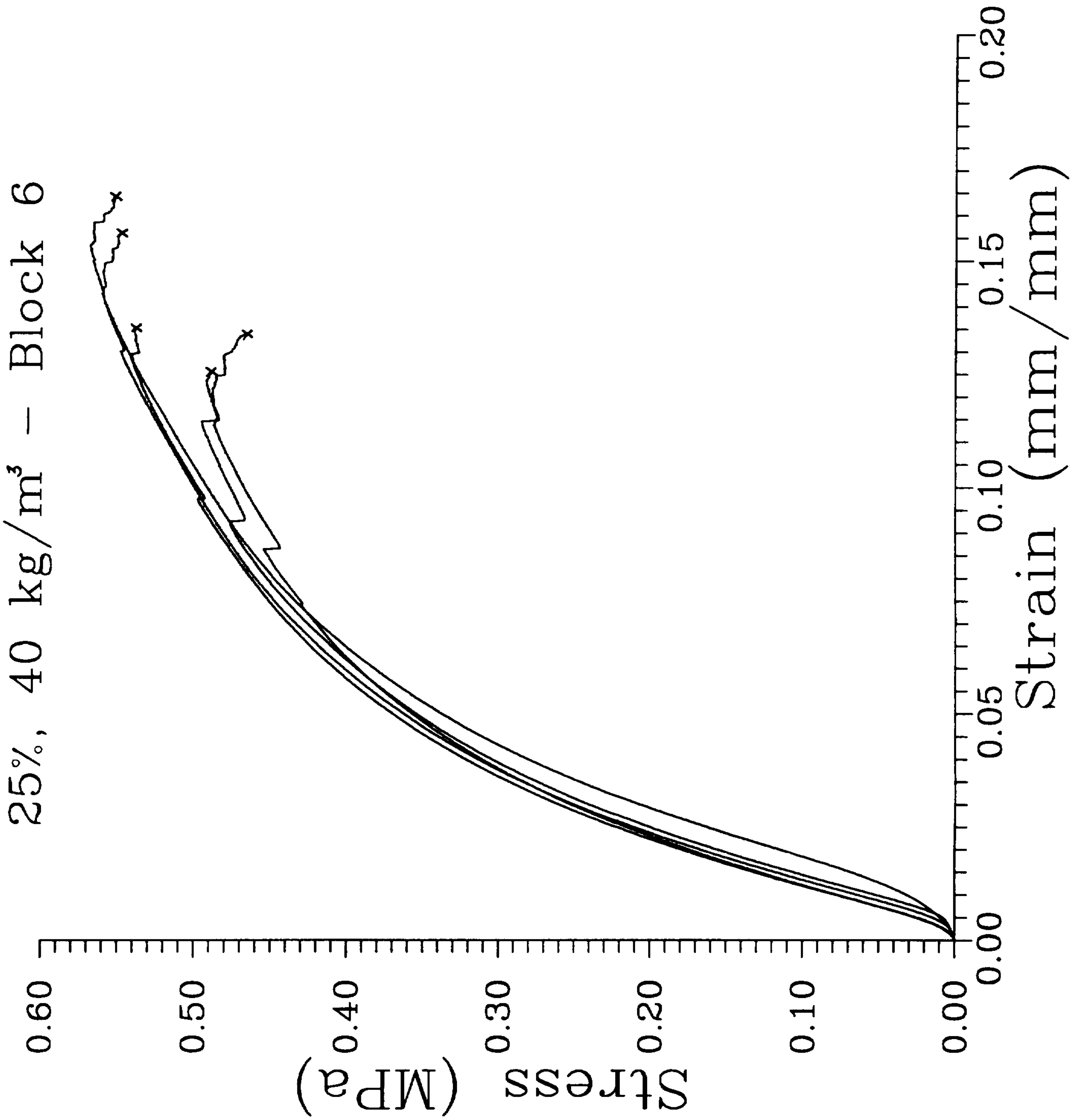

25%, 40 kg/m³ – Block 6
Stress (MPa)
Strain (mm/mm)
0.00
0.10
0.20
0.30
0.40
0.50
0.60
0.05
0.15

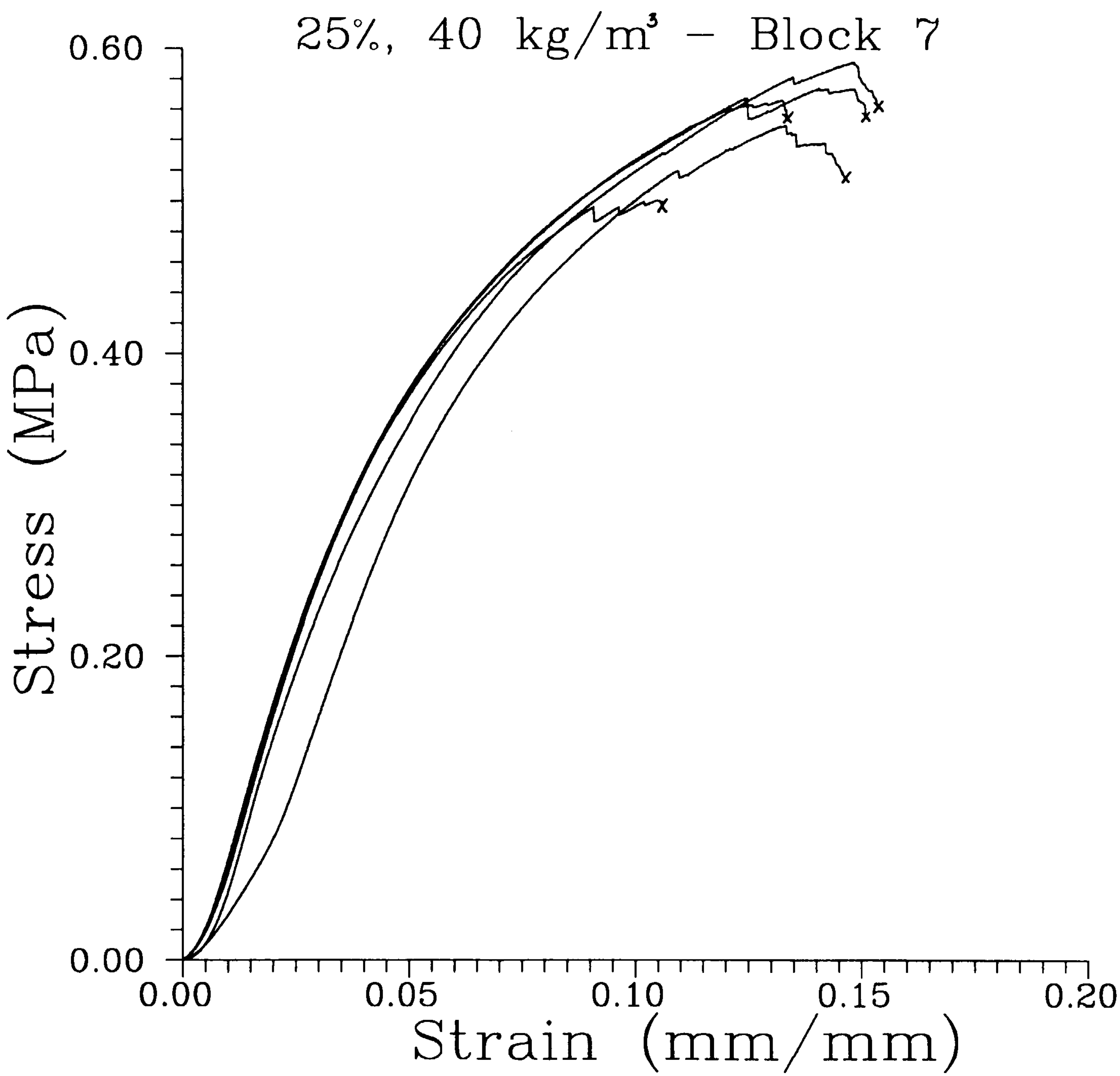
25%, 40 kg/m³ - Block 7
Stress (MPa)
0.60
0.40
0.20
0.00
0.00
0.05
0.10
0.15
0.20
Strain (mm/mm)

Summary of Compression Results

25%, 80 kg/m^3 - 1st, 2nd & 3rd block

2/21/95, 2/22/95 & /3/9/95 - Tests in Air

Avg Density = 240 kg/m^3

Expt. #	Compressive Strength (MPa)	Compressive Strain at Fracture (mm/mm)	E(50%) (MPa)	E(90%) (MPa)
1-1	-	-	-	-
1-2	-	-	-	-
1-3	0.81	0.067	26.5	17.6
1-4	0.80	0.069	24.9	16.3
1-5	0.81	0.071	25.1	16.3
1-6	0.78	0.088	21.6	13.6
1-7	0.75	0.062	25.5	17.7
1-8	0.77	0.068	22.3	16.2
1-9	0.81	0.080	23.9	15.3
1-10	0.82	0.079	22.3	15.3
1-11	0.79	0.087	17.1	12.6
2-1	0.75	0.094	16.9	11.5
2-2	0.80	0.085	19.5	12.1
2-3	0.82	0.094	18.0	11.6
3-1	0.75	0.068	25.9	17.0
3-2	0.81	0.082	22.9	15.1
3-3	0.77	0.068	22.9	16.3
Average	**0.79**	**0.077**	**22.3**	**15.0**
Std. Dev.	**0.02**	**0.010**	**3.1**	**2.1**

Notes:

1) The crosshead speed was 0.1016 mm/min
2) E(50%) is the secant modulus between the point A, of stress = 0.04 MPa, and point B, of stress = 50% of the compressive strength
3) E(90%) is the secant modulus between the point A, of stress = 0.04 MPa, and point C, of stress = 90% of the compressive strength
4) The specimens were 25% fiber loaded, target density = 80 kg/m^3
5) Tests were done at room temperature in air, with no prior desiccation

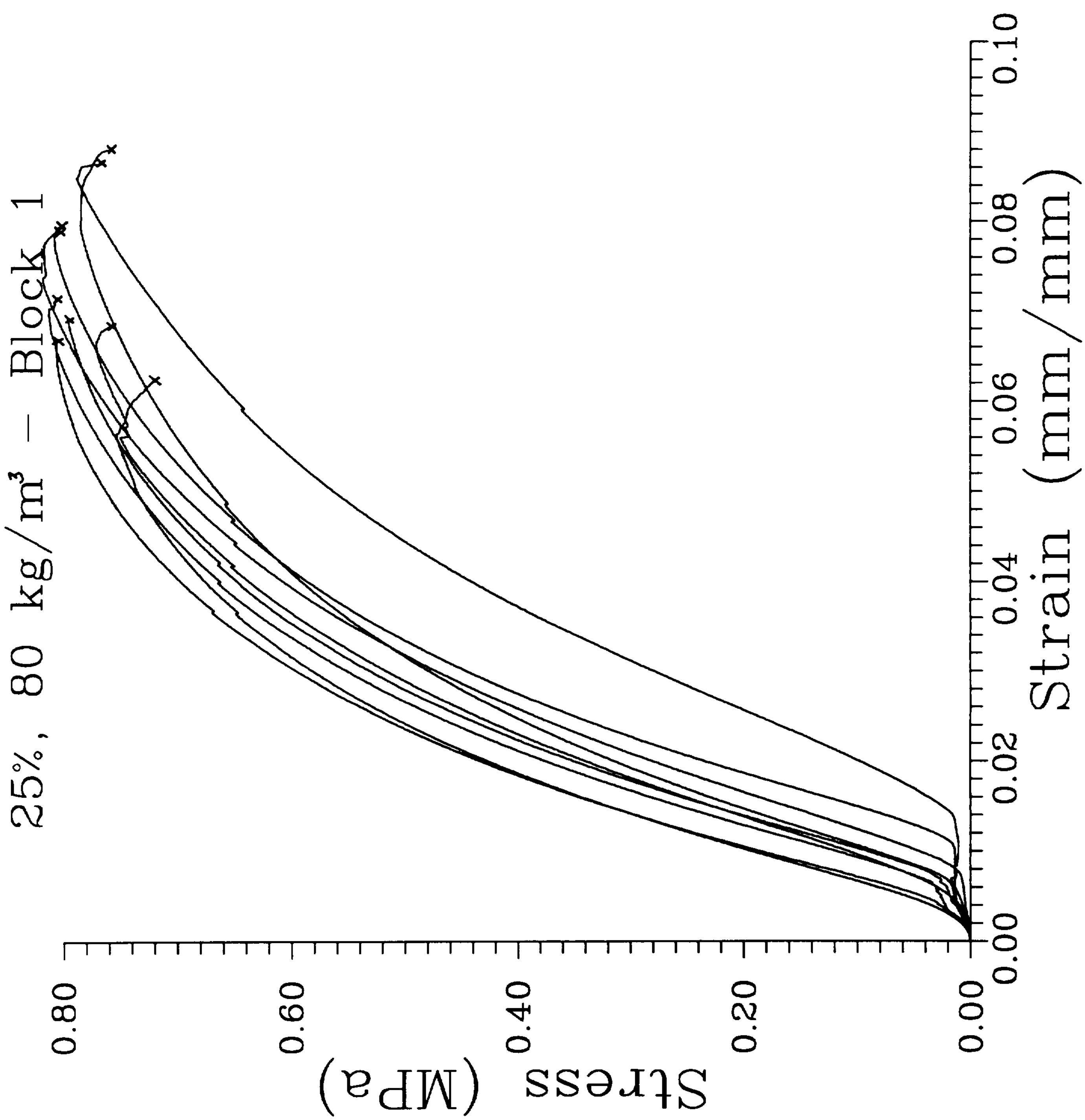
25%, 80 kg/m³ — Block 1
Stress (MPa)
Strain (mm/mm)
0.00
0.20
0.40
0.60
0.80
0.00
0.02
0.04
0.06
0.08
0.10

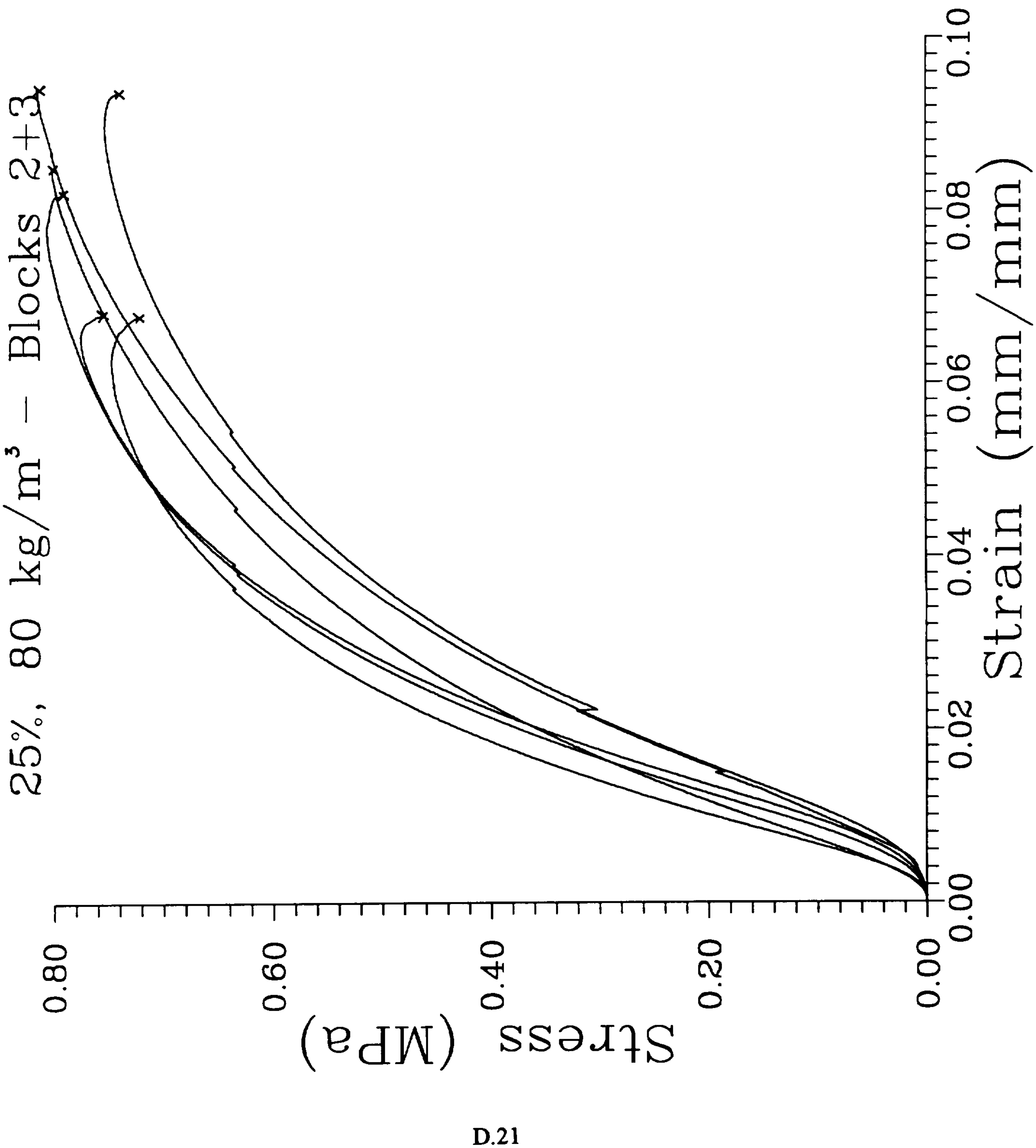
25‰, 80 kg/m³ — Blocks 2+3
Stress (MPa)
0.00
0.20
0.40
0.60
0.80
Strain (mm/mm)
0.00
0.02
0.04
0.06
0.08
0.10

APPENDIX E

Compression Results: Tests in Ethanol

Summary of Compression Results

10%, 50 kg/m^3 - 1st block

5/3/95 - Tests in Ethanol

Avg Density = 250 kg/m^3

Expt. #	Compressive Strength (MPa)	Compressive Strain at Fracture (mm/mm)	E(50%) (MPa)	E(90%) (MPa)
1	0.85	0.028	-	-
2	0.33	0.048	14.0	11.2
3	0.63	0.029	26.9	25.1
Average	**0.61**	**0.035**	**20.5**	**18.1**
Std. Dev.	**0.21**	**0.009**	**6.4**	**6.9**

Notes:

1) The crosshead speed was 0.1016 mm/min
2) E(50%) is the secant modulus between the point A, of stress = 0.04 MPa, and point B, of stress = 50% of the compressive strength
3) E(90%) is the secant modulus between the point A, of stress = 0.04 MPa, and point C, of stress = 90% of the compressive strength
4) The specimens were 10% fiber loaded, target density = 50 kg/m^3
5) Tests were done at room temperature in ethanol, with no prior desiccation

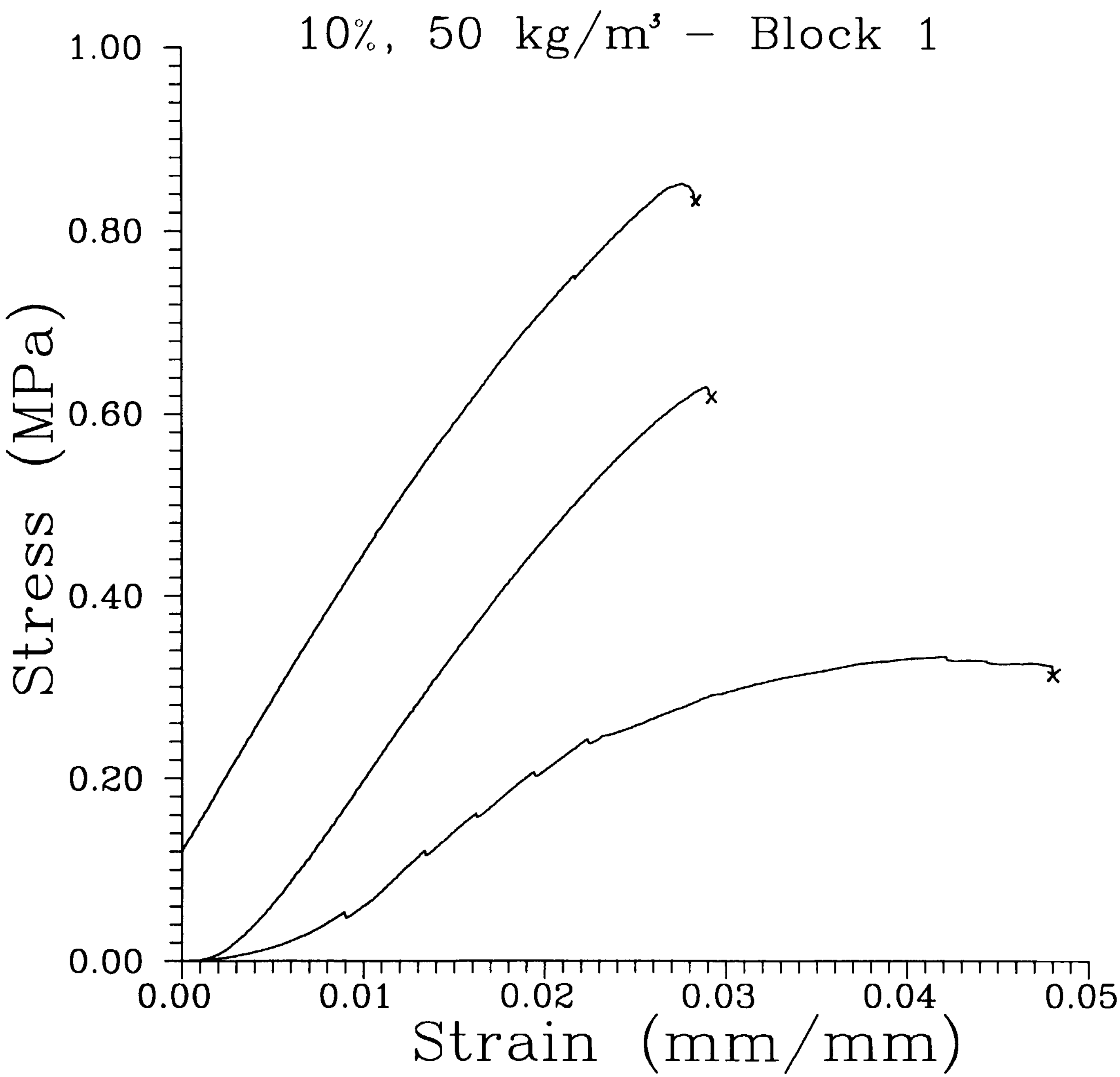
10%, 50 kg/m³ – Block 1
Stress (MPa)
Strain (mm/mm)
1.00
0.80
0.60
0.40
0.20
0.00
0.00
0.01
0.02
0.03
0.04
0.05

Summary of Compression Results

25%, 80 kg/m^3 - 2nd block

5/3/95 - Tests in Ethanol

Avg Density = 250 kg/m^3

Expt. #	Compressive Strength (MPa)	Compressive Strain at Fracture (mm/mm)	E(50%) (MPa)	E(90%) (MPa)
1	0.74	0.044	32.8	27.1
2	0.55	0.053	20.6	18.7
3	0.73	0.043	24.1	21.9
4	0.60	0.052	19.8	15.9
Average	**0.65**	**0.048**	**24.3**	**20.9**
Std. Dev.	**0.08**	**0.005**	**5.1**	**4.1**

Notes:

1) The crosshead speed was 0.1016 mm/min
2) E(50%) is the secant modulus between the point A, of stress = 0.04 MPa, and point B, of stress = 50% of the compressive strength
3) E(90%) is the secant modulus between the point A, of stress = 0.04 MPa, and point C, of stress = 90% of the compressive strength
4) The specimens were 25% fiber loaded, target density = 80 kg/m^3
5) Tests were done at room temperature in ethanol, with no prior desiccation

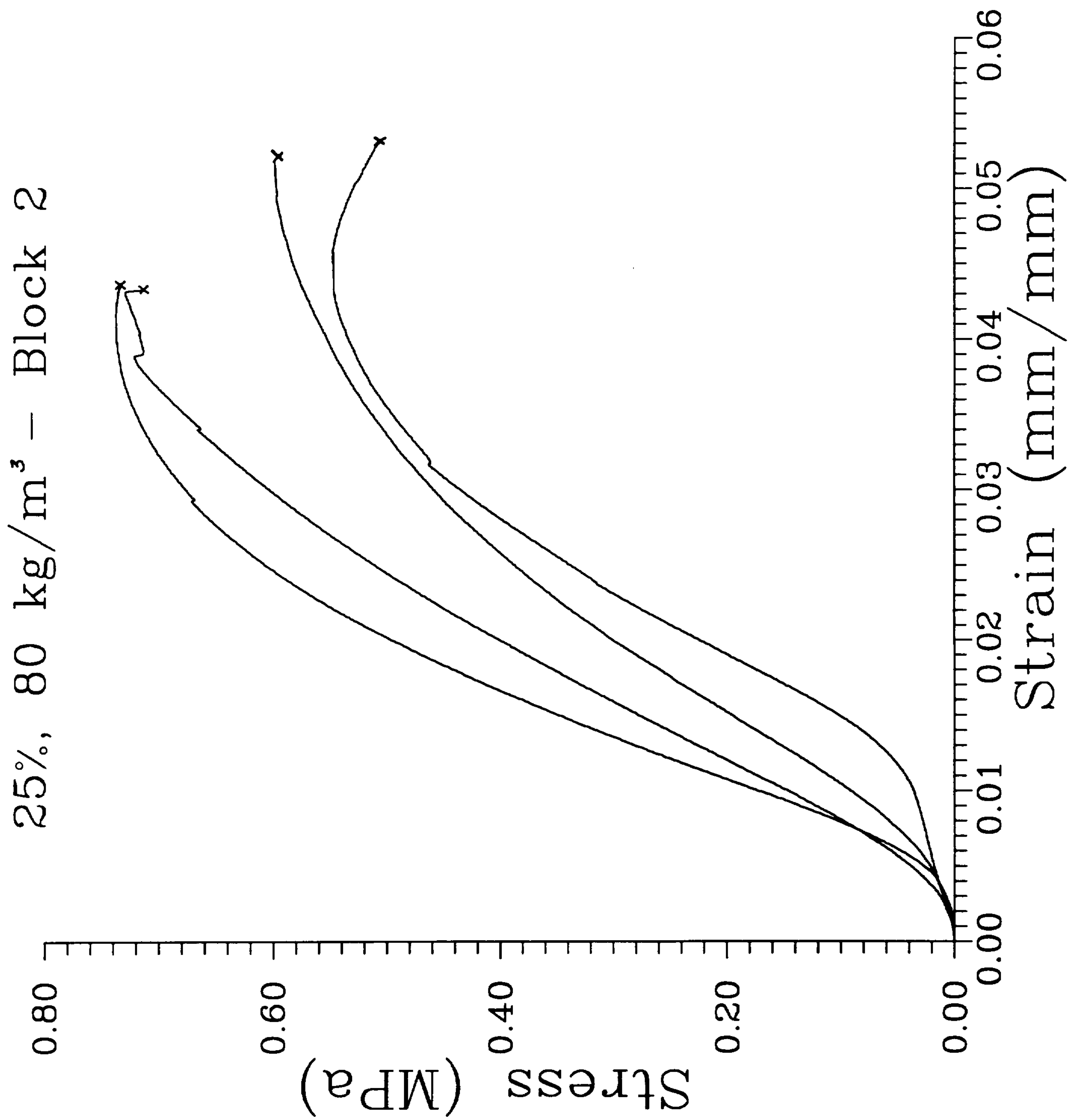
25%, 80 kg/m³ — Block 2
Stress (MPa)
0.00
0.20
0.40
0.60
0.80
Strain (mm/mm)
0.00
0.01
0.02
0.03
0.04
0.05
0.06

APPENDIX F

Compression Results: Specimens Aged in Air

Summary of Compression Results

10%, 50 kg/m^3 - 1st block

5/4/95 - Tests in Air

Avg Density = 250 kg/m^3

Expt. #	Compressive Strength (MPa)	Compressive Strain at Fracture (mm/mm)	E(50%) (MPa)	E(90%) (MPa)
1	1.02	0.043	34.0	28.5
2	1.12	0.047	34.4	28.3
Average	**1.07**	**0.045**	**34.2**	**28.4**
Std. Dev.	**0.05**	**0.002**	**0.2**	**0.1**

Notes:

1) The crosshead speed was 0.1016 mm/min
2) E(50%) is the secant modulus between the point A, of stress = 0.04 MPa, and point B, of stress = 50% of the compressive strength
3) E(90%) is the secant modulus between the point A, of stress = 0.04 MPa, and point C, of stress = 90% of the compressive strength
4) The specimens were 10% fiber loaded, target density = 50 kg/m^3
5) Tests were done at room temperature in air, with no prior desiccation
6) The specimens were aged for 2 months

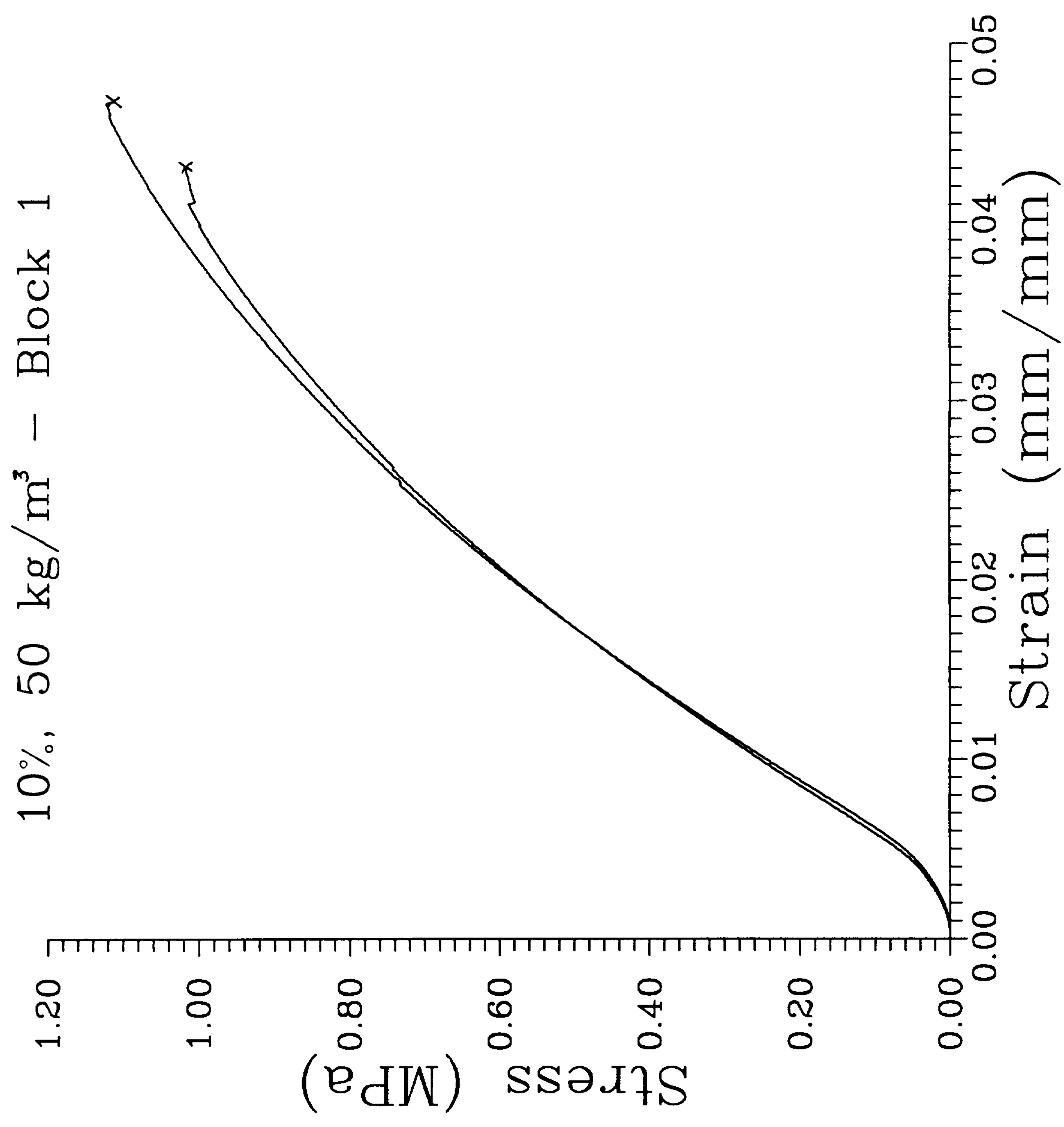

10%, 50 kg/m³ – Block 1
Stress (MPa)
1.20
1.00
0.80
0.60
0.40
0.20
0.00
Strain (mm/mm)
0.00
0.01
0.02
0.03
0.04
0.05

Summary of Compression Results

25%, 80 kg/m^3 - 2nd & 3rd blocks

5/4/95 - Tests in Air

Avg Density = 250 kg/m^3

Expt. #	Compressive Strength (MPa)	Compressive Strain at Fracture (mm/mm)	E(50%) (MPa)	E(90%) (MPa)
2-1	0.84	0.051	31.0	23.3
2-2	0.74	0.052	32.4	25.9
2-3	0.75	0.051	25.5	22.5
3-1	0.82	0.047	36.4	28.9
3-2	0.85	0.048	27.9	26.3
3-3	0.65	0.039	22.3	19.9
Average	**0.77**	**0.048**	**29.2**	**24.5**
Std. Dev.	**0.07**	**0.004**	**4.6**	**2.9**

Notes:

1) The crosshead speed was 0.1016 mm/min
2) E(50%) is the secant modulus between the point A, of stress = 0.04 MPa, and point B, of stress = 50% of the compressive strength
3) E(90%) is the secant modulus between the point A, of stress = 0.04 MPa, and point C, of stress = 90% of the compressive strength
4) The specimens were 25% fiber loaded, target density = 80 kg/m^3
5) Tests were done at room temperature in air, with no prior desiccation
6) The specimens were aged for 2 months

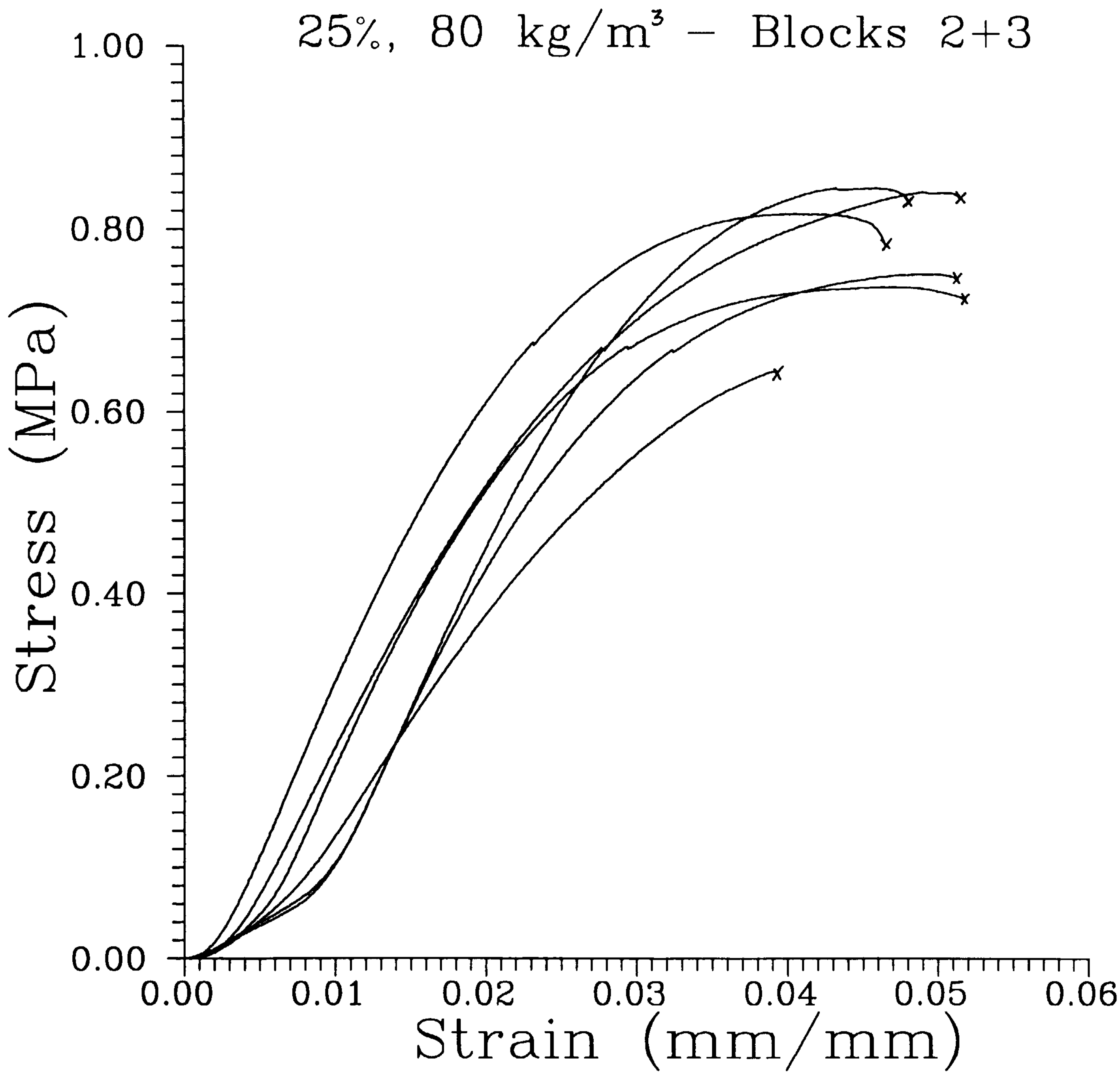
25%, 80 kg/m³ – Blocks 2+3
Stress (MPa)
Strain (mm/mm)
1.00
0.80
0.60
0.40
0.20
0.00
0.00
0.01
0.02
0.03
0.04
0.05
0.06

APPENDIX G

Compression Results: Specimens Aged in Air and Desiccated

Summary of Compression Results

25%, 80 kg/m^3 - 3rd block

5/12/95 - Tests in Air after Desiccation for 10 days

Avg Density = 240 kg/m^3

Expt. #	Compressive Strength (MPa)	Compressive Strain at Fracture (mm/mm)	E(50%) (MPa)	E(90%) (MPa)
1	0.87	0.040	31.6	28.7
2	0.98	0.051	33.4	26.1
3	0.86	0.049	27.9	24.9
4	0.89	0.047	29.5	27.7
Average	**0.90**	**0.047**	**30.6**	**26.9**
Std. Dev.	**0.05**	**0.004**	**2.1**	**1.5**

Notes:

1) The crosshead speed was 0.1016 mm/min
2) E(50%) is the secant modulus between the point A, of stress = 0.04 MPa, and point B, of stress = 50% of the compressive strength
3) E(90%) is the secant modulus between the point A, of stress = 0.04 MPa, and point C, of stress = 90% of the compressive strength
4) The specimens were 25% fiber loaded, target density = 80 kg/m^3
5) Tests were done at room temperature in air, with 10 days of desiccation

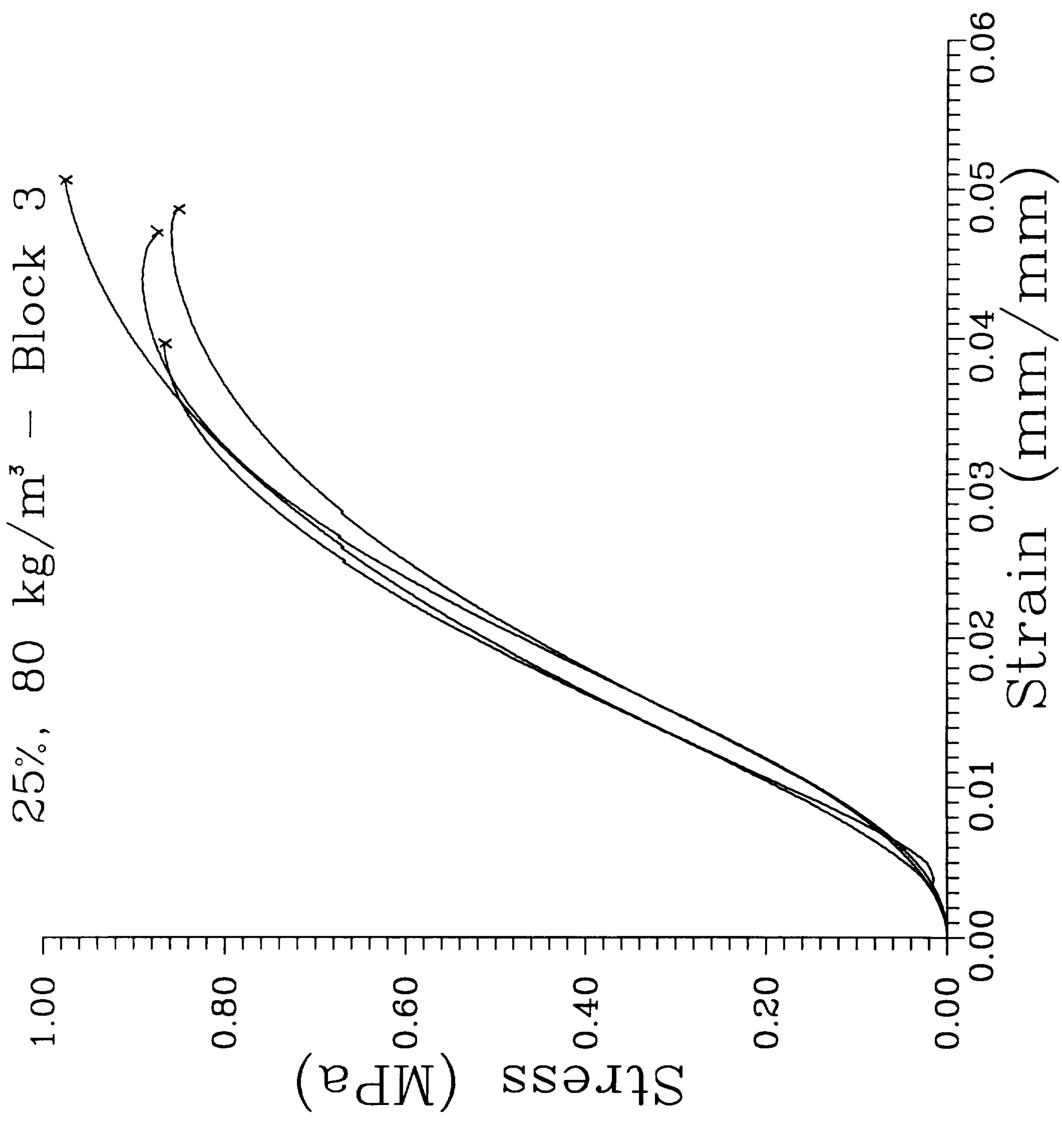
25%, 80 kg/m³ — Block 3
Stress (MPa)
Strain (mm/mm)
0.00
0.20
0.40
0.60
0.80
1.00
0.00
0.01
0.02
0.03
0.04
0.05
0.06